THE UNIVERSITY OF OKLAHOMA

GRADUATE COLLEGE

THE SORPTION KINETICS AND MECHANICAL PROPERTIES OF DILUTE COLUMBIUM-HYDROGEN SOLUTIONS

A DISSERTATION

SUBMITTED TO THE GRADUATE FACULTY

in partial fulfillment of the requirements for the

degree of

DOCTOR OF PHILOSOPHY

BY

THOMAS GLENN OAKWOOD

Norman, Oklahoma

1967

THE SORPTION KINETICS AND MECHANICAL PROPERTIES

OF DILUTE COLUMBIUM-HYDROGEN SOLUTIONS

APPROVED BY

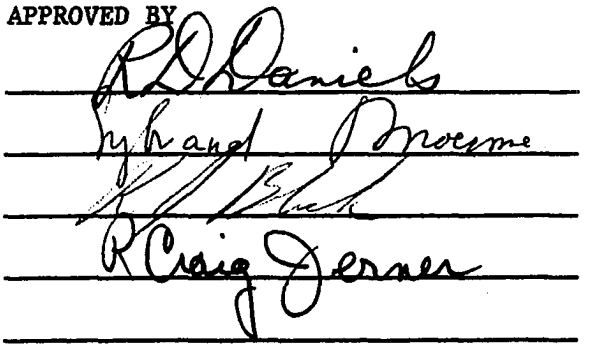

DISSERTATION COMMITTEE

ACKNOWLEDGEMENTS

This work was supported by the Atomic Energy Commission under Contract No. AT-(40-1)-2570. The author wishes to express his appreciation to Dr. Raymond D. Daniels, project director, for invaluable assistance and direction during the investigation and preparation of this manuscript. Special thanks are due Messrs. Magan Patel, David Stoner, and Robert Skinner for their assistance in the laboratory. The author wishes to thank the faculty and graduate students of the Department of Chemical Engineering and Materials Science of the University of Oklahoma for helpful suggestions during the course of this work.

ABSTRACT

The sorption kinetics and mechanical properties of dilute columbium-hydrogen solutions were investigated. The sorption kinetics, measured by a thermal equilibrium technique, were found to be sensitive to surface condition and insensitive to grain size. The sorption rate was adequately described by a diffusion controlled reaction in the temperature range 600°C to 750°C provided that the metal surface was abraded to remove effects of chemical etching. Below 600°C a surface step reaction apparently controls the sorption process, rather than bulk diffusion.

Hydrogen was found to have little effect on the strength of columbium in the temperature range 77°K to 300°K. The ductility of hydrogenated columbium, however, was found to be sensitive to hydrogen concentration, temperature, and microstructure. At 300°K, an abrupt loss in ductility was observed at a critical hydrogen concentration. A similar result was found at a lower hydrogen concentration at 191°K, with the ductility loss being greater at the lower temperature. At 77°K, however, a gradual loss in ductility with increasing hydrogen content was observed. Hydrogenated columbium was thus observed to undergo a ductile-brittle-ductile transition as the temperature was lowered from 300°K to 77°K.

Crack formation appears to be due to a hydride precipitation in localized regions of high hydrogen concentration. Hydrogen diffusion to

the microcracks from the surrounding regions is evidently responsible for crack propagation. Hydrogen apparently either adsorbs on the internal surfaces of a microcrack thereby lowering its surface energy, or diffuses to the tip of a crack resulting in a lower columbium atom bond strength.

The ductile-brittle-ductile transition suggests that the mechanism controlling crack propagation changes as the temperature is lowered. At 300°K, where hydrogen mobility is reasonably high, the rate of crack propagation appears to depend on the ability of columbium to flow plastically at crack tips. At 77°K, however, hydrogen mobility is reduced severely and, due to the inability of hydrogen to diffuse rapidly to a microcrack, a ductility return results.

TABLE OF CONTENTS

LIST OF TABLES

LIST OF ILLUSTRATIONS

SORPTION KINETICS AND MECHANICAL PROPERTIES OF DILUTE COLUMBIUM HYDROGEN SOLID SOLUTIONS

CHAPTER I

INTRODUCTION AND REVIEW OF LITERATURE

In recent years there has been a growing need for materials capable of withstanding extreme temperatures while still maintaining adequate strength. The demands of space flight technology are typical of these needs. The transition refractory metals, included in groups V-A and VI-A of the periodic table, have offered possible solutions to the problems of high temperature environments. These metals have extremely high melting points and, through the use of alloying, present attractive strength to weight ratios. However, a number of problems have been encountered in the use of these materials.

It has been determined that interstitial solutes have a profound effect on the mechanical properties of these metals. Hahn et al. (1) in a comprehensive investigation showed that interstitial elements such as carbon, oxygen, hydrogen, and nitrogen have a significant influence on the ductility and on the ductile-brittle transistion temperatures of refractory metals. Furthermore, Seigle and Dickinson (2) have also shown that mechanical and structural variables such as strain rate, state of stress, grain size and shape, etc., affect the ductile-brittle

transition.

The interaction of hydrogen with the refractory metals, and its subsequent effect on their mechanical properties, are of significant theoretical and practical interest. This interest comes about in part through the wide attention given to the commercially significant problem of hydrogen embrittlement of ferrous alloys.

Columbium is a refractory metal included in group V-A of the periodic table along with vanadium and tantalum. Pure columbium has a melting point of 2740°K (3). The columbium-hydrogen system has received attention in recent years both in terms of the thermodynamics and kinetics of interaction of hydrogen with columbium (4, 5, 6, 7, 8, 9, 10), and the embrittlement of columbium by hydrogen (11, 12, 13, 14). The investigation reported herein was concerned with the sorption kinetics of hydrogen in columbium and with the effects of small additions of hydrogen on the mechanical properties of columbium. The specific objectives of this investigation were essentially two-fold. The kinetics of the sorption of hydrogen by columbium were studied as a function of temperature and microstructure. In addition, the effects of hydrogen concentration, temperature, strain rate, and microstructure on the hydrogen embrittlement phenomenon were evaluated. Before proceeding with a discussion of this investigation, however, a review of pertinent literature regarding the interaction of hydrogen with columbium and the effects of hydrogen on the mechanical properties of columbium is in order.

Equilibria in the Cb-H System

In considering the sorption of a solid metal by a diatomic gas a number of possible steps must be considered. Fast (15) has broken

down the process into three separate steps: 1) the dissociation of the gas molecules at the entrance surface of the metal, 2) the transfer of atoms into solution within the metal (occlusion), and 3) diffusion through the metal.

In terms of the occlusion step, metals are generally catagorized as to whether they occlude a given gas exothermically or endothermically. Furthermore, Fast (16) has pointed out that if the heat of solution is positive (endothermic occlusion), the solubility at constant pressure should increase as the temperature is increased. Conversely, for the exothermic occluders, the solubility at constant pressure should decrease with temperature. Cotterill (17) has pointed out that endothermic occluders usually form true solutions, i.e., the metal will saturate with gas without the precipitation of a second phase. If, as in iron, the lattice solubility is exceeded, the gas will precipitate diatomically at various points in the material. The exothermic occluders are usually complicated by the formation of a second phase, e.g., a hydride. Thus, there is a finite temperature-pressure range over which a continuous solution may be formed.

McKinley (4) has shown columbium to be an exothermic occluder of hydrogen. This has been verified by other investigations (5, 6, 7). The phase diagram for the columbium-hydrogen system as determined by Albrecht et al. (6, 7) is shown in Figure 1. It can be seen that a miscibility gap occurs at low temperatures and pressures with the critical point being at 140°C, 0.01 mm. Hg, and a concentration of 0.3 H/Cb. A more recent study has refined this diagram and shows that the misicibility gap, shown in Figure 1, is confined between temperatures of 75°C

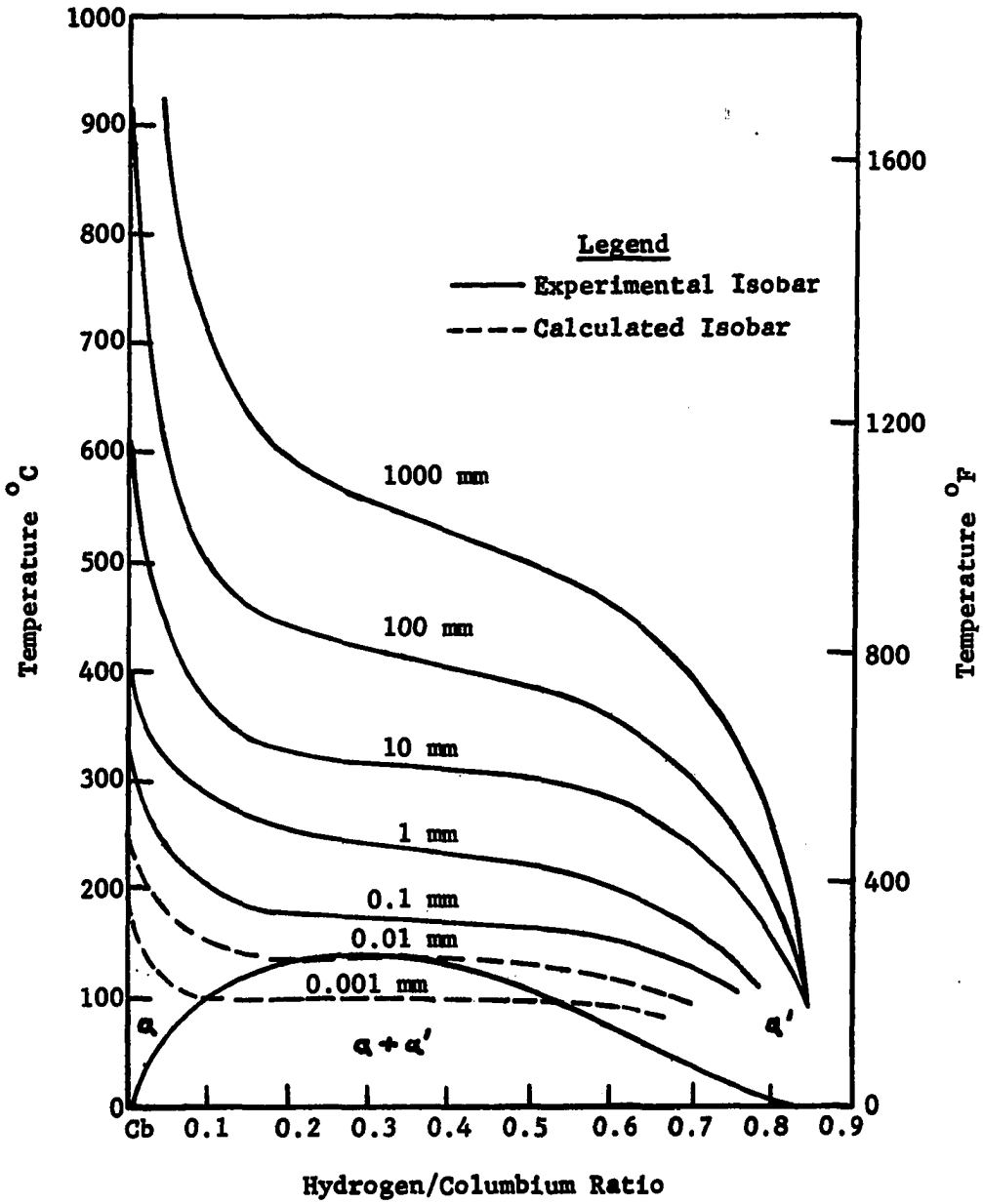

Figure 1. Phase diagram of the columbium-hydrogen system after Albrecht et al. (6,7).

and 140°C. Walter and Chandler (18) have shown that the α' phase decomposes in a eutectoid reaction to form the body centered cubic columbium rich α and a hydrogen rich orthorhombic hydride phase at about 75°C. The critical eutectoid composition is found to be at an H/Cb ratio of 0.585. There is also evidence of a peritectic reaction at higher hydrogen concentrations.

Kinetics of Cb-H Reactions

Information on the kinetics of hydrogen-columbium interactions is not very extensive. Gulbransen and Andrew (8) examined the kinetics of hydrogen-columbium reaction rates at temperatures ranging from 250°C to 900°C and at pressures up to 57 mm. Hg. Comparison of the experimental conditions with equilibrium data indicates that pressures were selected to give a hydrogen-columbium atomic ratio of about 0.6. No consistent reaction-rate law was followed. At 250°C the reaction was purported to increase with time; at 300°C, the reaction rate varied linearly with time; and, at 360°C, the reaction rate was found to decrease with time. At 700°C and 900°C, an initial parabolic rate law seemed to be established, indicating the possibility of a diffusion controlled reaction.

Paxton and Sheehan (9), utilizing a permeation technique in the range 300°C to 700°C, assumed a diffusion controlled reaction and found that the diffusivity of hydrogen in columbium could be expressed by:

$$D = 0.027 \exp \frac{-25,300}{RT} \qquad (1)$$

Albrecht et al. (7) investigated reaction rates at temperatures

ranging from 300°C to 700°C over compositions of 0.05, 0.10, 0.50, and 0.70 H/Nb. A closed system equilibrium technique was employed on cylindrical specimens. Up to 550°C initial sorption rates consistently varied linearly with time. After some time, determined by the conditions of the run, the reaction rates were observed to decrease with time and finally stop as equilibrium was established. In the temperature range 600°C - 700°C, initial sorption rates were found to be parabolic, and the reaction was treated as being diffusion controlled. It was determined that the diffusivity of hydrogen in columbium could be expressed by the relation:

$$D = 0.0215 \exp [(-9370 \pm 600)/RT] \qquad (2)$$

As can be readily seen, a number of discrepancies exist among various investigators. The inconsistencies in the low temperature data of Gulbransen and Andrew appear to be due to failure to allow the reactions to proceed to completion. Careful examination of the experimental results reveals that, at 360°C, the initial sorption rate is, in fact, approximately linear and the reaction rate begins to decrease only after a finite time. The increasing reaction rate at 250°C is incompatible with the fact that, under constant pressure, the composition of hydrogen in the columbium must eventually come to equilibrium with the surrounding gas. This latter discrepancy could be due to inaccuracies in the experimental technique of measuring weight gain as a function of time.

Comparison of the data of Paxton and Sheehan with that of Albrecht et al., reveals a striking discrepancy in the value of the activation energy for diffusion. Paxton and Sheehan obtained a value of 25,300 cal/mol., while that of Albrecht et al. was about 9300 cal/mol.

Furthermore, Paxton and Sheehan reported that the mathematical boundary conditions for a diffusion controlled reaction could be applied from 300°C to 700°C, while Albrecht found that only in the range 600°C to 700°C could the same analysis be applied. Albrecht presumed that some surface reaction altered the sorption rates at lower temperatures.

Paxton and Sheehan observed a discoloration of their specimens during hydrogenation, while Albrecht et al. reported that their specimens were consistently bright and void of any surface film. It is quite possible that a film formed on the surface of Paxton and Sheehan's specimens and retarded the sorption rate. It should also be pointed out that the solubilities of hydrogen in columbium below 600°C (1 atm.) reported by Paxton and Sheehan were in considerable disagreement with those of Albrecht et al. as well as other investigators. Examination of the activation energies for the diffusion of hydrogen in other metals (8700 cal/mol for Ni, 6800 cal/mol for Pd, and 9200 cal/mol for Fe) tend to support the reliability of Albrecht's kinetic data (19).

Assuming that Albrecht's values for the activation energy for diffusion in the range 600°C to 700°C are reasonably correct, there still remains the problem of sorption at lower temperatures. As was pointed out earlier, the initial rates at lower temperatures were linear rather than parabolic, and could not be fitted to a solution of Fick's second law for diffusion. These results suggest that the rate controlling step in the sorption process changes as the temperature is decreased. Evidence of this has been obtained by Webb (20) in a review of permeation experiments on the columbium-hydrogen system. A distinct change in the activation energy for permeation was noted at a temperature of about 500°C.

The possibility of a grain size sensitive sorption rate has been suggested, particularly at those temperatures where bulk diffusion may no longer be rate controlling. No systematic study of this has been made in columbium, however, a decrease in sorption rate with increasing grain size has been observed in the titanium-hydrogen system (21).

Fracture of Metals

Before examining the effects of hydrogen on the mechanical properties of metals, a brief review of the fracture characteristics of metals is in order. Based on the force necessary to shear atoms, the theoretical fracture strength of an ideal solid is about E/10 where E is Young's modulus (22). It is generally observed, however, that solids, and particularly metals, fracture at strengths one to three orders of magnitude less than their theoretical values (23).

One of the first attempts to explain this phenomena was the postulate of Griffith (24), that most materials contain tiny microcracks which provide stress concentrations on a localized basis sufficient to initiate fracture at applied stresses considerably below theoretical estimates. This analysis has led to the well-known Griffith formula:

$$\sigma = \left[\frac{2E\gamma}{\pi(1-\nu^2)C}\right]^{1/2} \qquad (3)$$

where σ is the stress sufficient to propagate a crack of length C, E is Young's modulus, and ν and γ are Poisson's ratio and the surface energy of the crack respectively.

Although the Griffith criterion seems to adequately explain the observed fracture strength of completely brittle materials such as

glass, it does not sufficiently explain some of the observed fracture phenomena in metals. In the first place, Stroh (25) has pointed out that to explain the observed fracture strength in many metals, cracks of several millimeters in length would have to be present. Furthermore, Cottrell (22) has pointed out that even the most brittle metals exhibit some plastic yielding prior to fracture. A most important consideration is the ductile-brittle transition from highly ductile to almost completely brittle fracture. None of the terms in Griffith's equation are particularly temperature dependent; thus the theory fails completely in this respect.

The inadequacies of the Griffith theory to explain the brittle fracture of metals have led to hypotheses that dislocations play an active role in this process. It has been proposed that fracture is initiated by the coalescence of dislocations to form microcracks which subsequently lead to fracture. The coalescence is considered to be the result of dislocation pile-ups at obstacles such as grain boundaries (25) or intersecting slip systems (22). In both cases the criteria in determining the mode of fracture is the relationship between the stress required to cause a microcrack to propagate and the tendency for the metal to yield at the crack vertex. If the "growth" stress of the crack, which depends on crack length and surface energy, is less than the yield stress of the metal at the crack vertex, the crack will propagate and brittle fracture will occur. Conversely, if the yield stress is lower than that required for crack propagation, the metal will yield in a ductile fashion, relieving any stress concentrations at crack tips, and thereby exhibit ductile behavior.

Effect of Hydrogen on Fracture of Metals

A profusion of data exists on the effects of hydrogen on the fracture characteristics of metals, with the greatest concentration placed in the area of the hydrogen embrittlement of ferrous alloys. A brief review of the effects of hydrogen in ferrous alloys is in order here, since much of the information regarding the effects of hydrogen on metal fractures in general has been derived from studies based upon phenomena observed in iron and steel.

A review of this topic by Tetelman (26) gives several conclusions which can be drawn from data on ferrous materials. First of all, it has been established that hydrogen existing in lattice sites is not responsible for the observed embrittlement in iron and steels. The room temperature interstitial solubility of hydrogen in iron at one atmosphere pressure is on the order of 5×10^{-4} ppm., yet the degree of embrittlement increases with increasing hydrogen concentrations up to 5 ppm. (27).

Secondly, there has been no conclusive verification that hydrogen locks dislocations. Diffusion studies by Hill (28) on deformed iron have indicated that hydrogen is not associated with defects such as vacancies or dislocations. This has been substantiated by Siede and Rostoker (29) and by Tetelman and Robertson (30) who have found that neither the yield strength of polycrystalline iron nor the critical resolved shear stress of single crystals is affected by the presence of hydrogen.

Thirdly, hydrogen can produce cracking in iron in the absence of an applied stress as well as in conjunction with it. Studies by Maringer *et al.* (31) have shown that iron charged electrolytically with

hydrogen contains severe structural damage resulting from the charging treatment alone.

Finally, it has been found that hydrogen must have mobility to cause embrittlement in ferrous alloys. Studies by Brown and Baldwin (32) have shown that the degree of embrittlement is quite sensitive to strain rate as well as temperature. High strain rates at normal temperatures tend to reduce the degree of embrittlement.

Theories of Hydrogen Embrittlement

A number of theories have been advanced to explain the embrittlement of ferrous alloys by hydrogen. An original treatment by Zapffe (33) proposed that molecular hydrogen precipitates into "internal voids" in the lattice causing sufficient pressure to initiate premature fracture. The strain rate and temperature dependence of the embrittlement phenomena were explained by pointing out that during straining, the voids expand causing a drop in hydrogen pressure; sufficient hydrogen must then diffuse from the surrounding lattice to maintain a damaging pressure. Fulfillment of this condition depends upon the rate of expansion of the voids and the temperature of straining.

Petch (34) has proposed that hydrogen is adsorbed on the surfaces of microcracks formed by the Stroh mechanism. It is pointed out that this adsorption lowers the surface energy of the crack so that it may propagate by the Griffith criterion. Once again continued crack propagation requires the diffusion of hydrogen during straining.

Theories postulated by De Kaxinczy (35) and Bastien (36) are essentially refinements of Zapffe's theory. In one case, the embrittlement mechanism depends upon the precipitation of molecular hydrogen in

a Griffith type crack (35). As the crack propagates the gas expands, releasing energy to the lattice, and thereby causing a lowering of the fracture stress. For this mechanism to operate during crack propagation, hydrogen diffusion to the microcracks is required. Bastien (36) considered hydrogen to be dissolved as protons in areas of lattice irregularities such as vacancies and dislocations. It was proposed that during straining the ionized hydrogen is carried along with glissile defects producing localized supersaturations. This in turn would induce precipitation of molecular hydrogen at high pressures resulting in embrittling stresses.

As can be seen, all of the above mechanisms rely on the segregation of molecular hydrogen to some sort of internal defect, be it a microcrack, void, or groups of vacancies or dislocations. All of the suggested processes require diffusion of hydrogen during straining, thus explaining the temperature and strain rate dependence of embrittlement. Garofalo et al. (37) have put forth rigorous calculations of these ideas showing that as little as 2 ppm. of hydrogen is sufficient to cause embrittlement.

The above considerations suggest that a prestrain and aging treatment should result in an immediate decrease in ductility as a function of aging time. However, Morlet et al. (38) have found that prestrain and aging of hydrogenated steels results in an initial increase in ductility. This phenomena has been explained by proposing that the embrittlement process is due to a segregation of hydrogen to highly stressed regions surrounding a void, rather than being due to hydrogen within the void itself. It is further proposed that the

concentration of hydrogen in the regions of maximum stress undergoes a reversal during the aging process. Initially hydrogen diffuses from the stressed regions to the void, thus decreasing the concentration and initially increasing the ductility. At longer aging times the stressed region is replenished with hydrogen from the surrounding lattice resulting in a loss of ductility.

With regard to the hypothesis of Morlet et al., Tetelman (26) points out that the theory does not explain how the Griffith criterion is satisfied; nor does it explain exactly how the hydrogen acts to embrittle. Tetelman has thus refined some of the earlier theories and proposed that hydrogen plays its most important role in the formation of a crack by means of a pressure buildup of molecular hydrogen at favorable points in the lattice. In considering single crystals it is suggested, moreover, that only a negligible amount of hydrogen can diffuse to a crack while it is moving; however, if a sufficiently large and constant stress is applied the Griffith criterion can always be satisfied and completely brittle fracture can occur. In the case of polycrystals, it is pointed out that completely brittle fractures are rarely observed, i.e., some reduction in area, usually on the order of 15 per cent is generally observed. Tetelman thus proposes that a propagating crack can be stopped by a barrier such as a grain boundary, and hydrogen diffusion sufficient to rebuild an internal pressure or an increase in external stress will be necessary to restart the propagation. If, in localized instances, the combined effects of pressure and stress are not sufficient to restart propagation, some ductility will be observed.

Troiano (39) has suggested a rather revolutionary mechanism.

Expanding the hypothesis of Morlet et al., it is pointed out that the cohesive strength of the transition metals is determined by the repulsive forces of the atoms in overlapping "d" bands of the electron cloud. It is therefore suggested that hydrogen produces an increase in electron concentration in these unfilled bands. Thus, an increase in repulsive forces is established, with a subsequent lowering of the cohesive strength.

Effect of Hydrogen on Fracture Characteristics of Group V-A Metals

Information on the effect of hydrogen on the fracture characteristics of the Group V-A metals is considerably less extensive than that available for ferrous alloys. However, enough data is available to draw some comparisons between the two groups of metals.

Roberts and Rogers (40) have found that vanadium can be embrittled by hydrogen. It was further demonstrated that fracture undergoes a ductile-brittle-ductile transition as the temperature is lowered from 150°C to -196°C, i.e., there is a ductility minimum observed at a certain temperature. The ductility is increased by either raising or lowering the temperature from this point. A more complete study by Eustice and Carlson (41) on vanadium containing 10-800 ppm. placed the ductility minimum at about -100°C with variations reportedly due to hydrogen content and strain rate. Van Fossen (42), however, did not find a ductility minimum in material containing 6 ppm. H, although embrittlement was observed. A minimum has also been found in tantalum at 7 ppm. H (43) and 140 ppm. H (11). At hydrogen concentrations above 270 ppm., the ductility return at low temperatures was considerably less (11). In the case of columbium some disagreement exists in the literature. Eustice and Carlson (12), Wilcox, et al., (13), and Imgram et al. (11),

failed to find a ductility minimum although a ductile-brittle transition was observed. Hydrogen concentrations in these investigations were 20 ppm. (12), 1-30 ppm. (13), and 200-390 ppm. (11). However, Wood and Daniels (14) observed a rather pronounced ductility minimum at hydrogen contents ranging from 19-252 ppm.

The effects of strain rate on the hydrogen embrittlement of Group V-A metals are less clear than the effects of temperature. Eustice and Carlson (41) observed an increase in the ductility minimum of about 10-20°C with an increase in strain rate by a factor of 60 on vanadium containing 10 ppm. hydrogen. Van Fossen (42) reported an increase in the ductility of vanadium containing 6 ppm. hydrogen at -125°C with an increase in strain rate by a factor of 100. In the columbium-hydrogen system, Wilcox et al. (13) show an increase in ductility with increasing strain rate at temperatures less than -150°C. Wood and Daniels (14), however, found little if any strain rate effect, irrespective of hydrogen concentration.

In comparing these results, careful attention must be paid not only to the presence of hydrogen, but to that of other interstitials as well. The vanadium used by Van Fossen contained considerably higher quantities of oxygen, nitrogen, and carbon than that used by Eustice and Carlson. This in all probability explains why Van Fossen failed to note a ductility return at low temperatures. It should also be pointed out that in most cases the ductility of Van Fossen's material was considerably less than that of Eustice and Carlson irrespective of test conditions.

With regard to columbium-hydrogen alloys, similar conclusions

can be drawn. Wilcox, et al. utilized columbium with substantially higher concentrations of interstitial impurities than that of Wood and Daniels; while the columbium used by Imgram et al., was of a commercial grade of fairly low purity. Eustice and Carlson hydrogenated finished tensile specimens rather than machining them following hydrogenation which may have been a source of surface contamination in the gauge section. As in the case of vanadium, excess impurities seem to be the reason why a ductility return may not be noted.

Attempts have been made to relate the effects of strain rate on the hydrogen embrittlement of refractory metals to the slow strain embrittlement phenomena observed in steels. The results reported by Van Fossen and Eustice and Carlson on vanadium tend to support this concept. However, the effects are small, and may well be within the range of experimental error. The strain rate effect reported by Wilcox et al. in columbium was found in as-received material containing only 1 ppm. hydrogen. Thus the effect may have been due to the presence of other interstitial impurities. As was mentioned earlier, Wood and Daniels found no strain rate effect in hydrogen columbium alloys.

Theoretical Considerations

A comparison of the Group V-A metals with ferrous alloys yields the similarity of a temperature dependent embrittlement process. However, this effect, along with the effect of strain rate, requires more investigation. From a theoretical standpoint, those theories of hydrogen embrittlement involving the precipitation of diatomic hydrogen do not seem to be applicable to the case of columbium and other exothermic occluders. As discussed earlier, such theories propose that extensive

crack formation and propagation occurs by the precipitation of diatomic hydrogen at internal voids and microcracks. However, photomicrographs of hydrogenated niobium do not show any evidence of damage introduced by the sorption and precipitation of diatomic hydrogen; rather, at high hydrogen concentrations, a hydride is precipitated (6, 7).

There is the possibility of the formation of microcracks, as is proposed by Stroh, through some sort of dislocation coalescence or pile-up. To investigate the possibility of microcracks formed by such a mechanism and, since pile-ups are usually associated with locked dislocations, it is necessary to investigate more completely the yield behavior of bcc metals. Such a consideration may also give some indication as to whether or not hydrogen along with other interstitial impurities may be effective in the formation of microcracks through dislocation locking.

Bcc metals often exhibit discontinuous yielding; i.e., during straining Hooke's law is followed to a certain stress level (upper yield stress) whereupon a sharp drop in stress occurs (lower yield stress) before the onset of work hardening. Furthermore, in polycrystalline materials serrations in an otherwise smooth stress-strain curve are often observed at the lower yield stress.

Considering polycrystalline materials, Cottrell (22) has proposed a model for yielding in bcc metals. According to this model, the upper yield point is due to the release of an avalanche of dislocations in a few grains from sources pinned by interstitial solute atom atmospheres. This avalanche will create pile-ups of dislocations in the yielded grains, giving rise to high stresses which in turn activate locked dislocation sources in adjacent unyielded grains. This grain to

grain yielding is proposed to be responsible for the lower yield stress.

It has been established that several parameters, σ, such as the upper and lower yield stress may be related to the grain diameter, 2d, according to the relation (44):

$$\sigma = C_1 + C_2 d^{-1/2} \tag{4}$$

Usually the lower yield stress is fitted to Equation (4) since the upper yield stress is extremely sensitive to specimen alignment during testing, surface preparation, etc. (45). This leads to the well known Petch equation (23):

$$\sigma_{lys} = \sigma_i + K_y d^{-1/2} \tag{5}$$

where σ_i is called a friction stress and is usually considered to be the sum of two parts: $\sigma_{i(st)}$ which is structure sensitive and temperature independent, and σ_i^* which depends on temperature and strain rate and is thought to be due to the Pierls-Nabarro force. K_y is considered to be a measure of dislocation locking and is defined by:

$$K_y = \sigma_d l^{1/2} \tag{6}$$

where σ_d is the stress required to unpin a dislocation from its solute atom atmosphere and (l) is the average distance from a dislocation source to the nearest pile-up. Thus K_y reflects the tendency for dislocation locking and, in turn, the probability of dislocation pile-ups.

Wilcox and Huggins (46) through strain aging studies and Petch analyses of the lower yield stress as a function of hydrogen content purported to show that hydrogen is responsible for strain aging in columbium, and that hydrogen could effectively lock dislocations. However,

it has been demonstrated by Adams et al. (47), and Johnson (48) that interstitial concentrations on the order of a few hundred ppm. do not give sufficiently large values of the locking coefficient in the Petch equation to indicate pile-ups of dislocations in columbium. Furthermore, Tankins and Maddin (49) attributed strain aging effects in columbium of similar overall purity to oxygen. Of more importance, however, is that a considerable amount of evidence has been compiled indicating that the temperature dependence of the yield stress is in fact related to the Pierls-Nabarro stress (σ_i^* in Equation (5)) rather than to impurity locking ($\sigma_{i(st)}$) (50, 51, 52, 53). The effects reported by Wilcox and Huggins are actually quite small, and appear to be within the range of experimental error when compared to the results of the other investigations cited above. Also, no strengthening effects due to hydrogen were reported as might be expected if hydrogen could efficiently lock dislocations.

It is important to note in this respect that dislocation pile-ups have never been observed in any bcc metals (54). In particular, Van Torne and Thomas (55) failed to note any pile-ups in columbium through transmission electron microscopy.

Since there is no likelihood of a pressure buildup of molecular hydrogen in columbium, and little evidence of dislocation pile-ups or hydrogen locking of dislocations, microcracks must initiate in some other fashion. Wood and Daniels (14) have put forth the possibility of a hydride precipitation. Work by Longson (56) has shown that hydrogen embrittlement of columbium parallels the bulk solubility limit; i.e., as the solubility increases, for instance with temperature, the amount of

hydrogen necessary to cause embrittlement also increases.

Although a hydride precipitation appears attractive as a means of nucleating microcracks in columbium, what require more intensive study are the low temperature anomalies which have been observed, i.e., the ductile-brittle-ductile transition. Also, the hydrogen concentrations where embrittlement occurs are often below the bulk solubility limits determined by Albrecht et al. (6, 7) and Walter and Chandler (18). This has led to the supposition that hydrogen can effectively embrittle columbium while still in solid solution (56).

As can be seen, the major unsolved problem is that of crack nucleation. Once microcracks are formed, the ideas of Petch (34) or Troiano (39) may very well explain their rapid propagation. An important point to be noted here is that the causes of brittle fracture per se have not been firmly established, to say nothing of the effects of impurities such as hydrogen. The more recent theories of brittle fracture have not as yet been verified to any substantial degree; in fact, many of the discrepencies outlined above in terms of hydrogen embrittlement could be applied to brittle fracture in the more general sense. As a result, it is still uncertain as to whether hydrogen simply enhances an inherent brittle fracture characteristic, or acts to initiate embrittlement independently of other causes.

CHAPTER II

EXPERIMENTAL PROCEDURE

Material Preparation

Two separate heats of columbium were used in this investigation. Material of reasonably high purity (hereafter called Heat I) was obtained from the Du Pont Company for kinetic studies. Ultra-high purity columbium (hereafter called Heat II) obtained from the Wah Chang Corporation, was used for the mechanical properties experiments. Chemical analyses of the two heats are given in Table 1.

TABLE 1

HEAT I COLUMBIUM

(DU PONT HEAT D-1190)

Element	Content in ppm. by Weight
Oxygen	206
Nitrogen	50 or less
Carbon	50
Iron	122
Nickel	75
Chromium	10 or less
Copper	10 or less

TABLE 1--Continued

HEAT II COLUMBIUM

(WAH CHANGE HEAT NO. 10-30987)

Analysis in ppm. by Weight

Element	Top	Bottom	Element	Top	Bottom
Al	<20	<20	Mo	<20	<20
B	<1	<1	N	50	40
C	40	50	Ni	<20	<20
Cd	<5	<5	O	80	90
Co	<10	<10	Pb	<20	<20
Cr	<20	<20			
Cu	<40	<40	Si	<50	<50
Fe	<50	<50	Sn	<10	<10
H	3.1	3.3	Ta	740	<500
Hf	<80	<80	Ti	<40	<40
Mg	<20	<20	V	<20	<20
Mn	<20	<20	W	195	85
			Zr	400	<100

Both heats were received in the cold worked condition in the form of 0.375 inch (Heat I) and 0.500 inch (Heat II) diameter rods. The 0.500 inch material was further reduced to a diameter of 0.350 inches by rotary swaging.

The Heat I material was cut into solid cylinders 0.75 ± 0.005 inches long. The cylinders were recrystallized by heating in a vacuum furnace to obtain several grain diameters as listed in Table 2.

TABLE 2

RECRYSTALLIZATION OF PURE Cb

Recrystallization Temperature	Avg. Grain Diameter
1200°C	110 microns
1500°C	350 microns
1850°C	550 microns

The Heat II material was cut into cylinders 1.50 $\pm$ 0.005 inches long. A portion of these specimens were given a stress relief anneal at 750°C to remove the effects of cold work for the purpose of investigating the effects of hydrogen on wrought columbium. The balance of the material was recrystallized at 1200°C and 1850°C to give both a fine and a coarse grain size.

All of the recrystallization treatments were carried out in a high temperature vacuum furnace (2400°C, 10^{-5} torr capacity) with the exception of the stress relief anneal. This was done under a vacuum of 10^{-6} torr in the alloy preparation apparatus to be described.

Extreme care was taken to prevent contamination of the material during heat treatment. No evidence of surface scaling was observed.

Cb-H Alloy Preparations

A closed-system equilibrium technique was used to prepare the Cb-H alloys. The apparatus employed was essentially a modification of that described by Wood (57). A block diagram is shown in Figure 2.

Basically the system consisted of a quartz reaction tube, two large calibrated reservoirs into which purified hydrogen was admitted prior to the reaction, a Pd-25 per cent Ag permeation leak for the purification of the hydrogen, an oil manometer, and appropriate valving and vacuum pumping apparatus. The reaction tube was enclosed by a Burrell glo-bar type furnace. Temperature control was maintained by a West stepless saturable reactor controller, and temperatures inside the reaction tube were measured by two chromel-alumel thermocouples connected through a glass-metal seal to an external potentiometer. Vacuum levels were measured by means of a Phillips Type PHG-010 gauge.

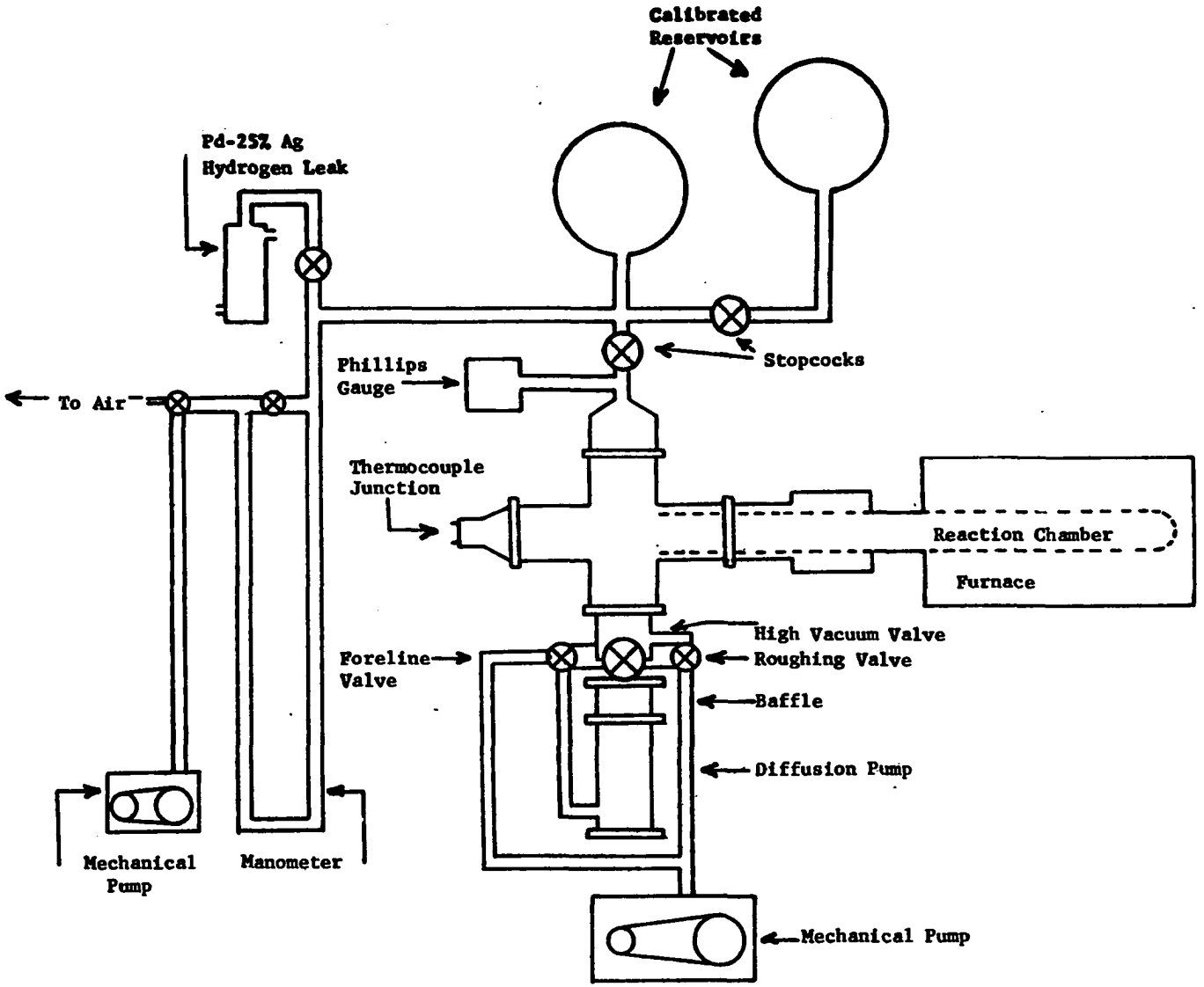

Figure 2. Schematic diagram of the hydrogenation system.

The system had a vacuum capability of 5×10^{-7} torr. Temperatures within the reaction tube could be controlled to within $\pm 2^{\circ}C$. The purification leak was capable of reducing the impurities in commercial tank hydrogen to a few parts in 10^{10}.

The hydrogenation procedure consisted of admitting to one or both of the reservoirs a quantity of hydrogen, determined by the temperature and the concentration of hydrogen in the columbium. The pressure of hydrogen in the reservoirs was measured on the oil manometer. Once this pressure reached its predetermined level, the reaction tube was blanked off from the pumping system and the hydrogen was admitted to the tube. The manometer now served to measure the pressure over the columbium, and the pressure drop as hydrogen was sorbed was recorded as a function of time until equilibrium was established.

Appendix I gives a detailed discussion of the calibration of the hydrogenation system. Appropriate formulae for the determination of hydrogen concentrations in the columbium under various conditions of temperature and pressure are also included.

Kinetic Studies

Sorption rates were measured on individual samples prepared from Heat I. Prior to insertion into the reaction tube, the specimens were etched in an HF, HNO_3, H_2O solution and weighed. Once the samples had been etched, they were handled remotely to prevent any surface contamination. It was presumed that the etching treatment would, in addition to revealing the grain structure, present an undisturbed surface for sorption. This method of surface preparation for sorption samples was later abandoned in favor of a treatment consisting of abrading the

surface lightly and then washing the sample in methanol. It is believed that the etching treatment produced a surface film which retarded sorption of hydrogen.

Once a given specimen was placed in the reaction tube, the system was pumped to a vacuum of at least 5×10^{-6} torr prior to heating the furnace. Each specimen was allowed to "soak" at its respective hydrogenation temperature under vacuum for several hours just prior to introduction of the measured quantity of hydrogen into the system.

Sorption rates were studied at temperatures ranging from 550° to 750°C. Hydrogen concentrations obtained were in the range of 160-220 ppm. by weight. Once hydrogen had been admitted to the reaction chamber, pressure readings were taken at convenient intervals, depending on the speed of the run, until equilibrium was established. Initial data were taken in the form of a pressure vs. time plot.

At no time was any contamination noted which has been evidenced by the presence of a black surface film (9). The specimens were clean and bright following hydrogenation.

Mechanical Properties Studies

The 1.5 inch cylinderical blanks prepared from Heat II were hydrogenated in groups of six to concentrations from 20 to 200 ppm. Hydrogenation treatments were carried out at temperatures ranging from 460°C to 650°C depending upon the final concentration desired. The specimens were etched and weighed prior to hydrogenation as described above.

The hydrogenation procedure was basically the same as that described for the kinetic studies with the exception that the soaking period prior to hydrogenation was deleted. In addition, the specimens

were allowed to remain at equilibrium with the hydrogen gas for several hours to insure as homogeneous a distribution of hydrogen as possible within the columbium. The specimens were then rapidly cooled to room temperature by rolling the furnace back from the reaction chamber. Once again no evidence of surface contamination was observed.

Upon removal from the alloy preparation apparatus, the samples were machined into button-head tensile specimens. Care was taken to prevent any pitting or notching of the specimens during machining. Original diameters and gauge lengths of the tensile specimens were determined using an optical comparator. Nominal gauge diameter was 0.150 inches, and nominal gauge length was 0.75 inches.

Tensile tests were performed on a floor model Instron testing machine equipped with a continuous strip chart recorder. Testing temperatures employed were $77^{\circ}K$, $191^{\circ}K$, $300^{\circ}K$; crosshead speeds varied from 0.02 in./min. to 2.0 in./min. Tests carried out below room temperature utilized an insulated container which surrounded the specimen with a cooling bath. A mixture of solid CO_2 and acetone was used to obtain a temperature of $191^{\circ}K$, and liquid nitrogen was used to obtain $77^{\circ}K$. Split friction type grips were used to support the tensile samples during testing.

CHAPTER III

DATA AND RESULTS

Equilibria in the Columbium-Hydrogen System

Table 3 gives the values of equilibrium pressures and corresponding compositions at various temperatures obtained from kinetics studies specimens. The data are in good agreement with earlier investigations. As can be seen from the data, there was no apparent sensitivity of composition to variations in surface condition or grain size; however, at 550°C, equilibrium was not established in the etched material.

Effects of Temperature on Sorption Rate

As was mentioned earlier, the initial kinetic data took the form of a plot of hydrogen pressure vs. time; a sample curve for an etched specimen is given in Figure 3. A comparison of several of these plots showed that, at sorption temperatures of 600°C and higher, initial sorption rates were very nearly parabolic with time. Many of the specimens, however, showed an "incubation time" before parabolic behavior was attained.

In an attempt to evaluate the kinetics of the sorption of hydrogen by columbium, the parabolic pressure-time data were fitted to an analysis which assumes that the sorption process is diffusion controlled. Wilson (58) has developed a time dependent solution to Fick's second

TABLE 3

EQUILIBRIA IN THE Cb-H SYSTEM

Spec. No.	Grain Size μ	H_2 Temp. ^{o}C	P_b^1 mm. Octoil	P_i^2 mm. Octoil	P_i^3 mm. Octoil	H/Cb Atomic ratio
U-9	110	750	1000.0	604.0	580.0	0.012
V-8	350	750	1000.0	603.5	579.0	0.012
W-4	550	750	1000.0	604.0	581.0	0.011
U-8	110	700	1000.0	602.0	573.5	0.014
V-7	350	700	1000.0	602.0	572.0	0.016
W-7	550	700	1000.0	602.0	574.0	0.015
U-1	110	650	963.0	576.5	538.0	0.021
U-4	110	650	965.5	577.0	540.0	0.020
V-2	350	650	961.0	575.5	537.0	0.021
V-6	350	650	959.5	576.0	540.0	0.021
W-1	550	650	962.0	576.0	538.5	0.021
W-6	550	650	959.0	576.5	540.0	0.020
U-2	110	600	565.5	338.0	301.5	0.023
U-7	110	600	566.0	340.0	310.0	0.018
V-1	350	600	565.5	338.0	303.0	0.022
V-4	350	600	564.0	338.0	306.5	0.020
W-2	550	600	566.0	338.0	300.5	0.022
W-5	550	600	565.0	339.0	310.0	0.018
U-3	110	550	312.0	185.0	157.5	*
U-6	110	550	311.5	185.0	159.5	*
V-3	350	550	311.5	185.0	167.5	*
V-5	350	550	310.0	185.0	162.0	*
W-3	550	550	312.0	185.0	169.5	*

TABLE 3--Continued

Spec. No.	Grain Size μ	H_2 Temp. °C	P_b[1] mm. Octoil	P_i[2] mm. Octoil	P_f[3] mm. Octoil	H/Cb Atomic ratio
U-8-a[4]	110	700	1000.0	597.0	574.5	0.0140
W-7-a	550	700	1000.0	598.0	576.5	0.0140
U-4-a	110	650	966.5	573.0	544.5	0.0180
W-6-a	550	650	960.5	570.0	543.0	0.0220
U-2-a	110	600	566.0	338.5	305.0	0.0200
W-5-a	550	600	565.5	338.0	305.5	0.0210
U-3-a	110	550	311.0	185.0	153.0	0.0180
W-3-a	550	550	311.0	185.0	152.0	0.0180

[1]Reservoir pressure.

[2]System pressure immediately after admitting hydrogen to reaction chamber.

[3]Final pressure obtained.

[4]Subscript (a) denotes abrasion, dehydrogenation, and resorption.

*Equilibrium not established.

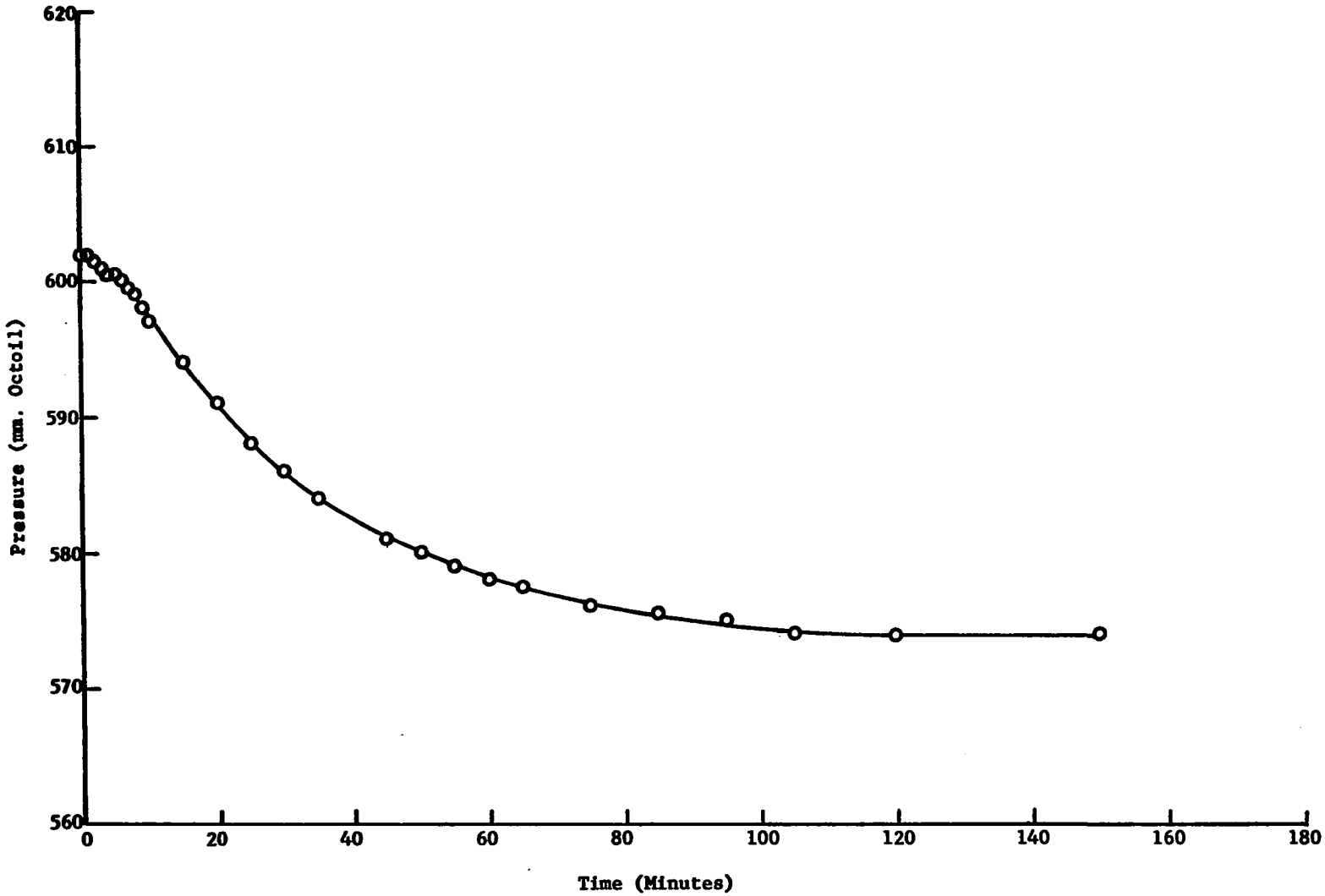

Figure 3. Sorption curve for etched columbium. Grain Size: 550 μ
Hydrogenation Temperature: 700°C

law of diffusion under conditions where the amount of diffusing substance is finite; i.e., for diffusion from a stirred solution of limited volume. For radial diffusion in a right circular cylinder the solution is

$$\frac{C}{C_0} = 1 - \sum_n \frac{4\alpha(1+\alpha)}{4 + 4\alpha + \alpha^2 q_n^2} e^{-\frac{Dt}{a^2} q_n^2} \qquad (7)$$

where q_n is a positive non-zero root of $q_n J_0(q_n) + 2J_1(q_n) = 0$, C is the concentration at time t, C_0 is the equilibrium concentrations, D is the diffusivity, (a) is the radius of the cylinder, and α is a constant dependent upon the percentage of the diffusing substance taken up by the specimen. A derivation of this equation appears in Appendix III.

Equation (7) may be graphed in the form of C/C_0 vs. $(Dt/a^2)^{1/2}$ for various values of α. For small percentages of uptake, as was the case in these experiments, such a theoretical plot appears as is shown in Figure 4. Thus experimental values of C/C_0, as determined from pressure-time data, should yield a straight line when plotted versus $t^{1/2}$ for the first 40-50 per cent of the sorption run. The experimental plot can be subsequently fitted to the theoretical curve by an appropriate selection of a value of D.

An example experimental plot is given in Figure 5; a complete tabulation of the D values obtained from the experimental plots is given in Table 4. All of the curves for etched columbium, obtained at 600°C and higher showed a linear portion; however, a rather pronounced sigmoid "tail" was evident at the beginning of each run. The time required to reach the linear portions of the curves varied from 10^2 to 10^3 seconds depending on the temperature of the run.

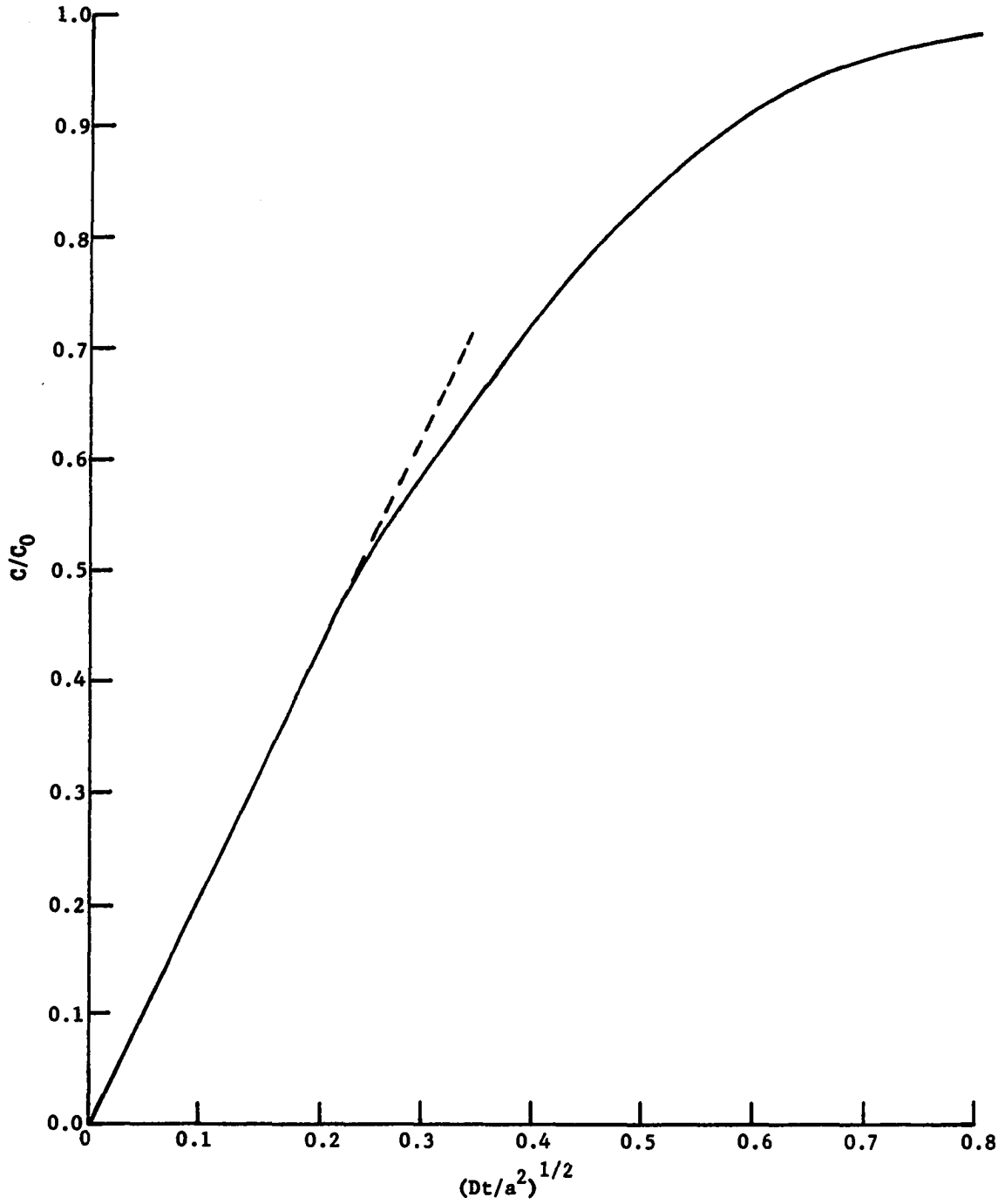

Figure 4. Theoretical plot of the solution of Fick's second law of diffusion for a cylinder immersed in a substance of finite volume.

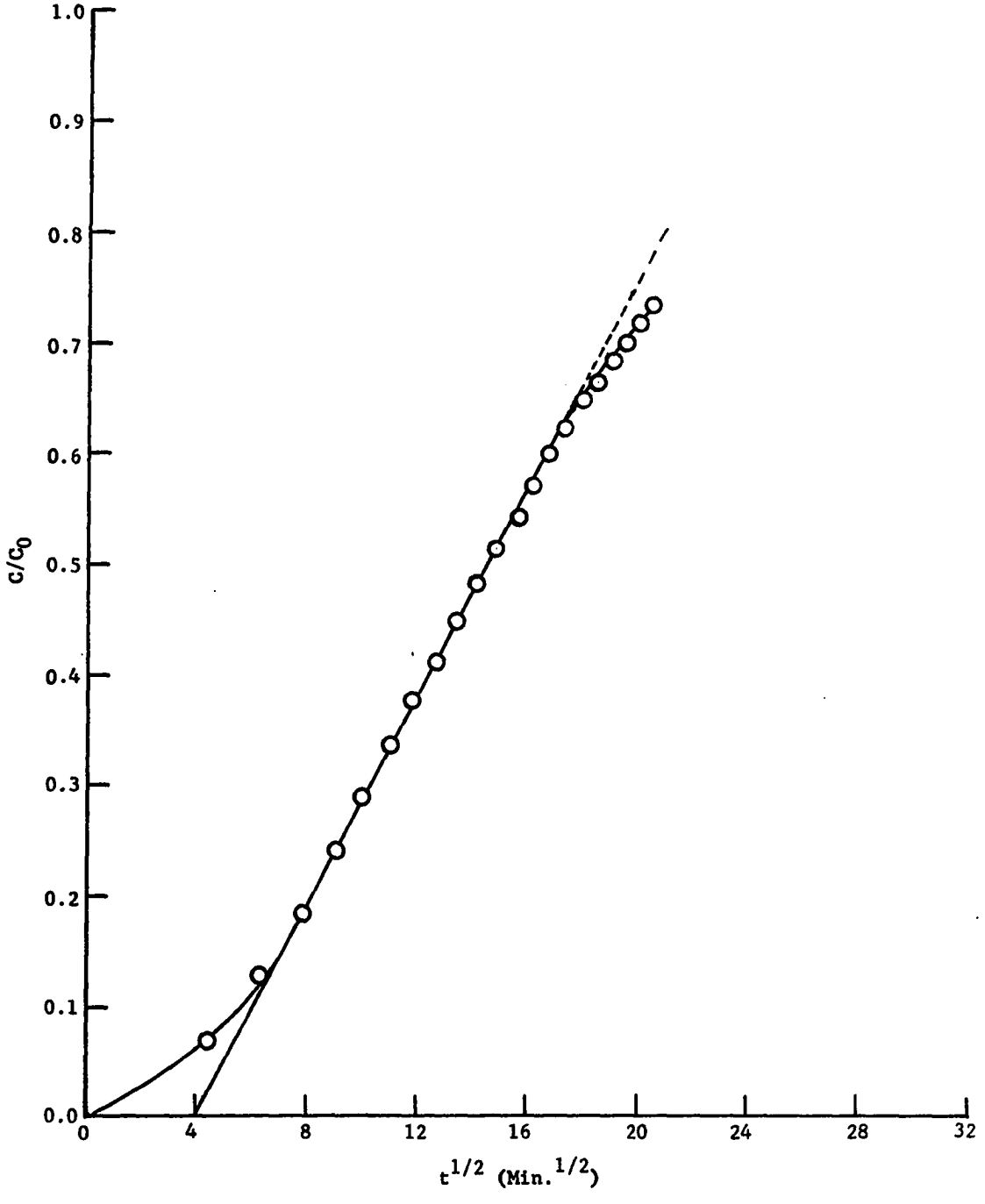

Figure 5. C/C_0 vs. $t^{1/2}$ for etched columbium. Grain Size: 110 μ
Hydrogenation Temperature: 600°C

TABLE 4

DIFFUSIVITIES IN THE Cb-H SYSTEM

Spec. No.	Grain Size, μ	H_2 Temp. ^oC	D $cm^2/Sec.$ x 10^5
U-9	110	750	7.330
V-8	350	750	6.340
W-4	550	750	10.000
U-8	110	700	4.160
V-7	350	700	1.840
W-7	550	700	2.720
U-1	110	650	0.795
U-4	110	650	2.210
V-2	350	650	1.360
V-6	350	650	0.665
W-1	550	650	1.450
W-6	550	650	2.080
U-2	110	600	0.204
U-7	110	600	0.285
V-1	350	600	0.190
V-4	350	600	0.132
W-2	550	600	0.399
W-5	550	600	0.196
U-8-a*	110	700	16.600
W-7-a	550	700	15.600
U-4-a	110	650	13.600
W-6-a	550	650	12.000
U-2-a	110	600	9.050
W-5-a	550	600	9.000

* Subscript (a) denotes abrasion, dehydrogenation, and resorption

If the reaction is truly diffusion controlled, the D values determined from the linear portions of the C/C_0 curves should give a linear curve if their logarithms are plotted against the reciprocal of the absolute temperature; i.e., diffusion data should fit an expression of the form:

$$D = D_0 e^{-Q/RT} \qquad (8)$$

where Q is the activation energy for diffusion. Such a curve, fitted

to the data by the method of least squares is shown in Figure 6. The activation energy obtained from the slope is about 40,000 cal/mol which is considerably higher than that reported for diffusion in most metals as was discussed in Chapter I. In particular, it is much higher than that obtained by Albrecht et al. (7) for the columbium-hydrogen system. *Thus the question is raised as to whether some surface step inhibits* the sorption rate of samples with chemically etched surfaces. This becomes a distinct probability in that the sigmoid shape of the C/C_0 curves has been shown by Crank (59) to be applicable to situations where the surface concentration of the diffusing substance does not reach saturation instantaneously. It thus appears possible that etching columbium in some way contaminates the surface so as to retard the sorption of hydrogen.

In order to investigate this latter point more completely, a series of these specimens were lightly abraded with a 240 grit silicon carbide paper to remove effects of chemical etching. Following a thorough cleaning, they were dehydrogenated and resorbed at their original hydrogenation temperature. A typical sorption curve for an abraded sample is illustrated in Figure 7. It can be seen that the sorption rate has increased considerably over the same specimen in the etched condition (see Figure 3). A similar increase in sorption rate was exhibited by all samples which were abraded. Also the "incubation" times exhibited during sorption by the etched specimens were no longer present. As discussed above initial reaction rates at temperatures of 600°C and higher were parabolic with time.

A fit of the parabolic data to Wilson's solution of the

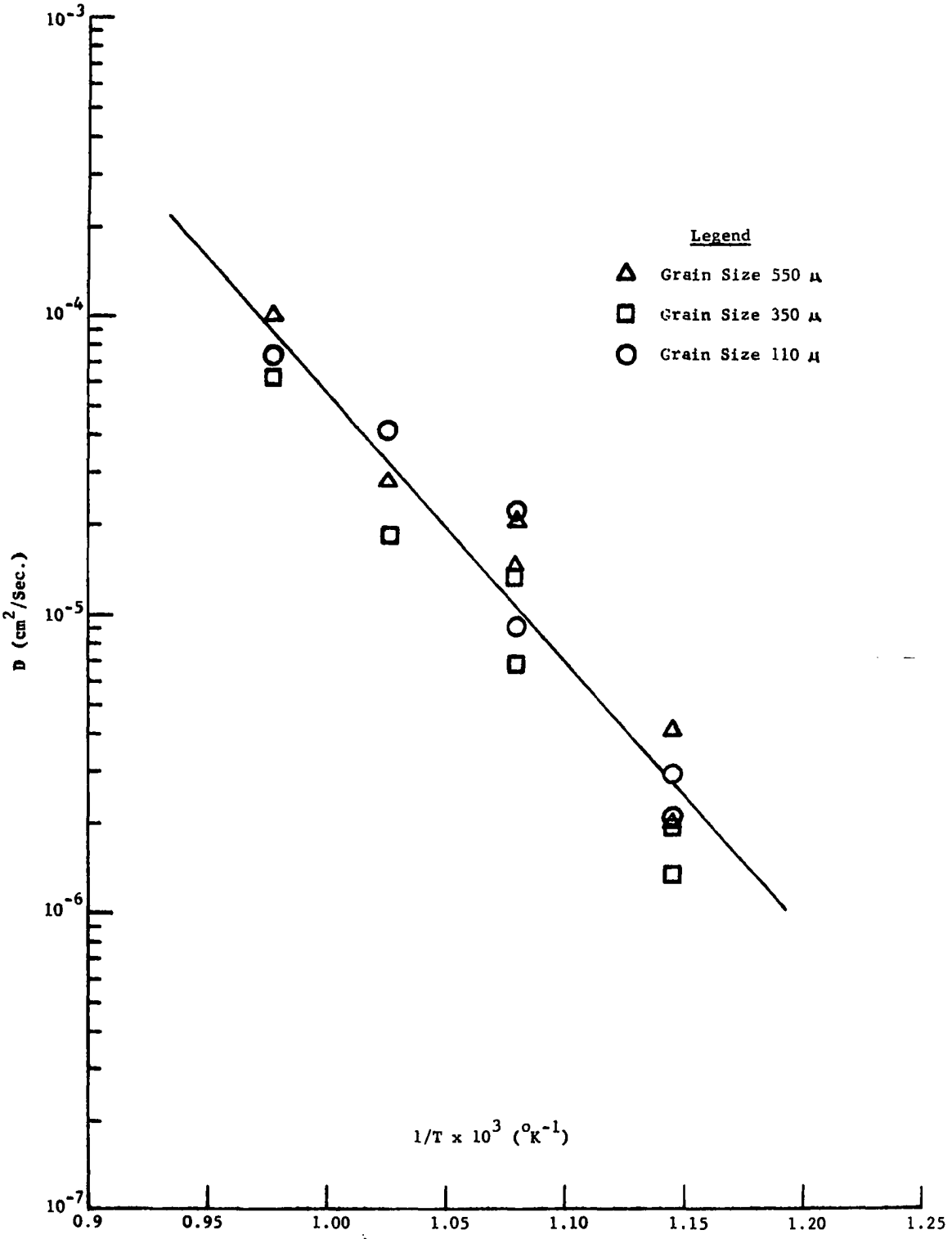

Figure 6. Ln D vs. 1/T for etched columbium.

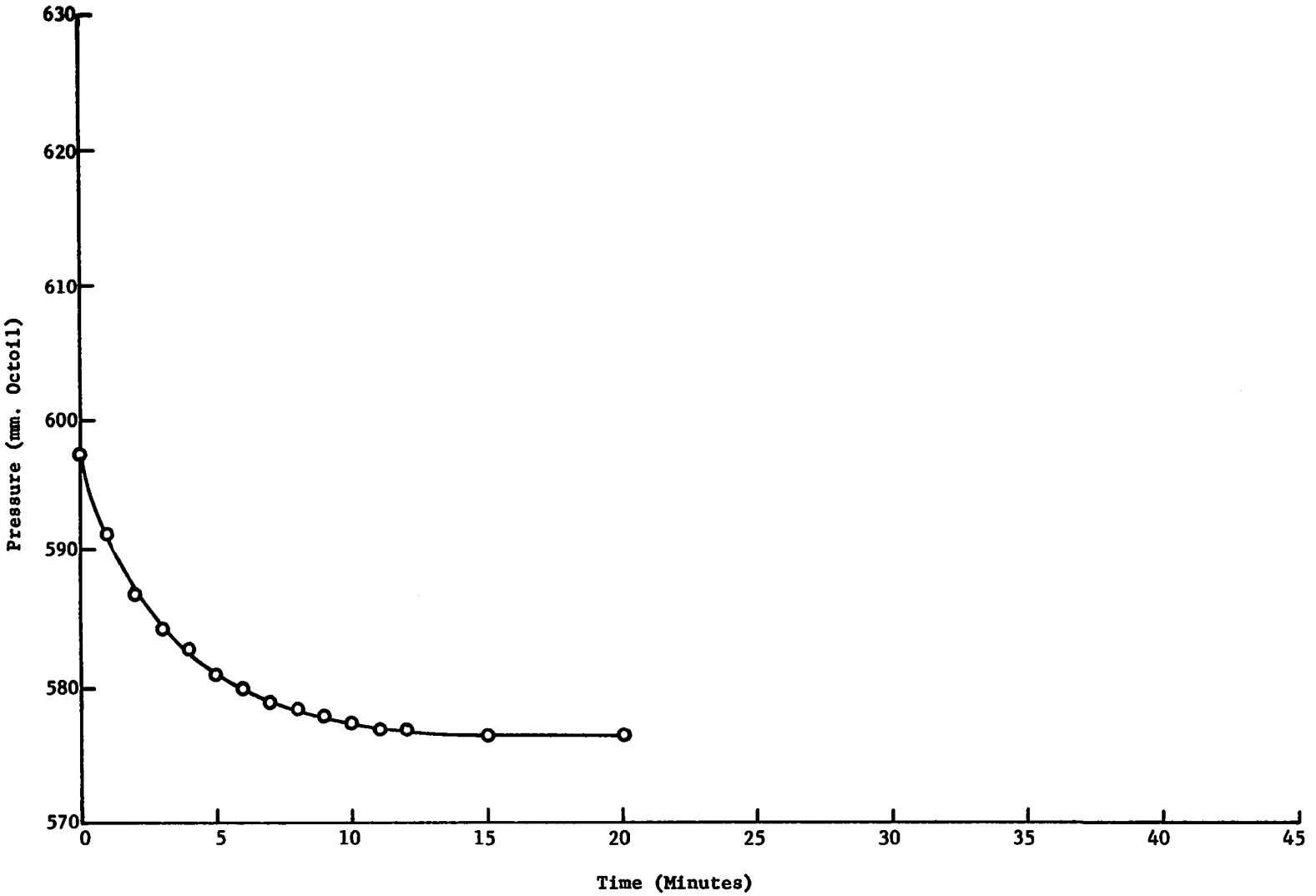

Figure 7. Sorption curve for abraded columbium. Grain Size: 550 μ
Hydrogenation Temperature: 700°C

diffusion equation gave curves as illustrated in Figure 8 (see Table 4 for a tabulation of D values). The slopes of the curves were considerably higher than that for the etched specimens (compare Figure 5 with Figure 8). Note that the abscissa of Figure 8 is in seconds while that of Figure 5 is in minutes. Of significance was the nearly complete disappearance of the sigmoid "tails" exhibited by the etched material. Slight deviations from the origin occurred, presumably due to instability in the manometer at the beginning of the run. The times involved for all specimens, however, were only on the order of 5-10 seconds.

A graph of ln D vs. 1/T for the abraded material is given in Figure 9. The slope of this curve gives an activation energy of about 9000 cal/mol which is consistent with the anticipated activation energy for a diffusion controlled reaction.

The discussion thus far has pertained particularly to that data which showed a parabolic initial reaction rate. The data obtained at 550^{o}C presented some difficulties in interpretation. The sorption curves for etched columbium were very irregular, and an initial rate law was not clearly definable. In some cases, the reaction did not proceed to completion even after extended periods of time. A sorption curve obtained from an etched specimen is shown in Figure 10. Also, the etched columbium, when fitted to a diffusion type analysis, gave poor results. As is shown in Figure 11 the C/C_0 curves had a poorly defined linear region. Where a linear portion can be found, such a curve still had a pronounced sigmoid "tail." The abraded material, on the other hand, showed a consistent linear initial reaction rate, as can be seen in Figure 12. However, when fitted to a diffusion type analysis, the data

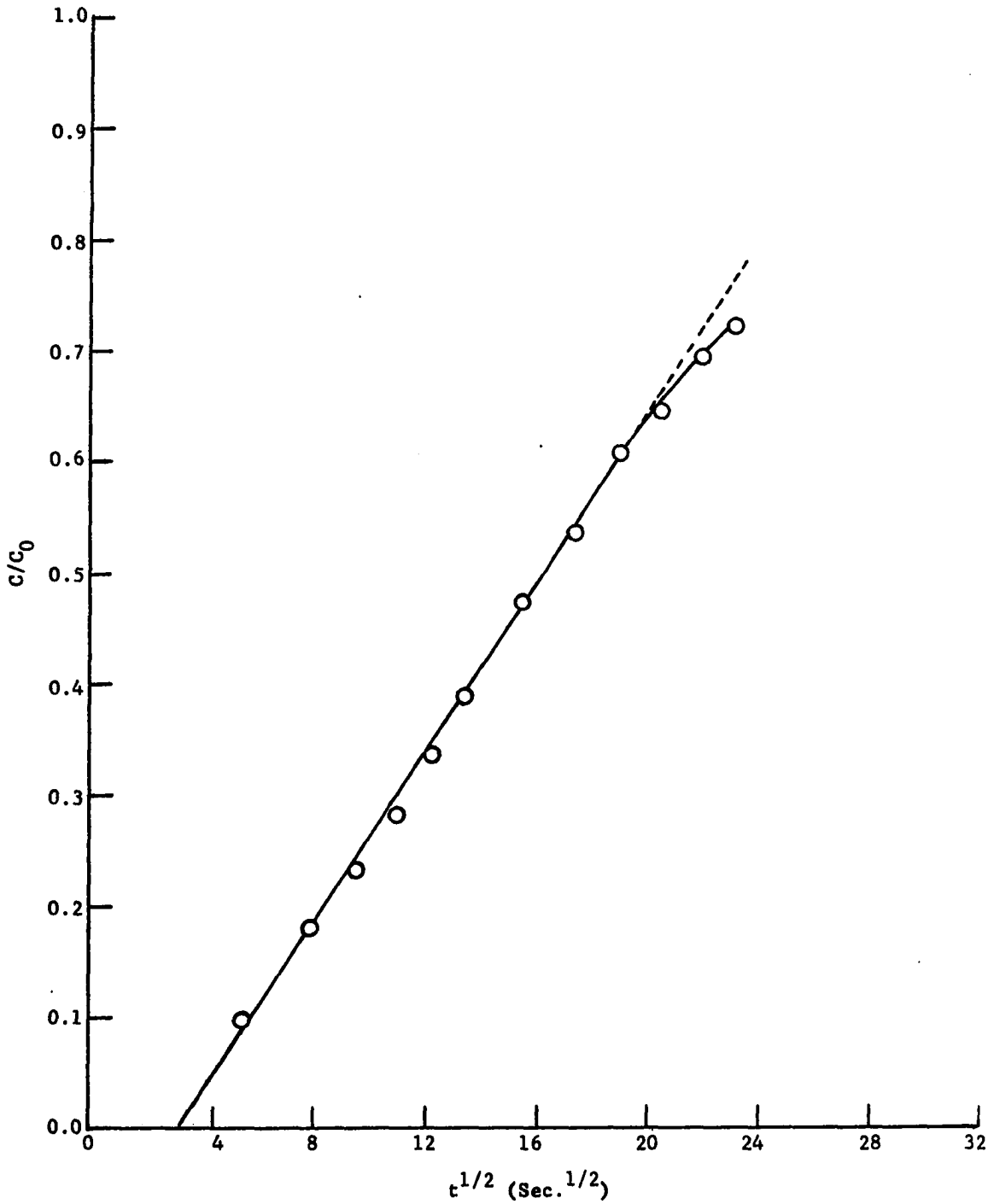

Figure 8. C/C_0 vs. $t^{1/2}$ for abraded columbium. Grain Size: 110 μ Hydrogenation Temperature: 600°C

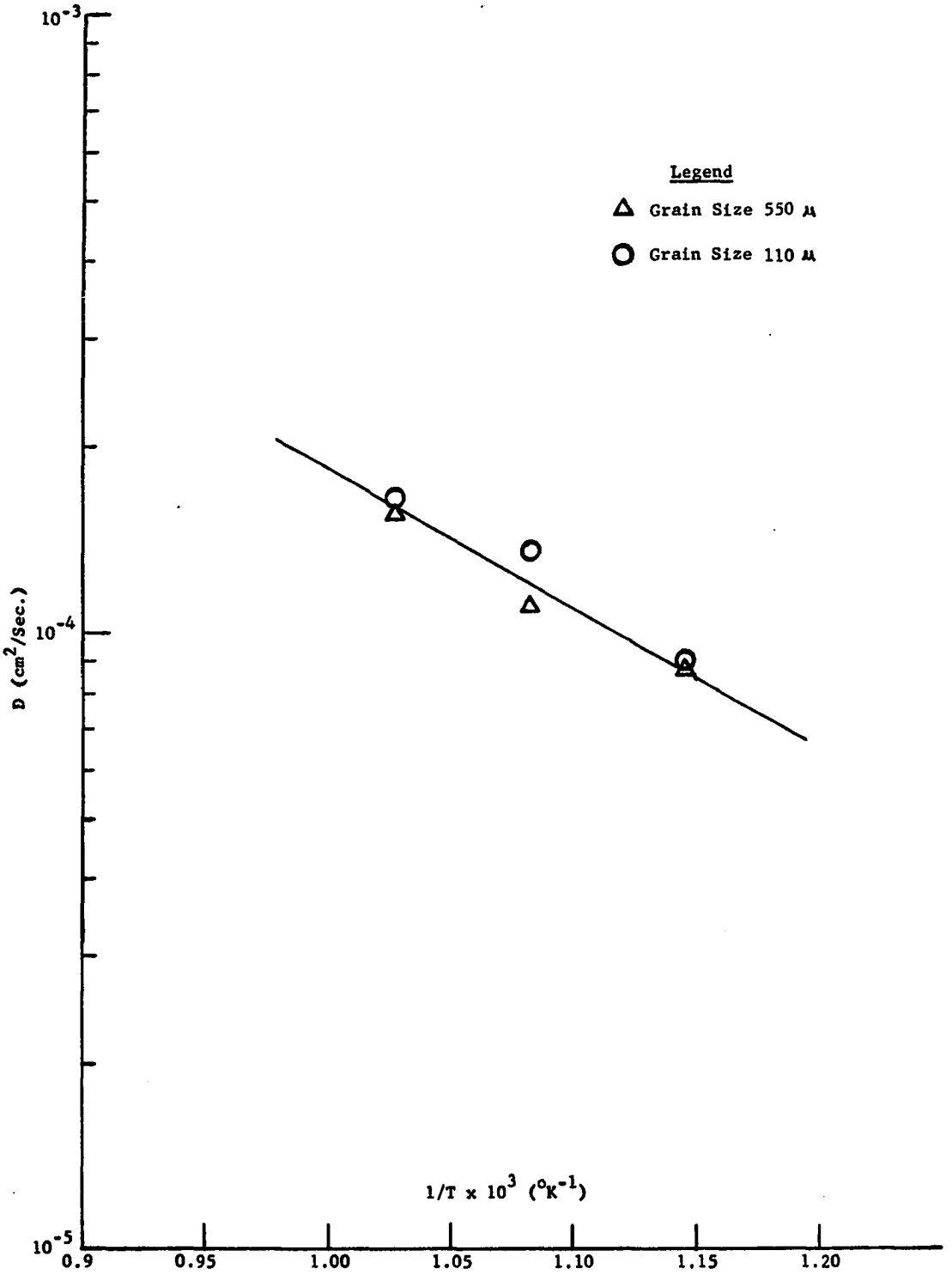

Figure 9. Ln D vs. 1/T for abraded columbium.

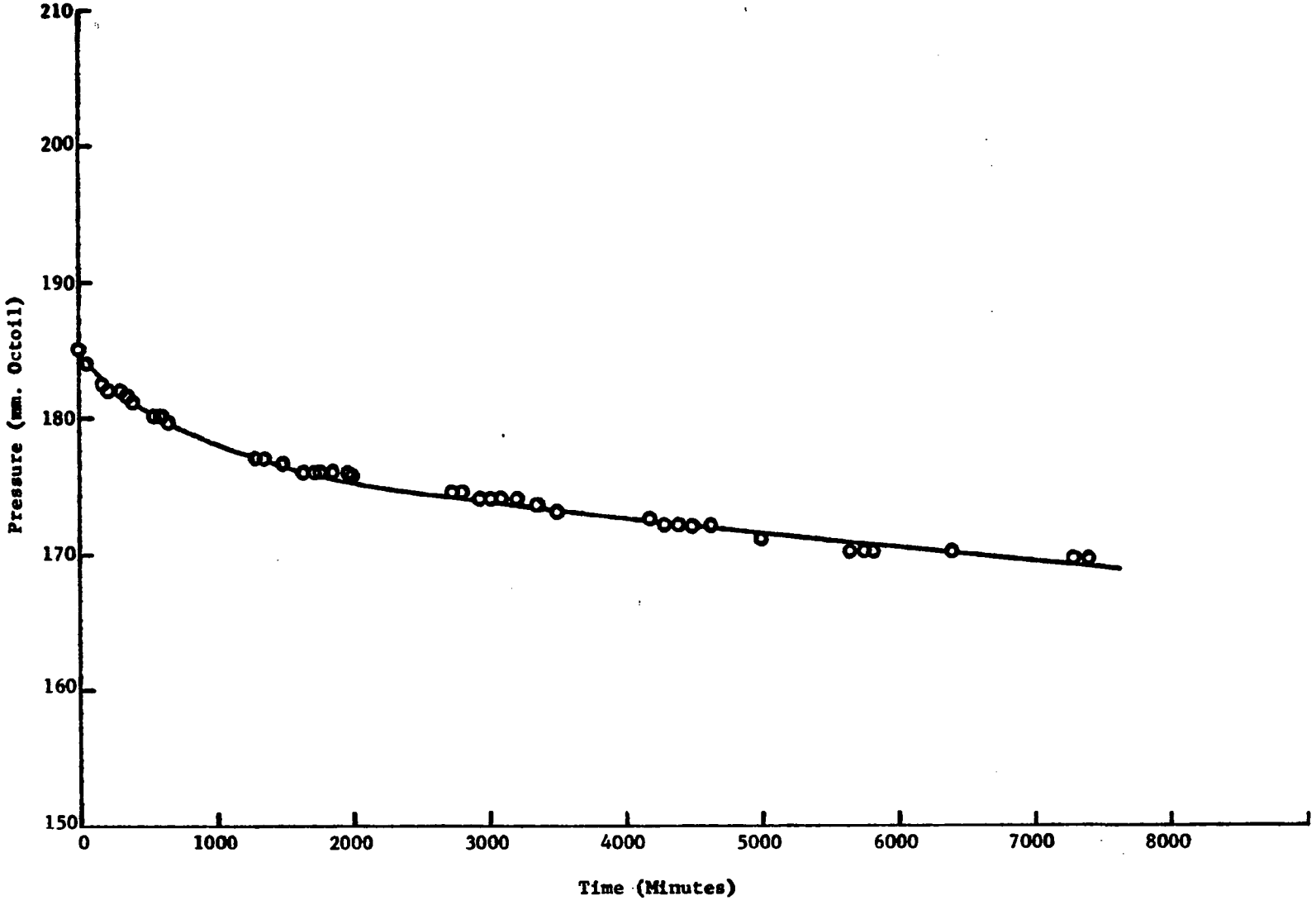

Figure 10. Sorption curve for etched columbium. Grain Size: 550 μ
Hydrogenation Temperature: 550°C

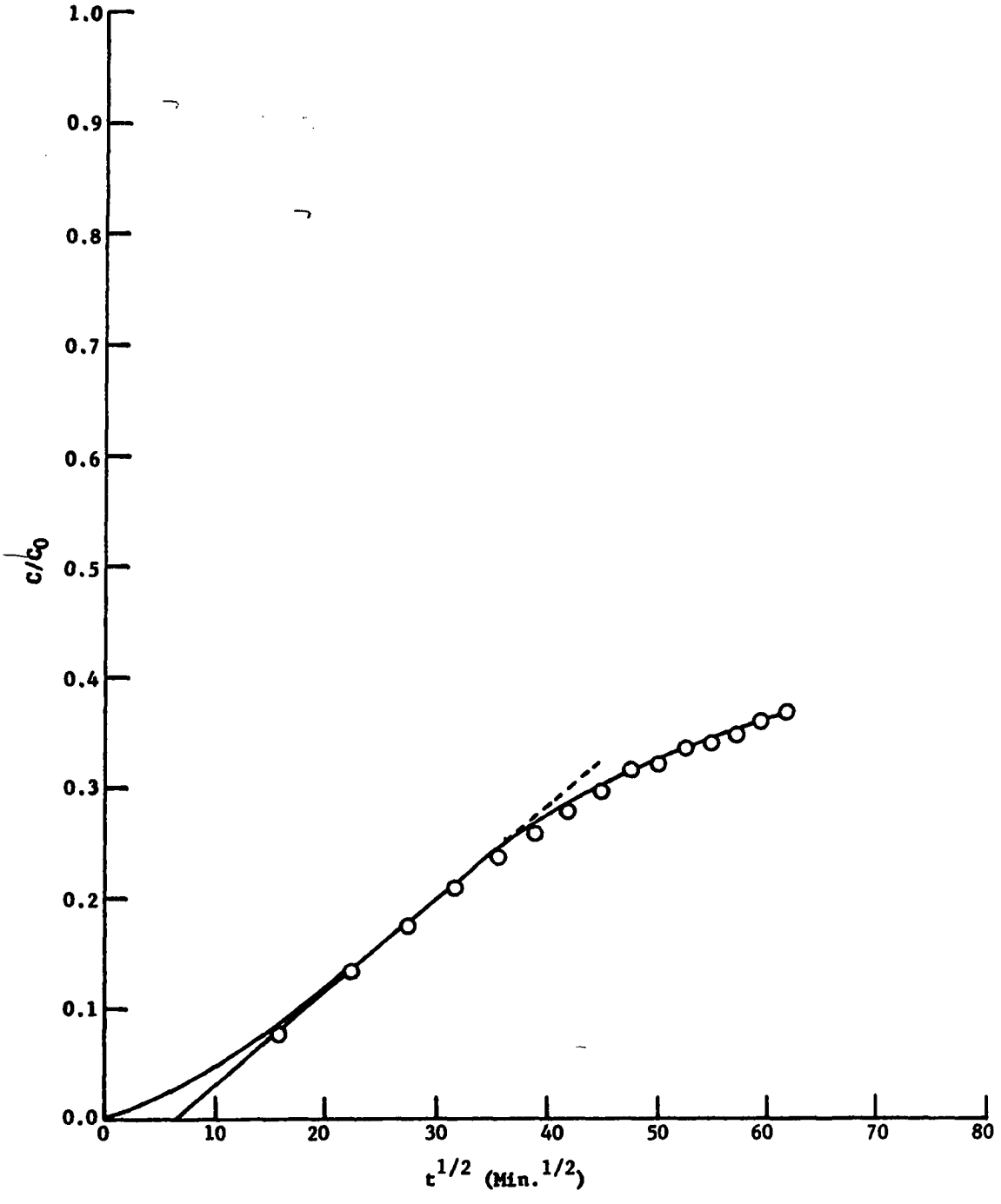

Figure 11. C/C_0 vs. $t^{1/2}$ for etched columbium. Grain Size: 550 μ
Hydrogenation Temperature: 550°C

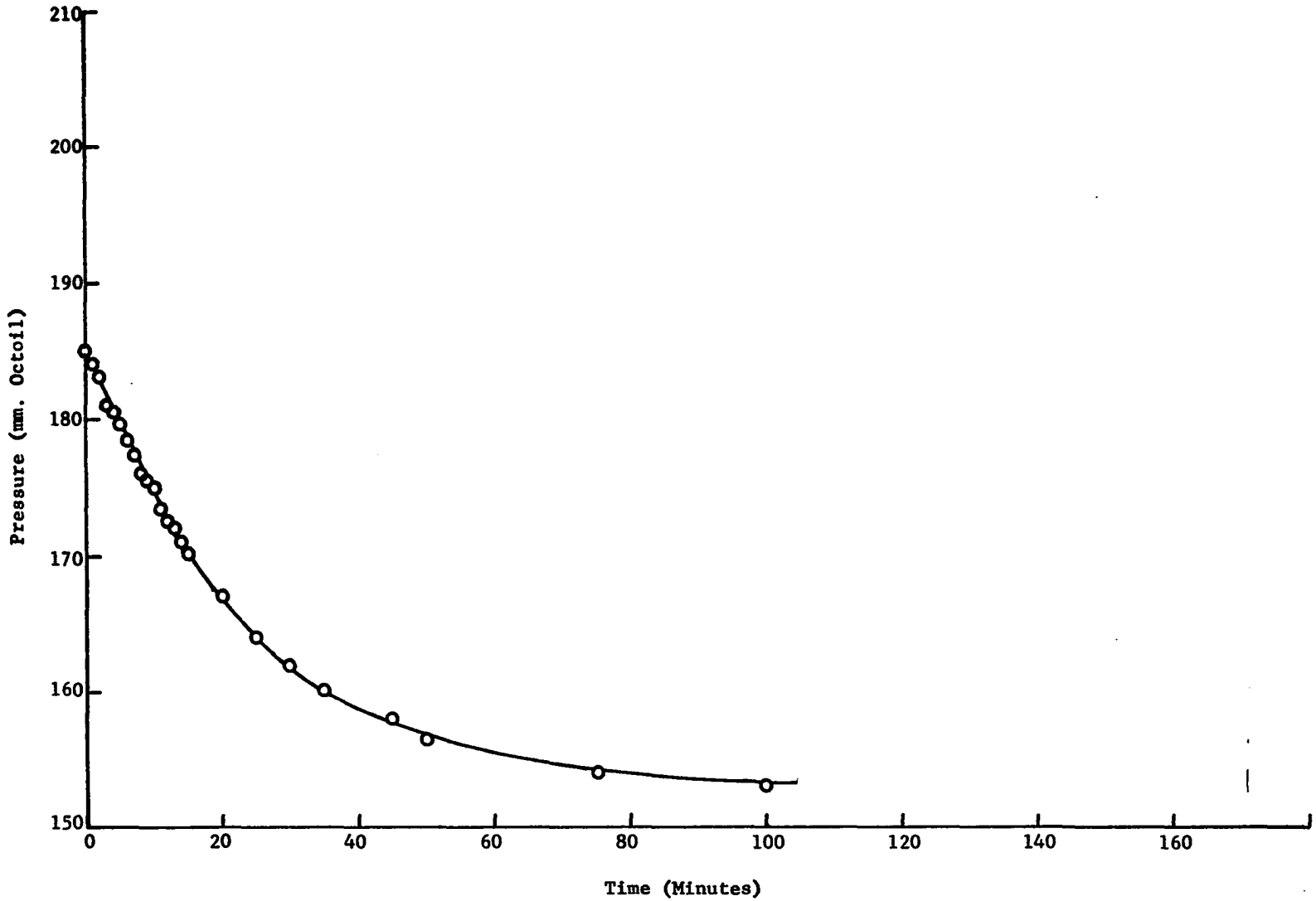

Figure 12. Sorption curve for abraded columbium. Grain Size: 110 μ
Hydrogenation Temperature: 550°C

still gave C/C_0 curves with a sigmoid "tail " preceding a linear portion (see Figure 13). Of particular significance is the fact that, where the slopes of the C/C_0 curves could be evaluated, the D values obtained were too low to fit the extrapolated values of the linear plots of ln D vs. 1/T obtained at higher temperatures.

Effect of Grain Size on Sorption Rate

As can be seen from D values in Table 4 and, particularly, the graphs of ln D vs. 1/T, there was no appreciable effect of grain size on the sorption rate. A rather large degree of scatter existed in the D values extracted from the C/C_0 curves of the etched columbium, and the scatter increased as the sorption temperature is decreased. However, no discernable grain size effect was evident. There was some indication of such an effect at 550°C, once again in the etched columbium, but, in view of the erratic sorption behavior, the effect is questionable.

In the case of the abraded material, the scatter in D values was reduced considerably. The values are in good agreement with those of Albrecht et al. (7) obtained in the same temperature range. Once again, however, no effect of grain size on sorption rate was observed irrespective of temperature.

Mechanical Properties of Hydrogen Free Columbium

The yield strength and ductility of the Heat II columbium is given in Table 5 for the various test temperatures and conditions of heat treatment. In general, the material showed only a slight tendency to work harden; a small amount of work hardening was observed at 300°K and at 191°K. At 77°K a plastic instability was often observed, i.e.,

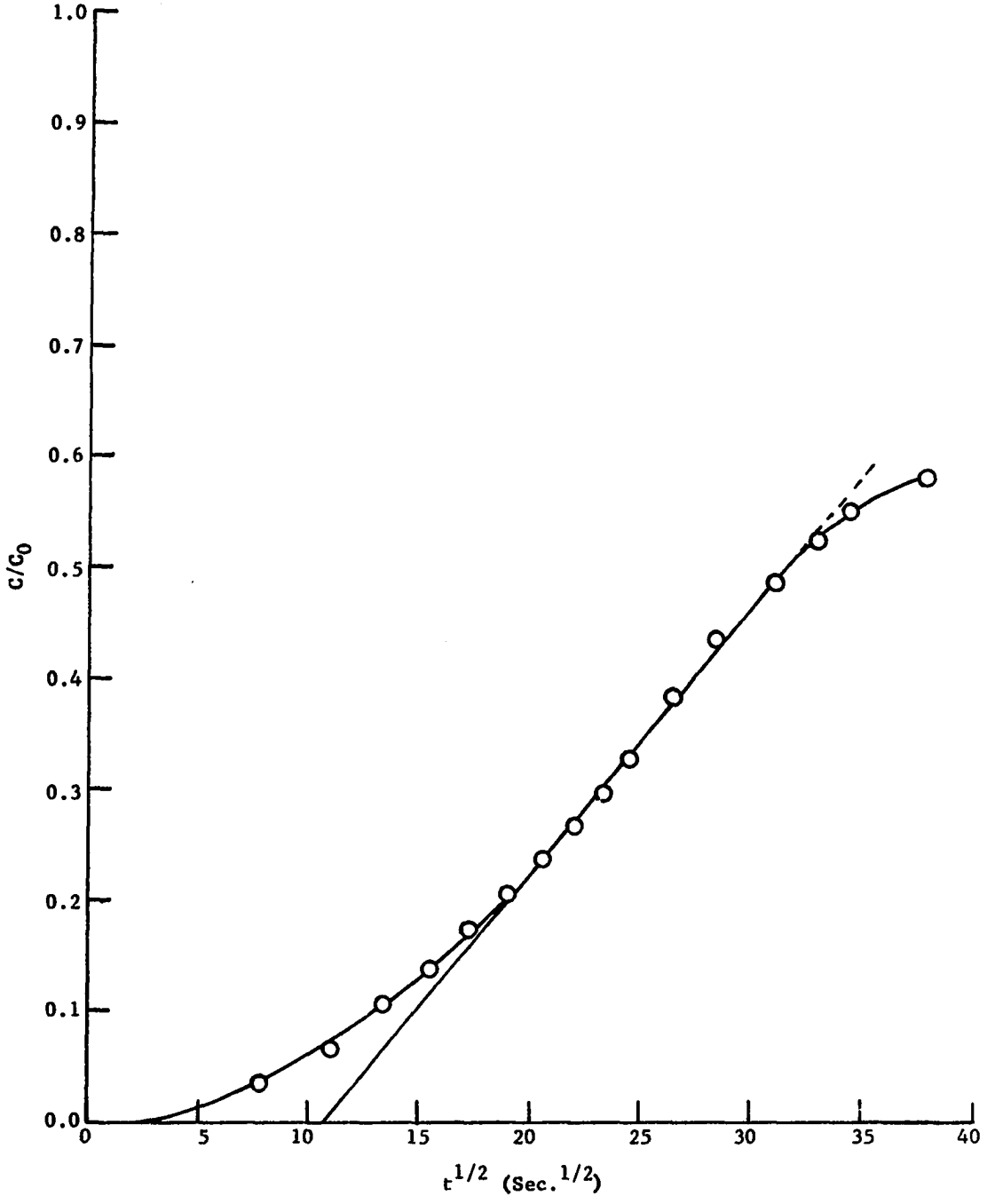

Figure 13. C/C_0 vs. $t^{1/2}$ for abraded columbium. Grain Size: 110 μ Hydrogenation Temperature: 550°C

a yield point occurred followed by a gradual reduction in the load until fracture took place. At no time were sharp upper and lower yield points observed, however, the yield stress increased greatly with decreasing temperature. The yield strength values were calculated using a 0.2 per cent offset method. Ductility values are given in terms of per cent reduction in area.

TABLE 5

TENSILE PROPERTIES OF PURE Cb

Condition	Test/Temp. deg. K	0.2% Offset Yield Strength psi	Ultimate Tensile Strength psi	Reduction in Area %
As swaged	300	55,300	58,300	94.0
As swaged	191	66,000	70,800	89.2
As swaged	77	129,400	129,400	77.5
Stress rel. (wrought)	300	41,800	50,800	95.7
Stress rel. (wrought)	191	51,100	62,500	92.6
Stress rel. (wrought)	77	128,700	128,700	77.8
Recrys. (1200°C)	300	21,700	33,200	97.5
Recrys. (1200°C)	191	35,000	45,400	96.5
Recrys. (1200°C)	77	97,700	103,400	83.4
Recrys. (1850°C)	300	19,400	24,000	66.30
Recrys. (1850°C)	191	32,200	37,900	68.75
Recrys. (1850°C)	77	98,800	100,500	49.5

Effects of Hydrogen on Mechanical Properties

The effect of hydrogen concentration on the yield strength of columbium is given in Figures 14, 15 and 16. Some scatter exists in the data, but it is evident that hydrogen concentrations up to 200 ppm. had little, if any, effect on the strength of columbium except at 77°K. It appeared that some slight strengthening occurred at 77°K in the recrystallized material, but the effect was quite small. Furthermore, only

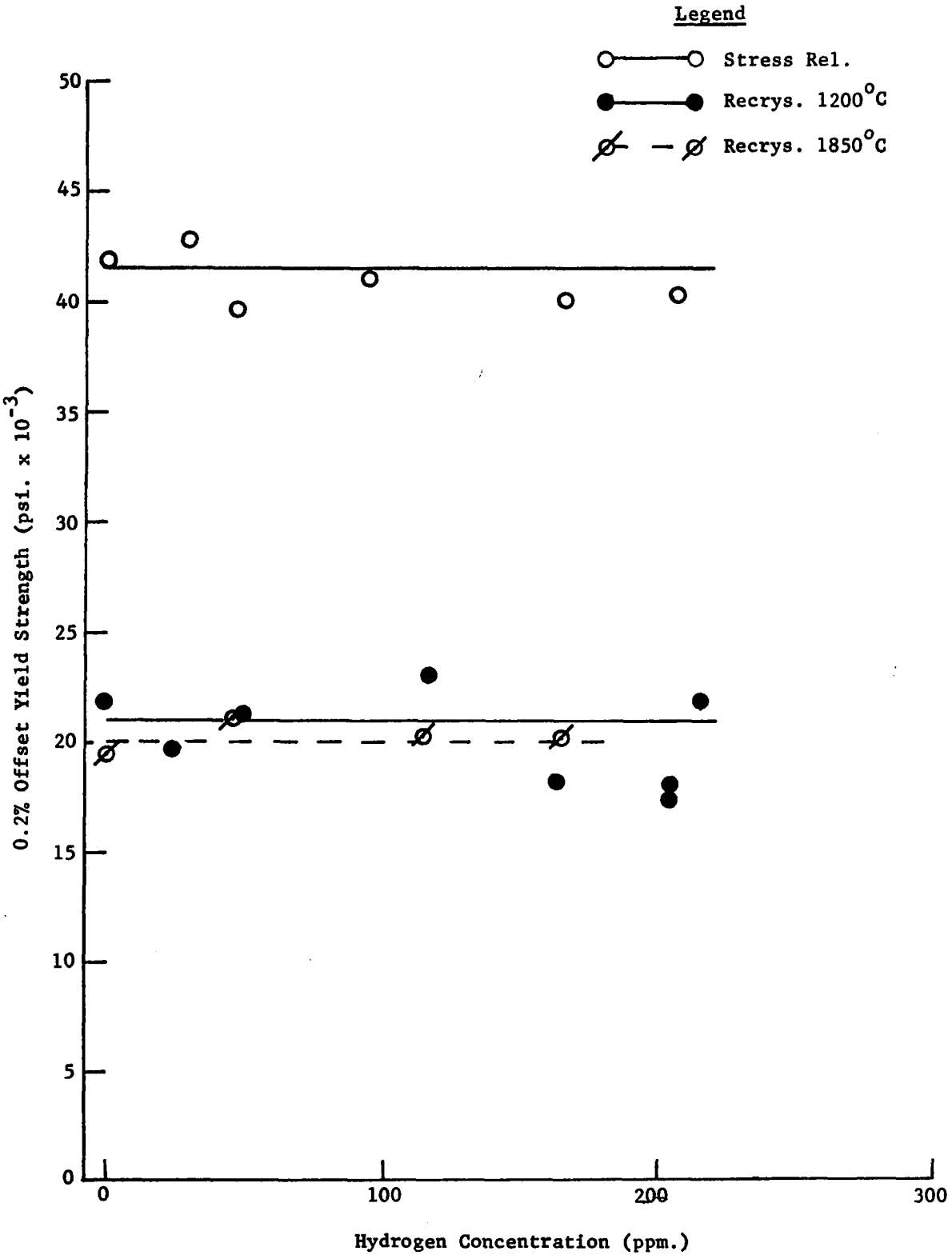

Figure 14. 0.2% offset yield strength vs. hydrogen concentration at 300°K.

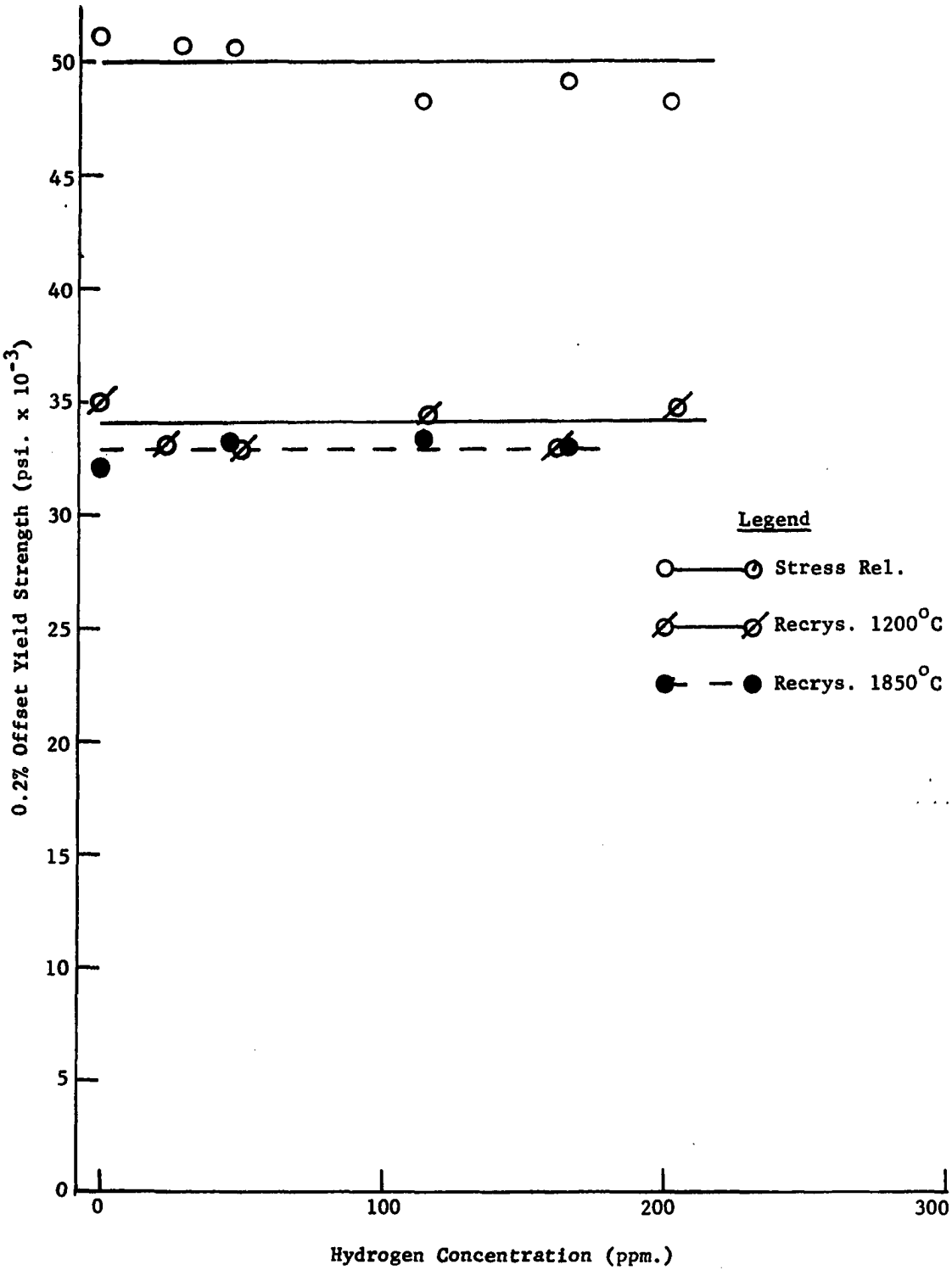

Figure 15. 0.2% offset yield strength vs. hydrogen concentration at 191°K.

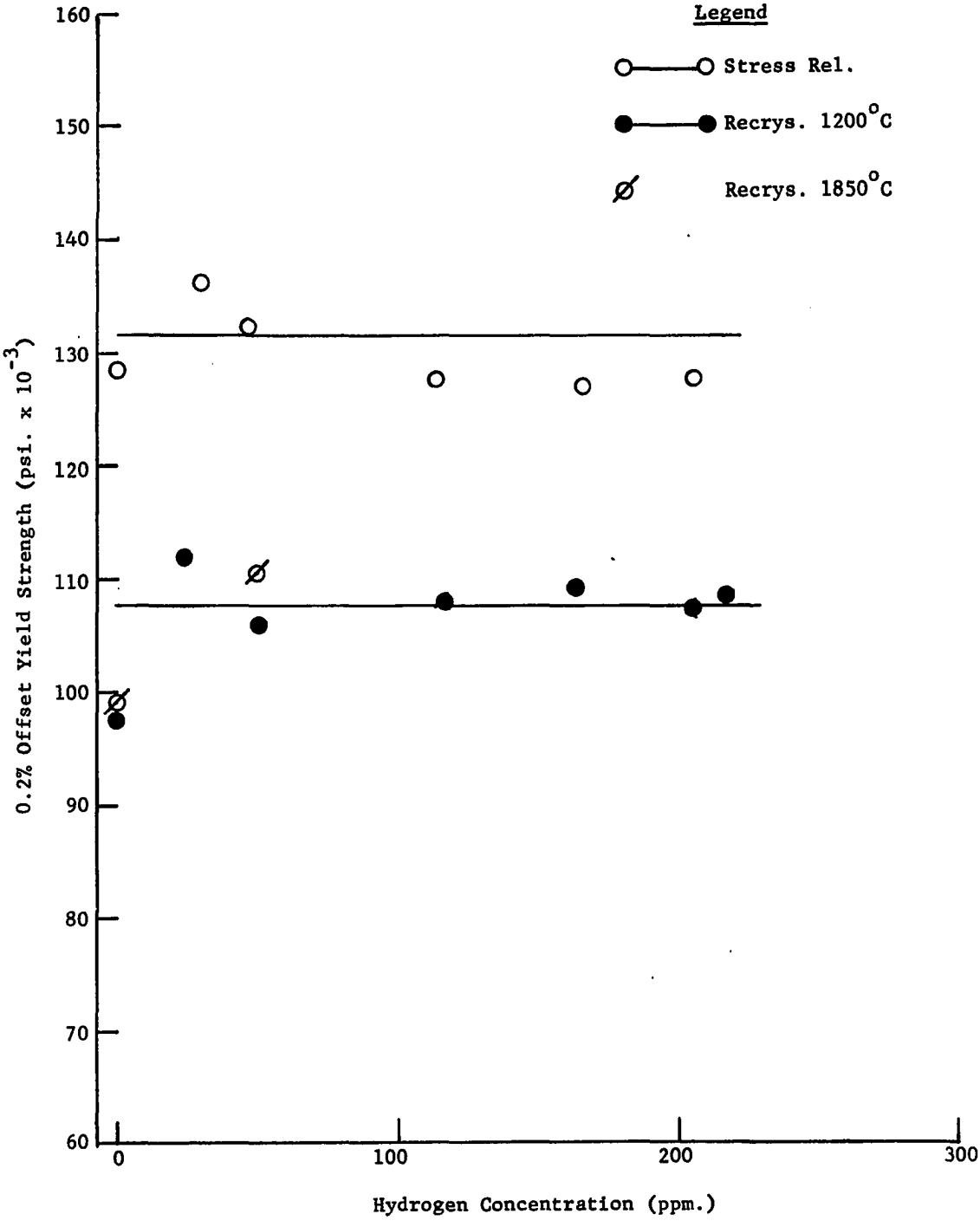

Figure 16. 0.2% offset yield strength vs. hydrogenation concentration at 77°K.

an initial strengthening of about 8-10 per cent was noted; continued addition of hydrogen did not produce a further increase in strength.

A point worth noting here is that even at higher hydrogen concentrations (up to 200 ppm.) no significant work hardening was noted. The material behaved much as it did without hydrogen except that fracture took place prematurely with little necking.

Only two values are shown for the coarse grained material at 77°K since extreme embrittlement was observed at higher hydrogen concentrations; in many cases the specimen fractured before the yield point was obtained.

Embrittlement due to the presence of hydrogen at various test temperatures can be seen in Figures 17, 18, and 19. At 300°K a distinct tolerance limit was observed at about 150 ppm. in the fine grained and wrought material. The coarse grained material, however, exhibited a tolerance limit at about 75 ppm. At 191°K only a small amount of hydrogen was necessary to cause embrittlement in all of the structures. Compositions on the order of 20-30 ppm. were sufficient to cause a severe loss of ductility. At 77°K the presence of hydrogen did not result in the abrupt transition from ductile to brittle behavior which was observed at higher temperatures. The ductility of all of the structures was reduced more or less gradually as the hydrogen concentration was increased. As in the case of 300°K an effect due to changes in microstructure is again evident. Fine grained recrystallized Cb-H alloys were slightly more sensitive to embrittlement than were the wrought alloys. The course grained material again showed a much greater rate of ductility loss than the other two structures. Above 100 ppm. the

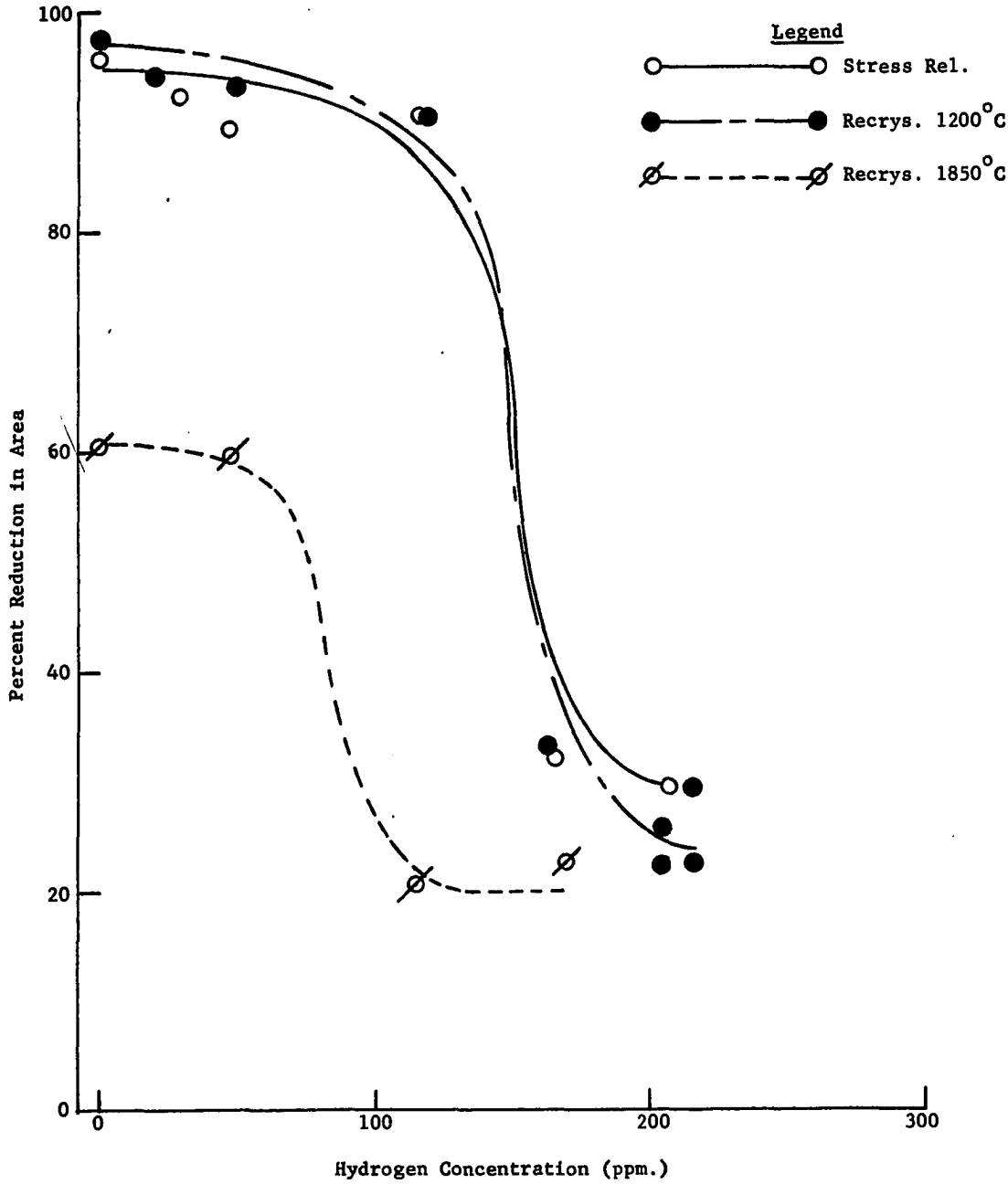

Figure 17. Ductility vs. hydrogen concentration at 300°K.

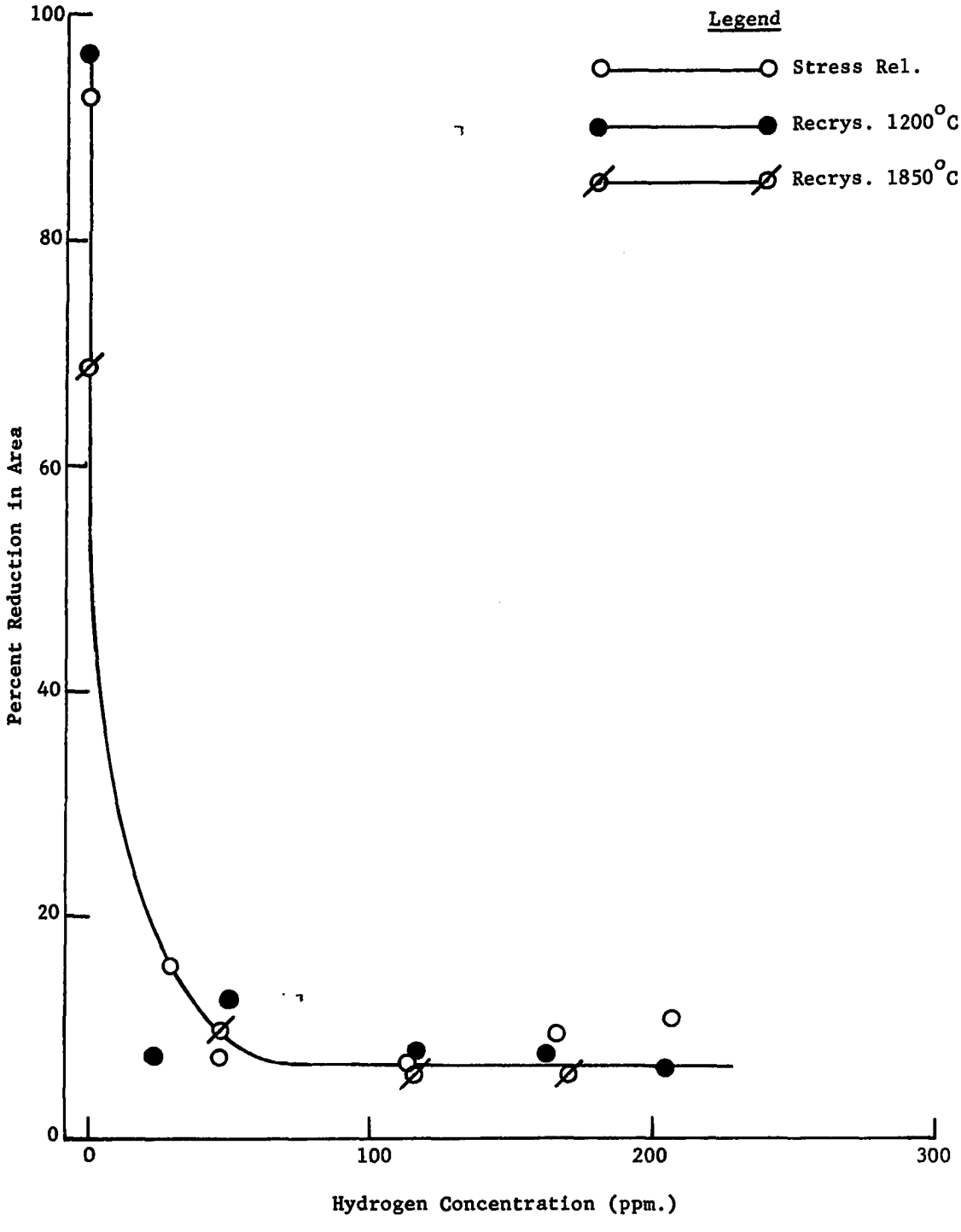

Figure 18. Ductility vs. hydrogen concentration at 191°K.

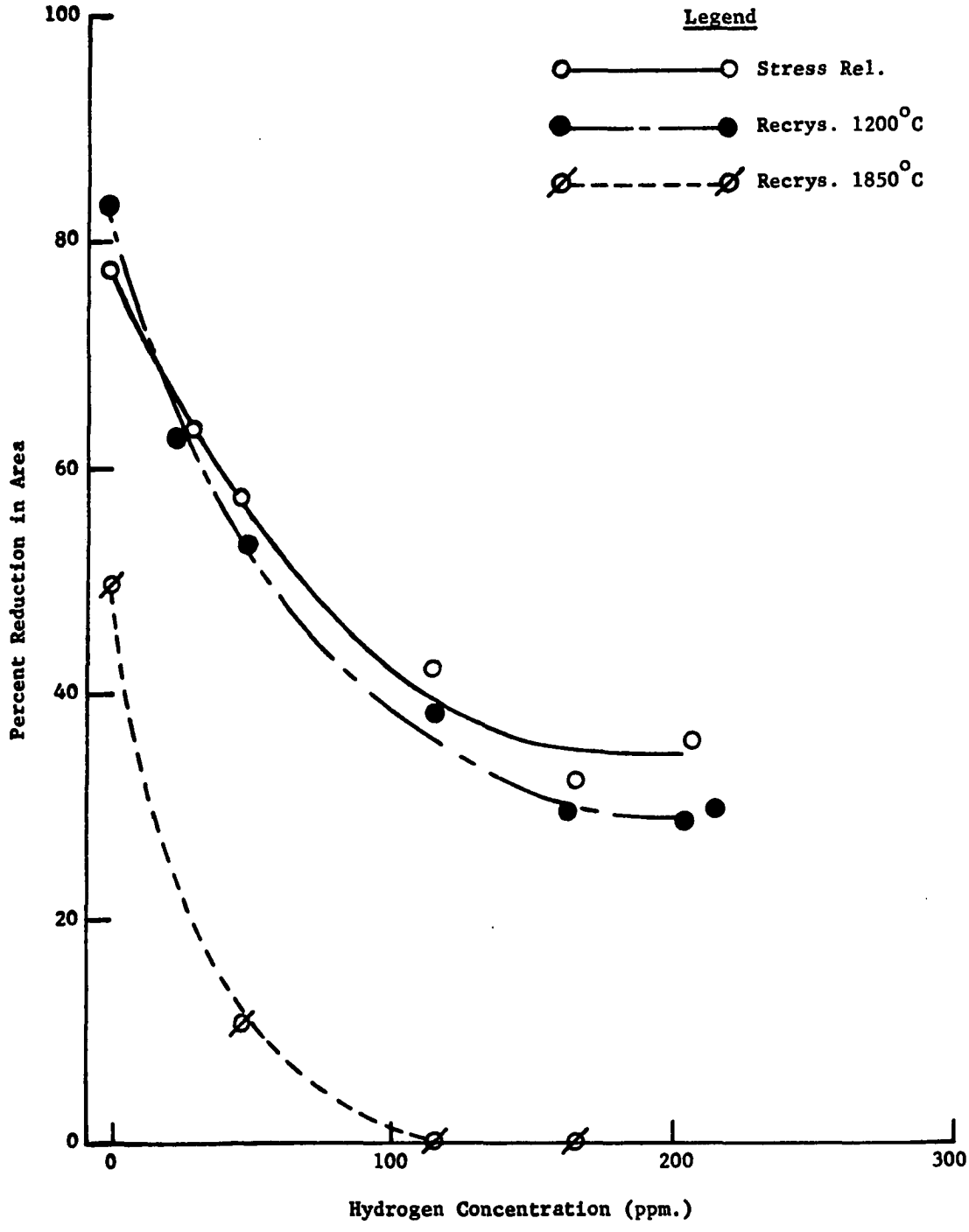

Figure 19. Ductility vs. hydrogen concentration at 77°K.

coarse grained material fractured before any yielding could be detected in a normal tensile test, while with the other structures some plastic deformation was noted prior to fracture.

Care must be exercised in evaluating the effects of grain size since the ductility of pure material will vary with grain size. Thus, a representation based upon per cent loss in ductility as a function of hydrogen concentration is necessary to account for this discrepancy. Table 6 gives the results of such a determination. The ductility loss is expressed as the difference in per cent reduction in area for pure columbium and columbium containing 115 ppm. hydrogen. The effects of microstructure are apparent as discussed above.

TABLE 6

PER CENT DUCTILITY LOSS FOR VARIOUS STRUCTURES

Structure	Test Temperature deg. K	Per cent Ductility Loss @ 115 ppm. Hydrogen
Wrought	300	5.60
Fine Grained Recrys.	300	7.50
Coarse Grained Recrys.	300	66.0
Wrought	77	45.5
Fine Grained Recrys.	77	53.2
Coarse Grained Recrys.	77	100

Ductility of Cb-H Alloys as a Function of Temperature

Plotting the data mentioned above in terms of ductility as a function of temperature rather than as a function of hydrogen concentration, reveals quite clearly the ductile-brittle-ductile transition discussed earlier. The coarse grained material, however, did not show

the ductility return at 77°K exhibited by the finer grained columbium. Only a slight return of ductility was observed at 48 ppm. hydrogen; at concentrations of 115 ppm. and above, the ductility dropped to zero (see Figures 20, 21, 22). It is interesting to note that at about 200 ppm. hydrogen concentration the ductility of the wrought and fine grained material was greater at 77°K than at 300°K.

Effect of Prestrain Treatment

In view of the above results, indicating the presence of a ductility minimum, it appears that the embrittlement process may be affected by a partitioning of mobile hydrogen. A series of specimens were given a 5 per cent prestrain at 300°K followed immediately by straining to fracture at 77°K. The purpose of the prestrain treatment was to enhance any partitioning of hydrogen to particular sites where brittle fracture might initiate. Thus re-testing at 77°K would be expected to reveal a higher sensitivity to embrittlement than would be observed by simply fracturing a specimen in a simple tensile test at the lower temperature.

The results of these tests are shown graphically in Figure 23. Comparison of this plot with Figure 19 indicates that for a given microstructure, prestraining in general tended to increase only slightly the embrittlement over a simple tension test at 77°K. However, a pronounced effect was observed in the fine grained recrystallized columbium at hydrogen concentrations of about 160-200 ppm. Here a sharp loss in overall ductility was observed compared to simple tensile testing at 77°K. The coarse grained material showed a slightly higher sensitivity to embrittlement in that some plastic deformation was observed at lower hydrogen concentrations in a simple test at 77°K; however prestraining produced

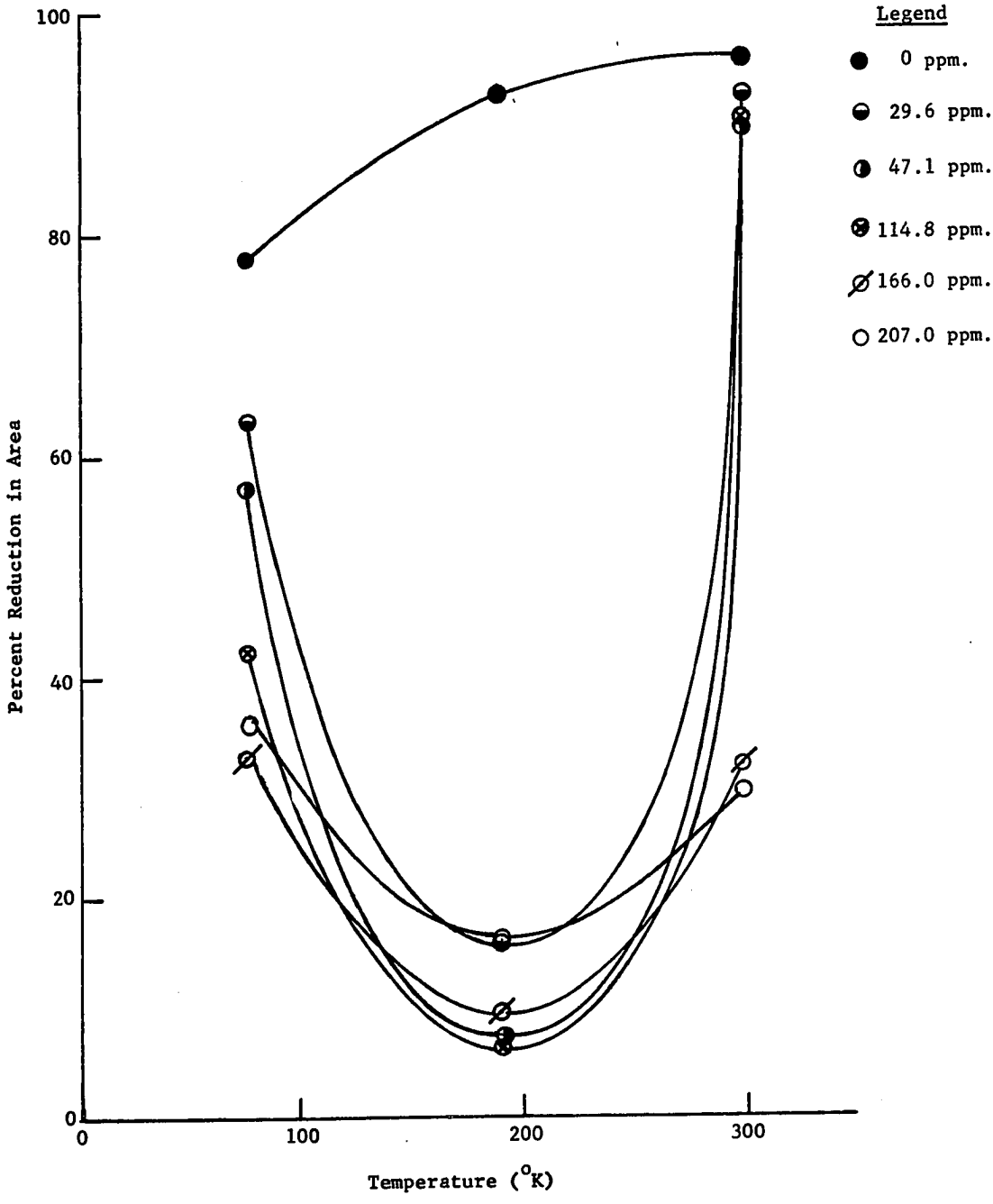

Figure 20. Ductility vs. temperature for stress relieved (wrought) columbium.

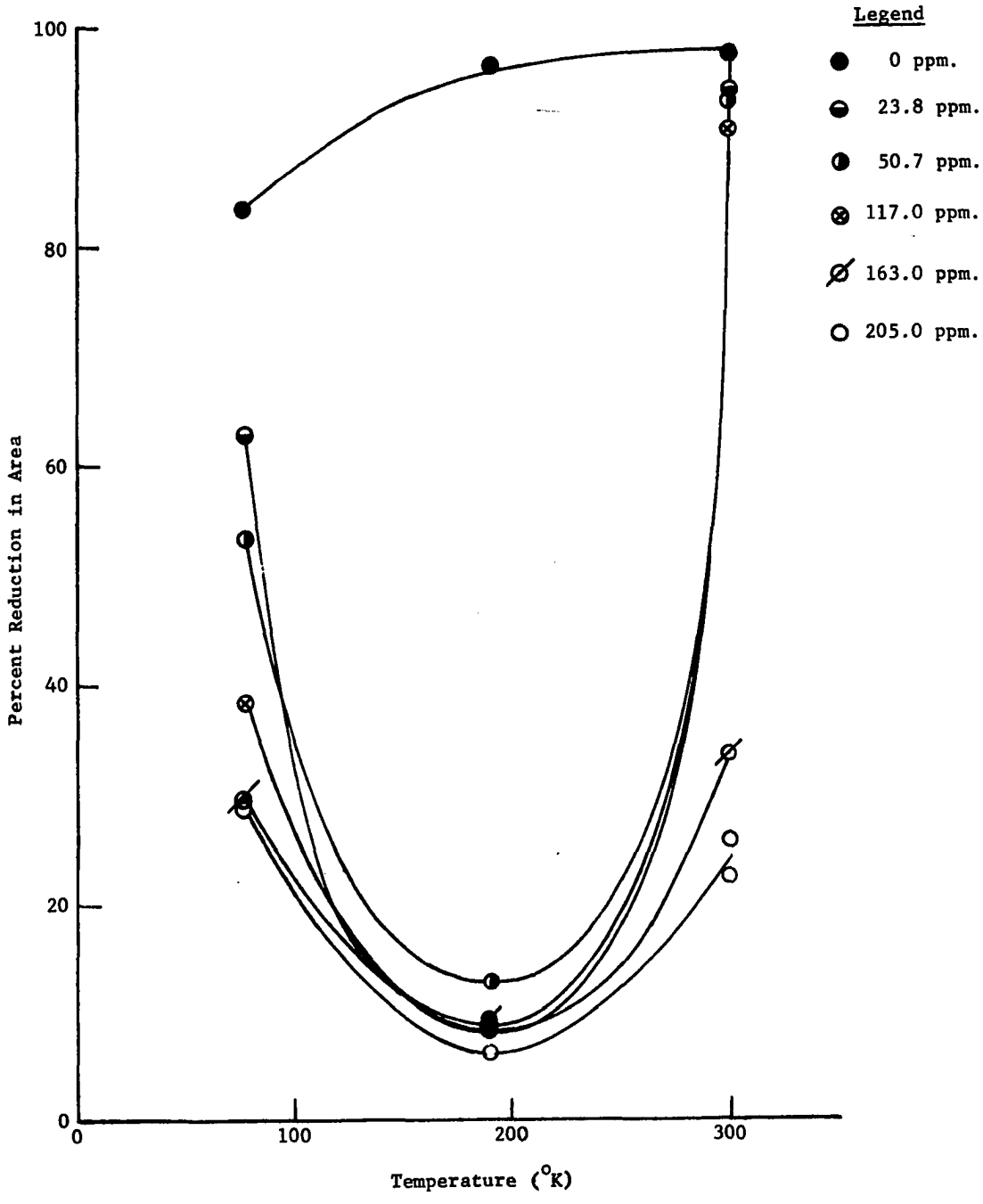

Figure 21. Ductility vs. temperature for recrystallized (1200°C) columbium.

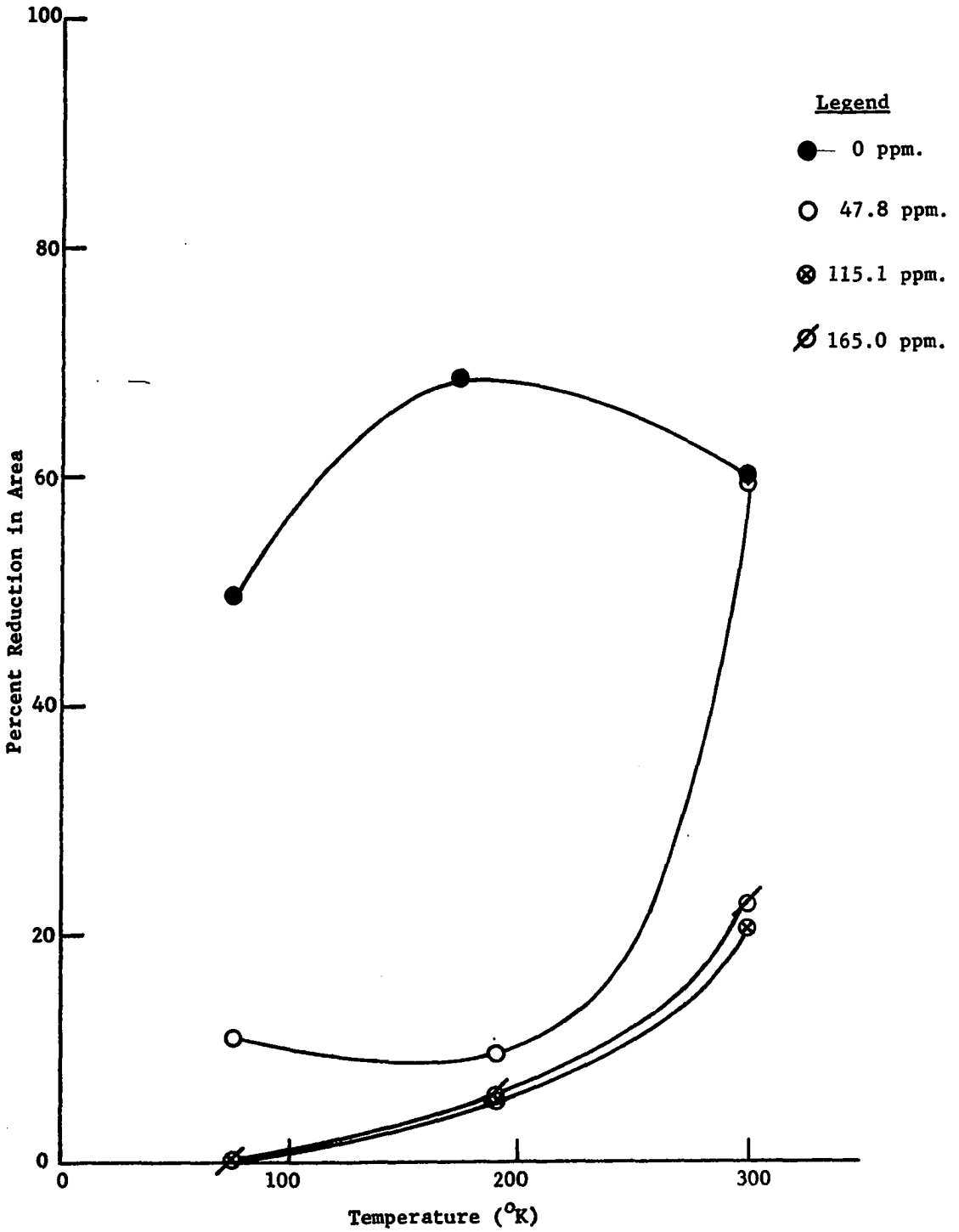

Figure 22. Ductility vs. temperature for recrystallized (1850°C) columbium.

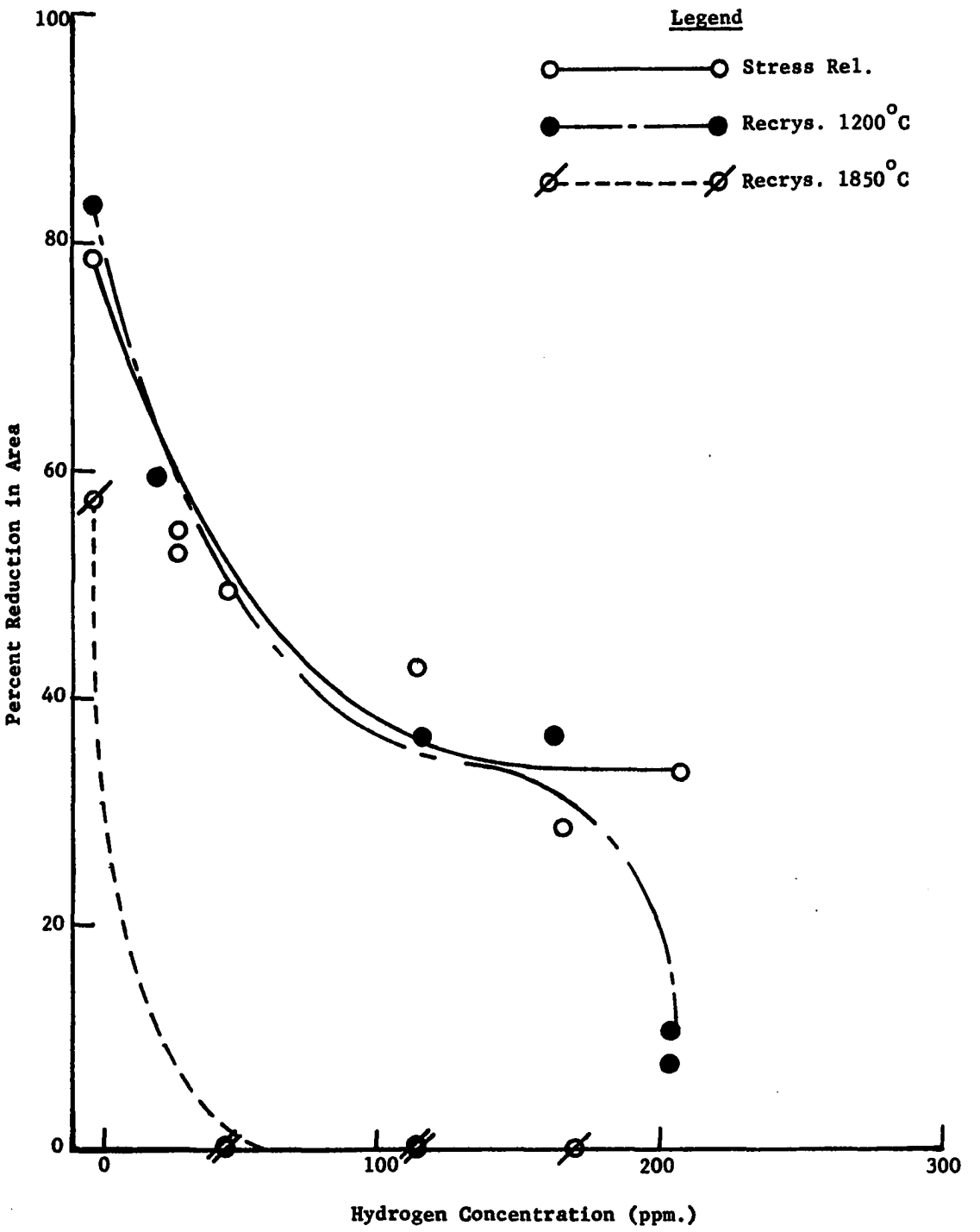

Figure 23. Ductility vs. hydrogen concentration at 77°K after 5% prestrain at 300°K.

failure without detectable yielding at all hydrogen concentrations studied.

Effect of Strain Rate

All of the data discussed above were obtained at a strain rate of 0.02 ipm. (actually 0.02 ipm. crosshead travel). To investigate the effects of strain rate, a random sample of specimens was tested at 300°K at strain rates up to 2.0 ipm. It can be seen from the data in Table 7 that a hydrogen tolerance limit was observed at high strain rates similar to that found at slow strain rates.

TABLE 7

EFFECTS OF STRAIN RATE ON HYDROGENATED COLUMBIUM AT 300°K

Structure	Hydrog. Conc. ppm.	Strain Rate	Yield Str.	% RA
Wrought	47.8	0.02	39,400	89.6
Wrought	47.8	0.20	42,600	89.2
Wrought	47.8	2.00	45,700	90.7
Wrought	114.8	0.02	41,100	90.4
Wrought	114.8	0.20	40,900	85.6
Wrought	114.8	2.00	46,500	89.0
Wrought	166.0	0.02	40,100	32.0
Wrought	166.0	0.20	42,200	13.29
Wrought	166.0	2.00	45,100	17.0
Wrought	207.0	0.02	40,300	29.4
Wrought	207.0	2.00	44,800	17.8
Recrys. (1200°C)	23.8	0.02	19,600	94.0
Recrys. (1200°C)	23.8	0.20	22,600	93.8
Recrys. (1200°C)	23.8	2.00	26,400	95.8
Recrys. (1200°C)	163.0	0.02	18,000	33.4
Recrys. (1200°C)	163.0	0.20	21,000	23.9
Recrys. (1200°C)	163.0	2.00	29,000	14.4

Little effect of strain rate on ductility was observed until

the tolerance limit was reached. At this point increasing the strain rate resulted in a noticeable loss in ductility. It is also evident that raising the strain rate by a factor or 100 increased the 0.2 per cent offset yield strength by roughly 10 per cent, independent of hydrogen content.

CHAPTER IV

DISCUSSION OF RESULTS

Kinetic Studies

Effect of temperature

It seems apparent that the sorption of hydrogen by columbium can be described by a diffusion controlled reaction in the temperature range 600°C - 750°C provided that the metal surface remains uncontaminated. The pronounced sigmoid shapes of the C/C_0 plots for the etched specimens sorbed in this temperature range are in good qualitive agreement with what has been observed in the sorption of hydrogen by etched zirconium (60). Gelezunas et al. (60) proposed that the retarded sorption rate was due to the presence of a "chemical film" at the surface of the metal formed during the etching treatment; however, the exact nature of such a film was not explained. The possibility exists that the etching treatment introduces large numbers of oxygen atoms to interstitial sites near the surface of the metal, thus retarding the hydrogen sorption rate. The activation energy obtained when fitting the data for etched columbium obtained in this investigation to a diffusion type analysis is also in good agreement with the results of the above mentioned study of hydrogen sorption by zirconium. This agreement suggests that the nature of the film is similar in both cases. The large scatter

in "D" values obtained in this study for the etched samples is presumably due to differences in the thickness of the inhibiting layer.

Whatever the nature of the film, it evidently exists only at the surface of the metal. The short abrasion treatment apparently removes it, since sorption rates increased drastically. The activation energy obtained on the abraded samples from an analysis which assumes a diffusion controlled reaction is more consistent with that obtained for hydrogen diffusion in other bcc metals (19), and in good agreement with the data of Albrecht et al. on columbium (7).

The sorption data obtained at 550°C is not consistent with that obtained at the higher temperatures studied. Considering first the abraded material, the initial reaction rates were distinctly linear as opposed to the parabolic rates obtained at the higher temperatures. This behavior indicates that the rate controlling step in the sorption process changes as the temperature is lowered. It was pointed out earlier that a sigmoid "tail" on a C/C_0 curve suggests that the sorption reaction is inhibited by some surface step (59). However, since any inhibiting chemical surface film has presumably been removed by abrading, as suggested by data obtained at higher temperatures, the sigmoid curves obtained here evidently represent an inherent change from a diffusion controlled to a surface controlled reaction. The rather erratic sorption behavior of the etched material at this temperature can now be more clearly understood since a surface step controlled reaction would presumably be extremely sensitive to any surface contamination. In addition, the increased scatter in D values as the sorption temperature is lowered from 750°C to 600°C is understandable since, as

the sorption temperature approaches that for a surface controlled reaction, the surface film would become a more effective barrier to sorption.

Effect of grain size

The sorption rates do not appear to be sensitive to grain size as was evidenced in Table 3 of the preceding chapter. Thus it appears that volume diffusion masks the effects of diffusion along short circuiting paths such as grain boundaries, irrespective of surface condition. The surface preparation and the grain size do not seem to affect the quantity of hydrogen sorbed by columbium at any given temperature (see Table 4 in Chapter III); however, the surface condition will affect the rate of approach to equilibrium.

It is intuitively expected that the equilibrium solubility and distribution of hydrogen in columbium will vary with grain size, but these effects are not apparent from the data obtained in this study. The mechanical properties, to be discussed in succeeding sections, are apparently more sensitive indicators of the hydrogen distribution within the metal.

Yield Point and Temperature Dependence of Yield Strength in Columbium

There has been some discrepancy in the literature regarding the presence or absence of a sharp yield drop in columbium. Adams, et al. (47), Wessel et al. (53), and Tankins and Maddin (49) observed it; whereas, in the work of Johnson (48), as well as in this investigation, sharp yield points were not observed. It should also be noted that where yield points were found at room temperature, they often were not evident at low temperatures (49).

As was pointed out in Chapter I, the yield point is usually associated with the unlocking of dislocations from solute atom atmospheres. However, in view of the evidence that impurities in columbium do not lock dislocations to any great degree, the presence or absence of a sharp yield point cannot be attributed to varying concentrations of impurities for reasonably pure material. This is pointed out significantly in that there is no correlation between the presence or absence of a sharp yield point and the interstitial atom concentration in the investigations mentioned above.

Van Torne and Thomas (55), moreover, have shown that a sharp yield drop in columbium is associated with a rapid increase in dislocation density due to dislocation multiplication. Thus it may be that the degree of yield drop observed in columbium depends on the ability of dislocation sources to operate during straining. It seems reasonable to expect that the rate of multiplication would be influenced by temperature, grain size, and initial dislocation arrangements as well as impurity concentration. Any of these factors would presumably affect the operation of dislocation sources and explain differences in the yield drop of columbium among various investigators.

What is of considerable importance is that the yield strengths observed in this investigation do not vary appreciably with hydrogen concentration regardless of test temperature. This, in turn, points up a distinct lack of sensitivity of the temperature dependence of the yield strength to hydrogen concentration. This result is in qualitative agreement with the investigations discussed in Chapter I which show that the temperature dependence of the yield strength is not due to impurity

locking (50, 51, 52, 53). Thus it appears that hydrogen does not embrittle through blocking of dislocation motion leading to a strengthening of the lattice or to dislocation pile-ups.

Effect of Hydrogen on the Ductility of Columbium

Metallographic observations

Metallographic examination of tensile specimens of the fine grained recrystallized material and the wrought material at various hydrogen concentrations revealed, in many cases, extensive porosity. The recrystallized columbium showed extensive pitting at 300°K and 77°K. As can be seen in Figures 24 through 28, the porosity is a distinct function of hydrogen concentration. At 300°K, 163 ppm. produces extensive pitting, whereas at 117 ppm. the pitting is virtually eliminated. At 77°K, the amount of porosity, particularly in terms of pit size, decreases more slowly with hydrogen concentration. Porosity appears to develop preferentially at grain boundaries. The pits appear to be extended in a direction perpendicular to the tensile axis. Although not apparent in the photomicrographs, due to the limited area which could be viewed under the microscope, the pit density gradually decreased with increasing distance along the gauge length away from the point of fracture.

The wrought columbium exhibited no significant pitting at 300°K irrespective of hydrogen concentration; rather, secondary cracks initiated at the surface of tensile specimens at hydrogen concentrations of 165 ppm. and higher. As can be seen in Figure 29, these cracks appear to be blunted. At 77°K, however, pitting was observed along the striations

Figure 24. Porosity in recrystallized (1200°C) columbium plus 163 ppm. hydrogen tested at 300°K. X200

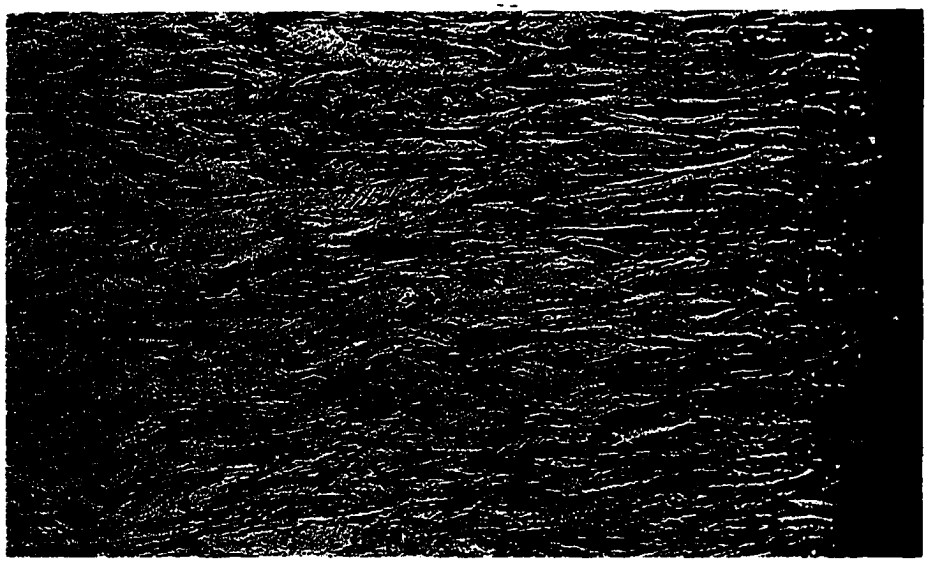

Figure 25. Microstructure of recrystallized (1200°C) columbium plus 117 ppm. hydrogen tested at 300°K. X200

Figure 26. Porosity in recrystallized (1200°C) columbium plus 205 ppm. hydrogen tested at 77°K. X200

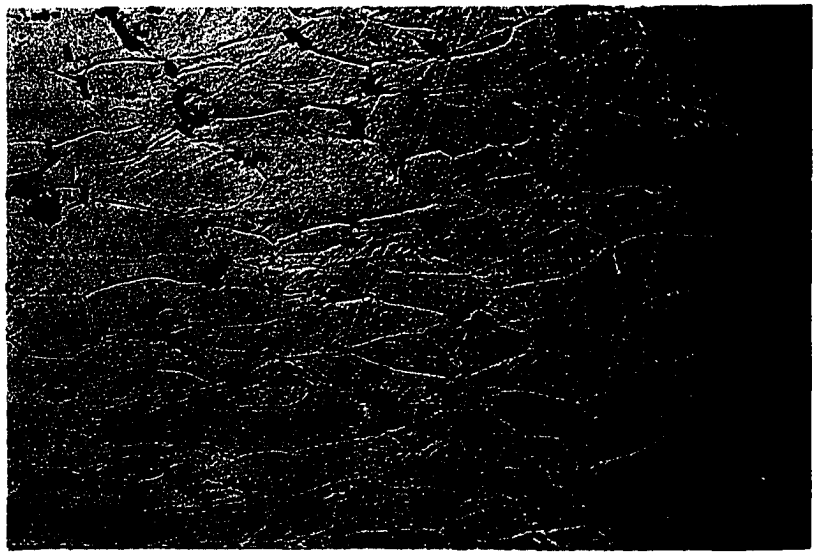

Figure 27. Porosity in recrystallized (1200°C) columbium plus 117 ppm. hydrogen tested at 77°K. X200

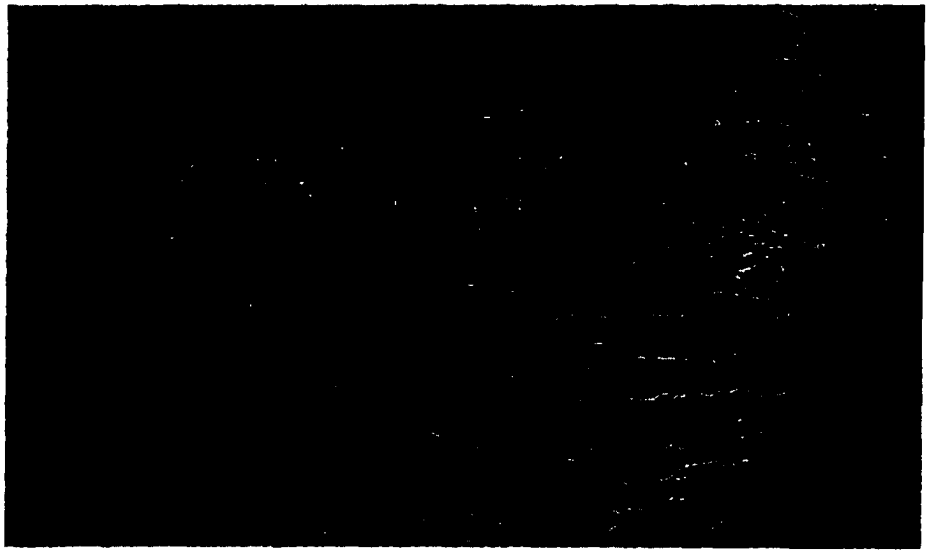

Figure 28. Porosity in recrystallized (1200°C) columbium plus 50.7 ppm. hydrogen tested at 77°K. X200

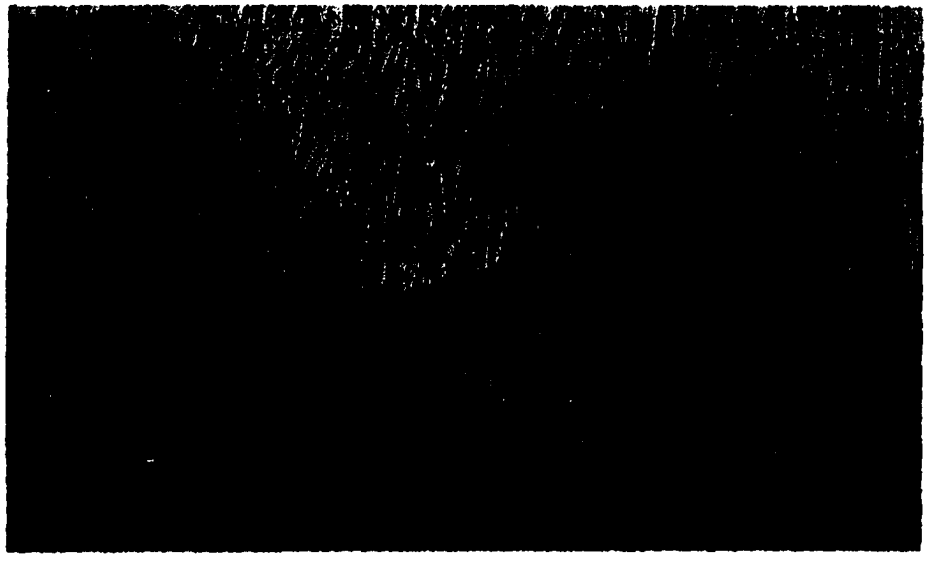

Figure 29. Blunted cracks stress relieved (wrought) columbium plus 207 ppm. hydrogen tested at 300°K. X200

of the wrought structure. Similar to what was observed in the recrystallized material tested at this same temperature, the amount of porosity decreases gradually with decreasing hydrogen concentration as can be seen in Figures 30, 31 and 32. Again, the pit density was highest near the point of fracture.

At the intermediate test temperature of 191^{o}K, little or no porosity was observed in either structure except in the region very near the fracture in the wrought samples. Figure 33 shows some pitting in a wrought specimen but it is in a very localized area near the point of fracture. The recrystallized material usually exhibited small cracks near the fracture surface as can be seen in Figure 34.

It should be pointed out that the porosity illustrated above could be observed during the latter stages of specimen preparation prior to the application of a chemical etch. The specimens were prepared for metallographic observation by the conventional methods of abrasion and mechanical polishing. In addition a chemical polish was employed, consisting of 50 ml lactic acid, 30 ml nitric acid, and 2 ml hydrofluoric acid, prior to etching. The etch was a mixture of 2 parts nitric acid, 3 parts sulfuric acid, 4 parts hydrofluoric acid, and 10 parts water by volume. Figures 35 and 36 show typical porosity both after mechanical polishing and after etching.

The coarse grained columbium showed little tendency toward extensive pit formation. This was to be expected, since this material was comparatively brittle for all test conditions except for the lowest hydrogen concentrations at room temperature. Rapid crack propagation took precedence over pit formation during straining at all test temperatures.

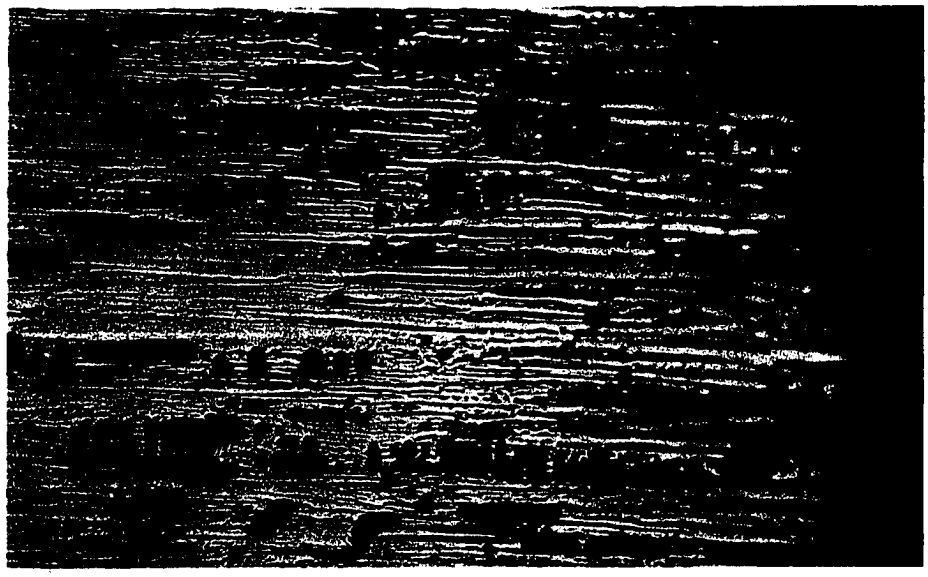

Figure 30. Porosity in stress relieved (wrought) columbium plus 207 ppm. hydrogen tested at 77°K. X200

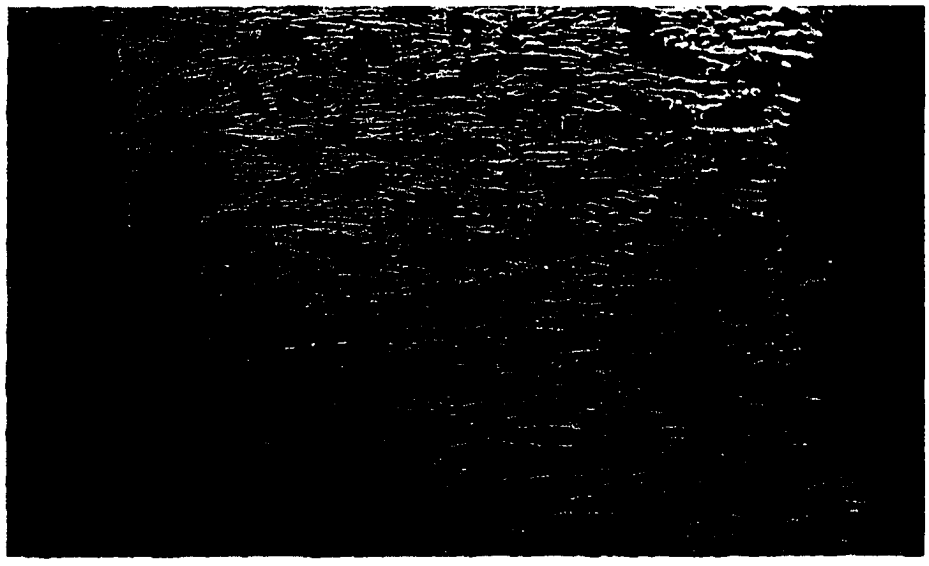

Figure 31. Porosity in stress relieved (wrought) columbium plus 114.8 ppm. hydrogen tested at 77°K. X200

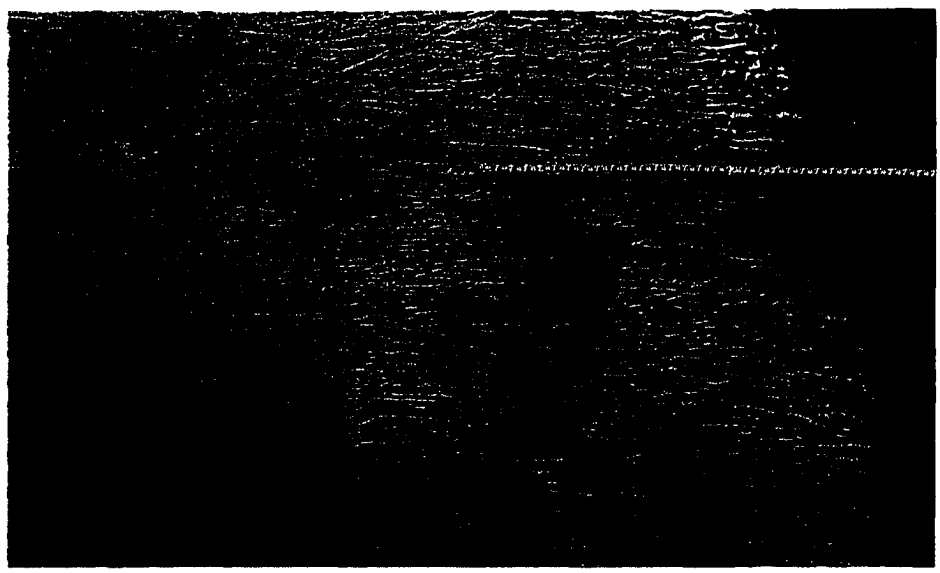

Figure 32. Porosity in stress relieved (wrought) columbium plus 47.1 ppm. hydrogen tested at 77°K. X200

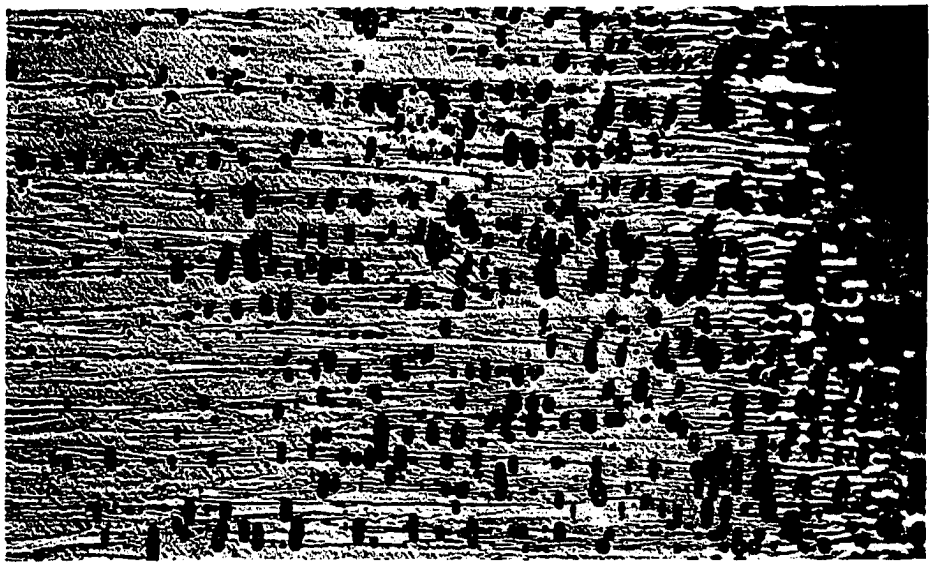

Figure 33. Localized porosity in stress relieved (wrought) columbium plus 47.1 ppm. hydrogen tested at 191°K. X200

Figure 34. Secondary cracks in recrystallized (1200°C) columbium plus 50.7 ppm. hydrogen tested at 191°K. X200

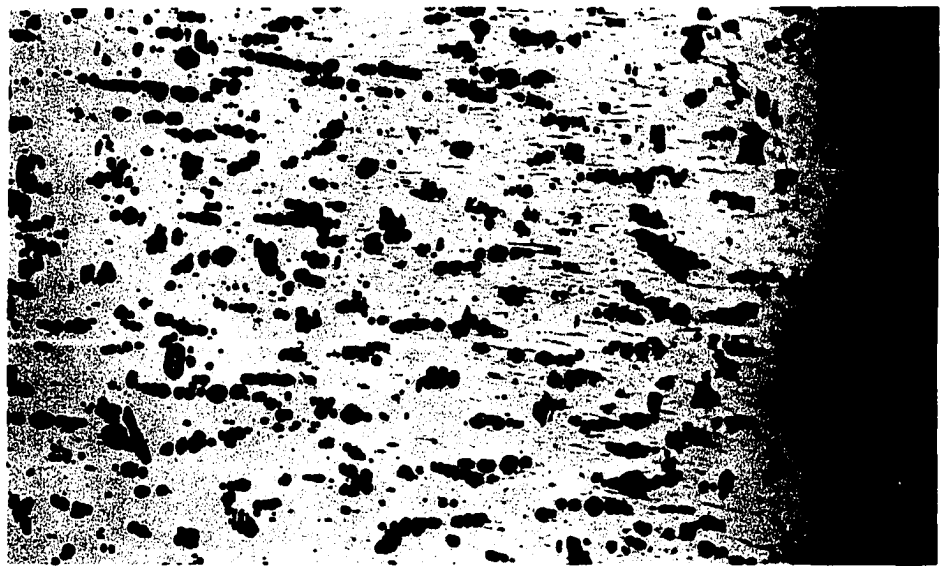

Figure 35. Porosity revealed in hydrogenated columbium after mechanical polishing. X200

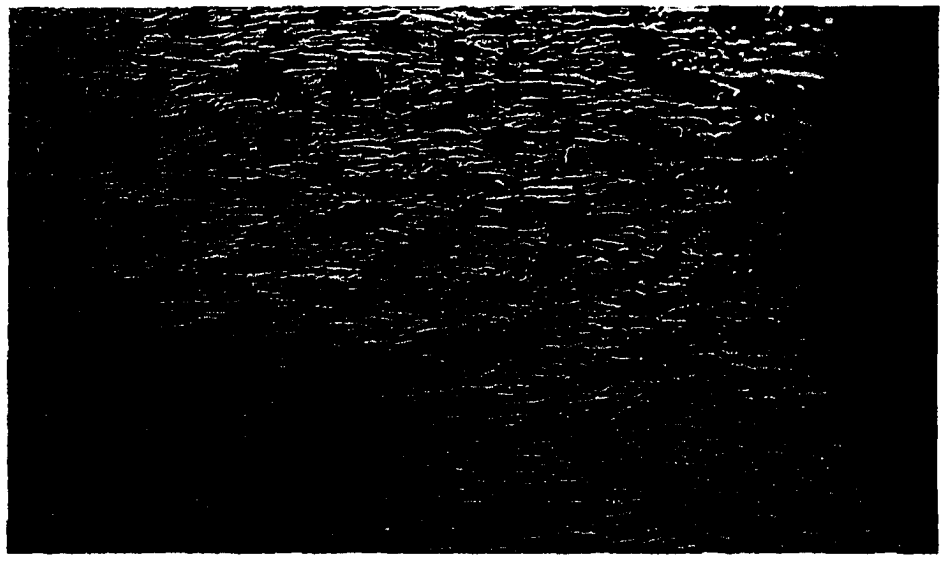

Figure 36. Porosity revealed in hydrogenated columbium after etching. X200

Examples of this can be seen in Figures 37 and 38, where secondary cracks can be observed. In some instances only one or two cracks were evidently responsible for failure since very little secondary cracking could be found. Cracking appeared to initiate both from internal sources and from surface fissures.

A rather interesting phenomenon occurred in the coarse grained columbium tested at 77°K. At hydrogen concentrations in excess of 100 ppm., a considerable amount of twinning was observed in the tensile samples (see Figure 39). Twinning was not observed in hydrogen-free material or in samples containing 50 ppm. hydrogen. Also, no twinning was found in the fine grained recrystallized or wrought columbium tested at this temperature irrespective of hydrogen concentration.

Comparison of metallographic results with tensile data

A comparison of the metallographic observations with the tensile ductility data yields some distinct correlations. First of all, in the finer structures tested at both 77°K and 300°K, the profuse pitting observed at higher hydrogen concentrations appears to be responsible for the decrease in ductility observed with increasing hydrogen concentration. However, the development of porosity is evidently associated with the higher ductility observed at 77°K and 300°K compared to the extreme embrittleness and rapid crack propagation found at 191°K. Apparently many of the voids and fissures formed during plastic straining at the two extreme test temperatures were in some way blunted during straining, while, at the intermediate temperature, a few rifts in the lattice expanded rapidly into cracks of sufficient length to propagate to failure, Thus, the formation and subsequent growth of voids observed as porosity

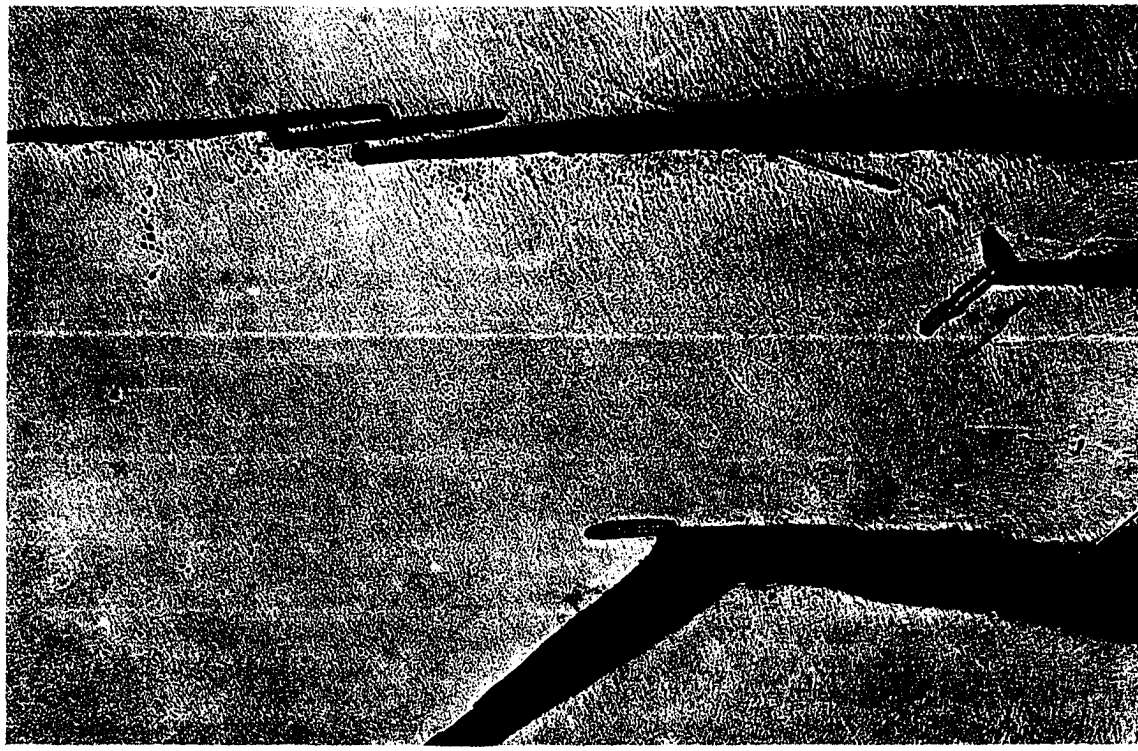

Figure 37. Secondary cracks in recrystallized (1850°C) columbium plus 47.8 ppm. hydrogen tested at 191°K. X200

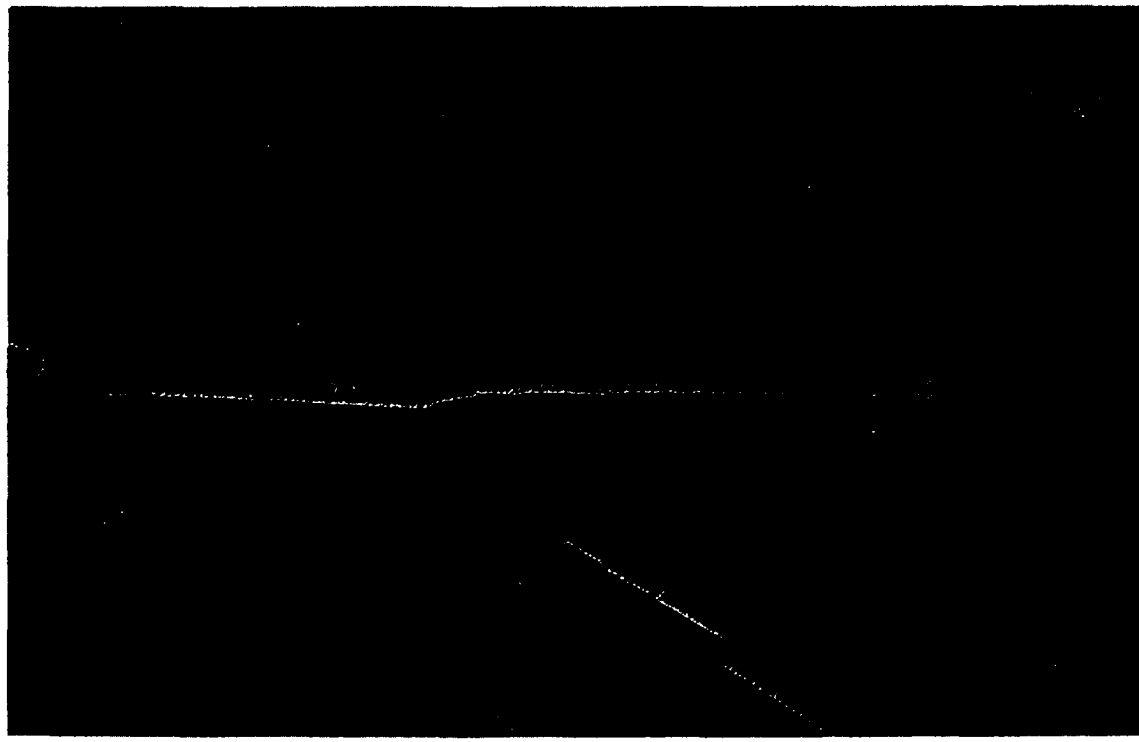

Figure 38. Secondary cracks in recrystallized (1850°C) columbium plus 47.8 ppm. hydrogen tested at 77°K. X200

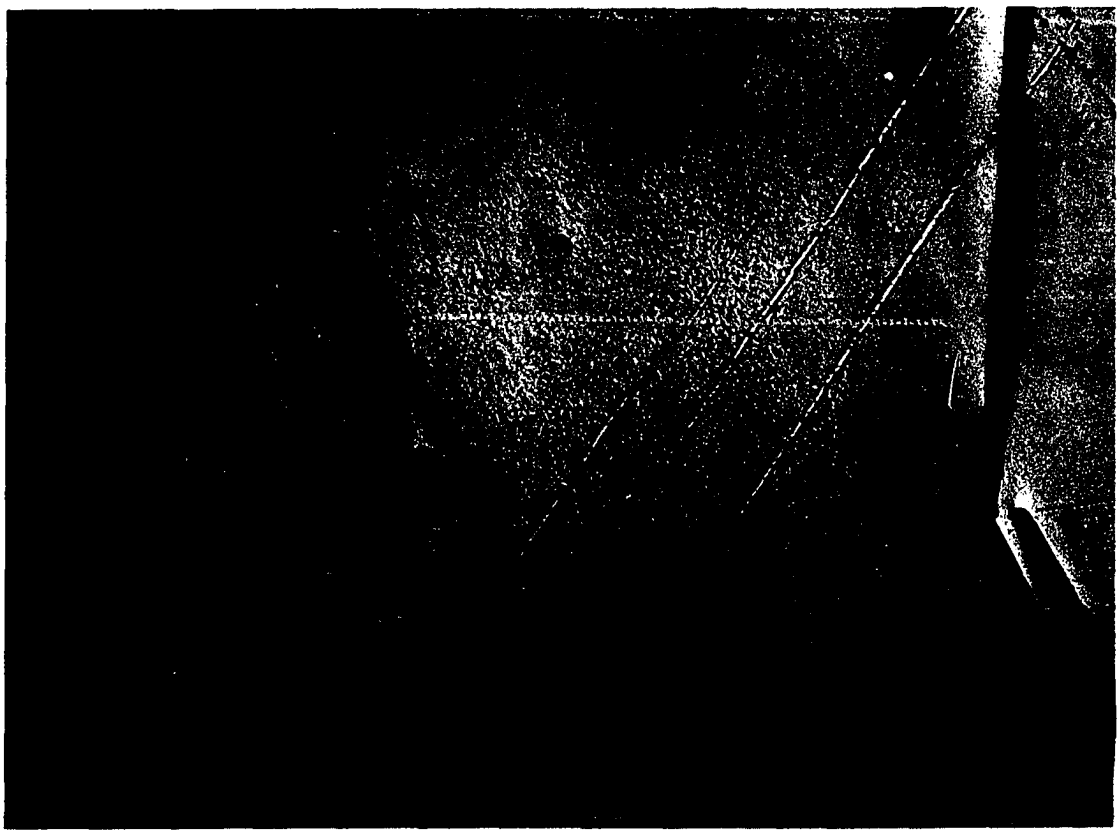

Figure 39. Twinning and secondary cracking in recrystallized (1850°C) columbium plus 115.1 ppm. hydrogen tested at 77°K. X200

on fractured samples is dependent on some ductility in the metal matrix.

Secondly, a coarsening of the microstructures seems to enhance embrittlement as is evidenced bythe lower ductility of the coarse grained hydrogenated columbium and the rapid crack propogation observed. Both phenomena were found at all test temperatures. To a certain degree the above results might be expected since the ductility of pure columbium was reduced by enlarging the grain size. Thus a higher susceptibility to the presence of hydrogen might be anticipated.

As was pointed out earlier, concentrations of hydrogen in excess of 100 ppm. resulted in nearly zero ductility at 77^{o}K in the coarse grained material, i.e., fracture took place before detectable yielding, along with profuse twinning. However, specimens with less than 50 ppm. hydrogen tested at this same temperature produced a measurable yield stress, and no twinning was observed. The first implication is that the addition of a critical quantity of hydrogen results in twinning during deformation at low temperatures with subsequent brittle failure. However, evidence has been accumulated to show that hydrogen has little, if any, effect on the ease of twinning in columbium. McHargue and McCoy (61) investigated columbium with up to 1000 ppm. hydrogen. Some cracks were noted at the intersections of twins with hydride platelets, although it was concluded that hydrogen additions had little effect on the twinning behavior of columbium. Adams, et al. (47) have shown that twins in coarse grained columbium may result from the shock generated by extremely brittle fractures at low temperatures. This seems to be a plausible explanation in this case since no serrations were observed in the stress-strain curves, nor was any audible "clicking" evident to

signify twinning during deformation. Furthermore, no twinning was evident in the finer structured materials as might be expected if the presence of hydrogen per se had any effect on twinning behavior.

Theoretical Aspects of Hydrogen Embrittlement of Columbium

The "knee" in the ductility vs. hydrogen concentration curves at 300°K (Figure 17) indicates that a critical quantity of hydrogen is necessary for embrittlement at this temperature. The concentration evidently is dependent on grain size. The sharp loss in ductility observed at a concentration of 160 ppm. for the wrought and fine grained recrystallized material is in good agreement with the room temperature tolerance limit observed by Longson (56). The abrupt onset of embrittlement strongly suggests that a process such as the precipitation of a brittle hydride phase may be occurring. Fast (16) has pointed out that, in the columbium-hydrogen system, where a miscibility gap occurs, it is more energetically favorable for the hydrogen to segregate to localized regions than to distribute itself randomly through the material. Thus, even though the observed tolerance limit is below the most recent determination of the bulk solubility limit at 300°K (approximately 500 ppm. (18)), brittle hydride particles could be precipitated under the influence of applied stress, and serve as nuclei for microcracks. In the concentration ranges studies in this investigation, such hydride precipitates would probably be of submicroscopic size and unresolvable by normal optical microscopy.

Hydrogen remaining in solution at 300°K in regions surrounding precipitates of microcracks could serve to aid crack propogation by

adsorbing on the internal surfaces of microcracks thereby lowering their surface energy (34), or by diffusing to crack tips and lowering the columbium bond strength (39). Such processes would continue until several microcracks propagated to sufficient lengths to cause failure, or until the cracks were blunted either through ductile yielding or depletion of the localized regions of hydrogen.

At 300°K, the mobility of hydrogen in columbium is high enough that diffusion of hydrogen to a crack from the surrounding regions, under the influence of applied stress, is sufficient to support crack propagation. However, since columbium is inherently ductile at this temperature, many of the cracks formed would be blunted by plastic flow at their tips. Thus, though a sharp loss in ductility will be observed due to the formation and propagation of microcracks near hydride precipitates, some ductility will be observed since many of the cracks will be blunted through ductile yielding. The porosity observed above the critical hydrogen concentration, along with the sharp loss in ductility observed, is evidence in support of such a postulate.

When the test temperature is lowered to 191°K, the solubility of hydrogen in columbium is greatly reduced. Also, the yield strength of the material will increase significantly over that at 300°K, which, in conjunction with the lower solubility, would lead to severe embrittlement at very low hydrogen concentrations. The presence of a few large secondary cracks and little porosity indicates that cracks formed early in the test were of nearly critical size and propagated almost immediately to failure. Comparison of the tensile data and the metallographic information obtained at this temperature with that obtained at 300°K

and 77°K suggests that a temperature at or near 191°K represents a critical temperature; at this point the low hydrogen solubility, high yield strength, and adequate hydrogen mobility combine to provide optimum conditions for crack propagation and brittle fracture. The hydrogen mobility, although presumably reduced at this lower temperature, is evidently still high enough that crack expansion is not retarded by the inability of hydrogen to diffuse to regions of stress concentration.

The ductility return noted at 77°K suggests that the process which controls hydrogen embrittlement in columbium undergoes a change in this temperature range. Presumably the solubility has been reduced to a very low level, and the yield strength of the material is several times that at 300°K. Both of these factors would favor crack nucleation and propagation. It appears therefore that the availability of hydrogen still in solution to expand a crack becomes the controlling factor. At 77°K, hydrogen mobility is quite low, so that hydrogen is unable to promote crack growth by diffusion to a crack from the surrounding lattice. The ductility and porosity observed in hydrogenated material support this concept.

At 300°K and 191°K, there is an apparent correlation between the solubility of hydrogen in columbium and the observed embrittlement. At 77°K, however, there is no such correlation. At 300°K additions of hydrogen have little effect until a critical concentration is reached where severe embrittlement occurs. Once a second phase has been nucleated and microcracks formed, the main factor controlling the rate of crack expansion is ductile yielding at crack tips since hydrogen mobility is reasonably high. At 191°K, a similar process evidently takes place except

that the solubility of hydrogen is reduced; the mobility of hydrogen is apparently still sufficient to support crack growth. At 77°K, however, where the mobility of hydrogen is nil, even though microcracks appear to form readily, they do not grow to a critical length. The numerous rounded pores in Figures 30 and 31 illustrate this behavior. The decrease in ductility with increasing hydrogen content is a gradual one and may be related to the number of microcracks formed rather than to the growth of a few such cracks.

Up to this point only the finer structured materials have been considered in detail. As was pointed out earlier, the increased susceptibility of the coarse grained columbium might be expected due to its overall lower initial ductility. This lower initial ductility in agreement with the observations of Seigle and Dickinson (2) which showed that, by increasing the grain size of columbium, the ductile-brittle transition temperature could be raised. Figure 40 shows an effect which could account for this phenomena. A number of cracks can be observed in unhydrogenated material deformed at 77°K, believed to be due to tearing at "river lines" formed by non-uniform elongation (26). Thus hydrogen could serve a dual role in coarse grained columbium. Embrittlement could occur not only by initiation and propagation of microcracks formed by precipitation of a hydride, but also through the segregation of hydrogen to cracks formed as described above.

In summary, observations on the ductility of hydrogenated columbium at 300°K, 191°K, and 77°K indicate that hydrogen embrittlement in dilute solutions gives rise to a "pseudo" ductile-brittle transition. This transistion is characterized by a return of ductility at 77°K. The

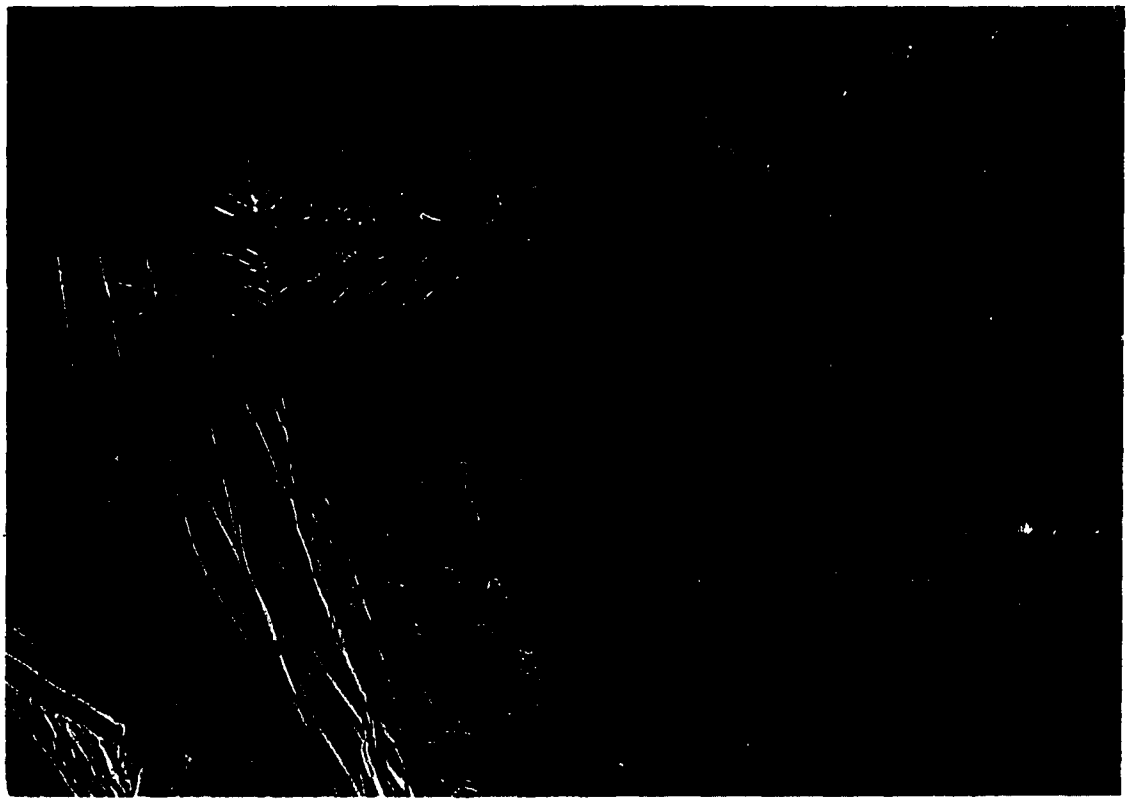

Figure 40. Secondary cracks at "river lines" in recrystallized (1850°C) columbium tested at 77°K. X200

embrittlement observed with increasing hydrogen content at 77°K may be characterized as an increase in the normal ductile-brittle transition temperature induced by the addition of an impurity.

Effects of Strain Rate and Prestrain

As is evident from Table 7 in Chapter III, slow strain rate embrittlement is not observed in columbium at room temperature. Cottrell's theory of brittle fracture states that embrittlement will occur when (22):

$$(\sigma_i d^{1/2} + k_y)K_y \geq \beta \mu \gamma \qquad (9)$$

where β is a constant approximately equal to unity, μ is the modulus of rigidity, and γ is the crack surface energy. The other terms are as defined in the Petch equation (Equation 5). As can be seen, embrittlement may be enhanced if, in some way, σ_i could be increased. The results in Table 7 show that by raising the strain rate, the yield strength of columbium was increased, as was observed by Wessel et al. (53). As noted earlier, σ_i is considered to be a function of strain rate. Thus, in the presence of a hydrogen concentration sufficient to form microcracks, conditions for propagation of these cracks are enhanced by an increase in strain rate. The lower ductilities observed at higher hydrogen concentrations tend to support this premise.

As was shown in Chapter III, prestraining has only a slight, if any, effect on the hydrogen embrittlement of columbium with the exception of the fine grained recrystallized material with a hydrogen concentration in excess of 160 ppm. The differences in ductility at high hydrogen concentrations between the fine grained recrystallized

material and the wrought material is interesting in that there was no difference in a simple tensile test at 77°K. It appears quite possible that, in the recrystallized columbium, the porosity observed at 300°K developed in the early stages of deformation. Hydrogen segregation to these cracks would occur quite rapidly at room temperature. Thus retesting at 77°K, after a prestrain of 5 per cent at 300°K, would favor rapid propagation of such cracks. In the wrought material, however, no porosity was observed at 300°K, thus a similar prestrain treatment would be expected to have little effect on the low temperature ductility. Porosity in prestrained tensile samples is shown in Figures 41 and 42.

The coarse grained columbium prestrained at 300°K exhibited twinning when tested to failure at 77°K as can be seen in Figure 43. As in the case of a simple tensile test at 77°K, the twinning was associated with failure before detectable yielding. The only difference noted was that, in the prestrained sample, the twinning and associated brittle failure occurred at a lower hydrogen concentration. The twinning again appears to be the result of the shock of brittle fracture as was discussed earlier.

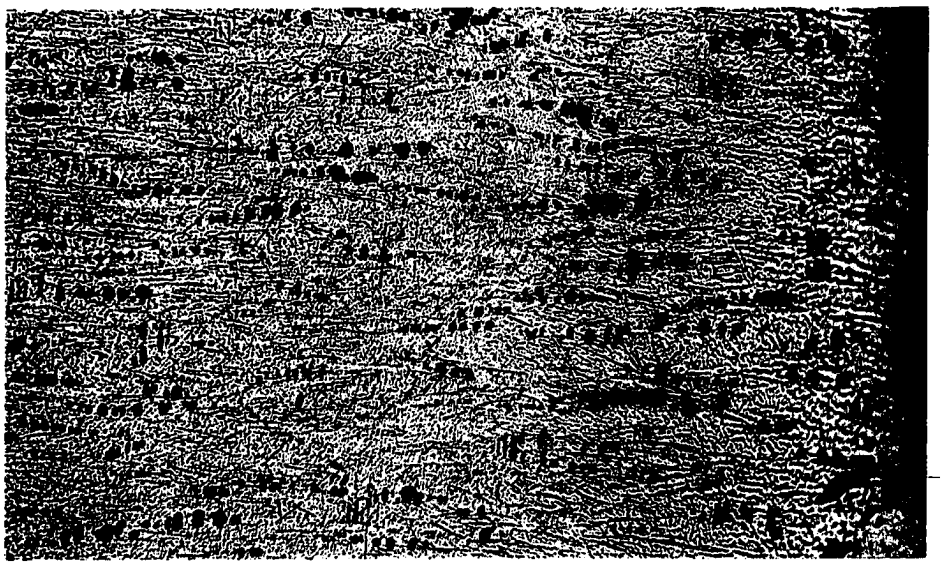

Figure 41. Porosity in stress relieved (wrought) columbium plus 166 ppm. hydrogen tested at 77°K after 5% prestrain at 300°K. X200

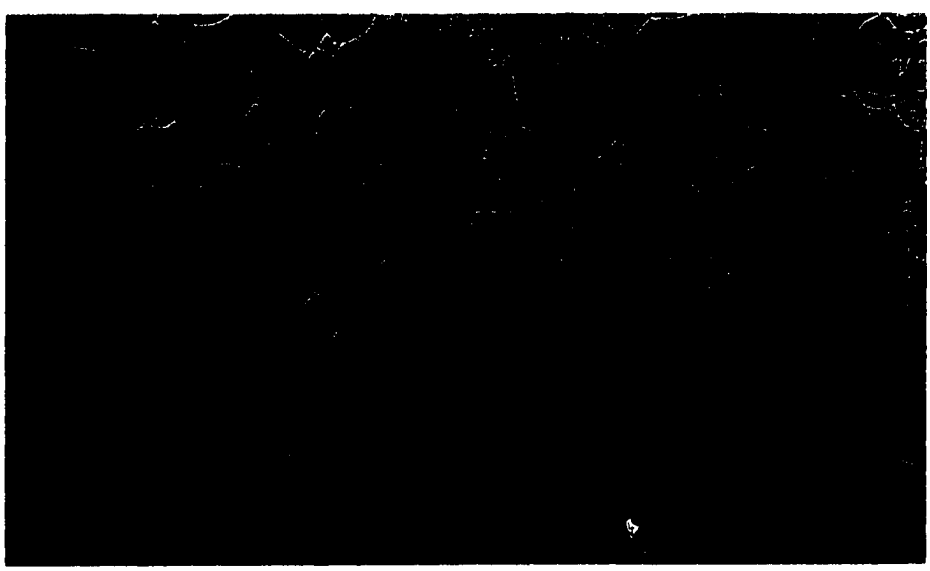

Figure 42. Porosity in recrystallized (1200°C) columbium plus 205 ppm. hydrogen tested at 77°K after 5% prestrain at 300°K. X200

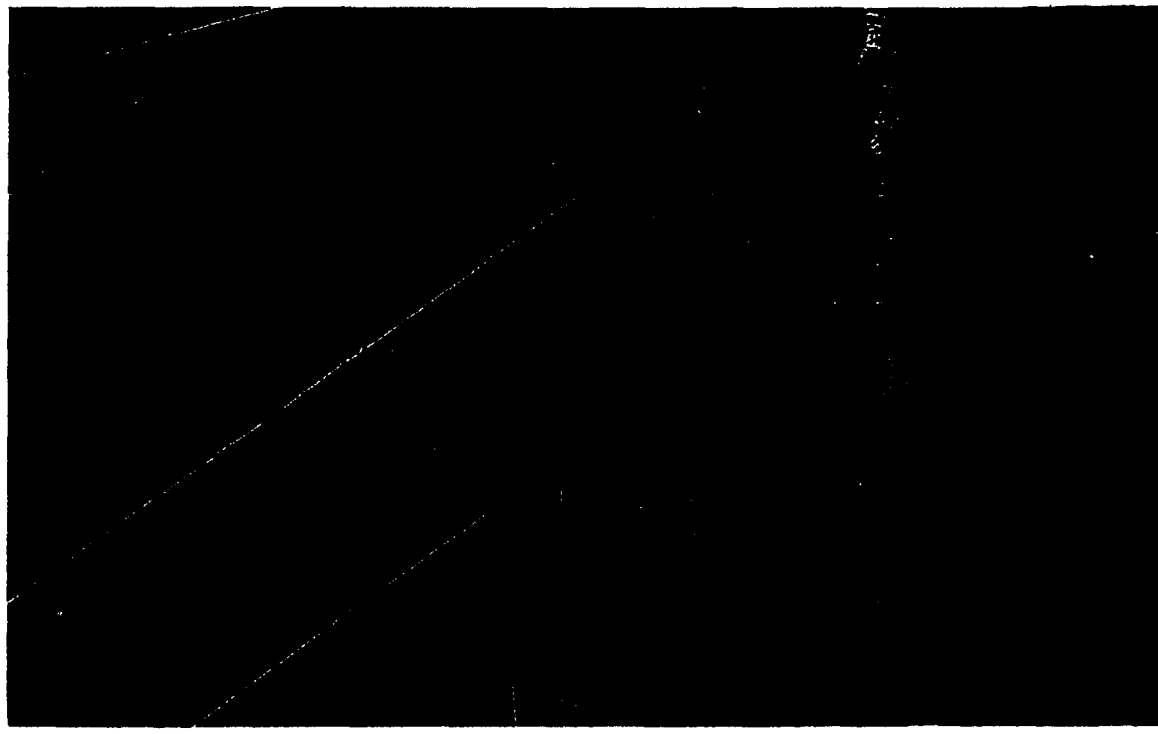

Figure 43. Twinning and secondary cracking in recrystallized (1850°C) columbium plus 47.8 ppm. hydrogen tested at 77°K after 5% prestrain at 300°K. X200

CHAPTER V

SUMMARY AND CONCLUSIONS

1) The effects of temperature and grain size on the sorption kinetics of hydrogen in columbium have been studied. In addition, the effects of hydrogen concentration, temperature, microstructure, and strain rate on the mechanical properties of hydrogenated columbium were evaluated.

2) It was found that chemical etching of columbium produces a surface barrier to sorption. The sorption of hydrogen may be described by a diffusion controlled reaction in the temperature range 600°C - 750°C provided that this surface barrier is removed by abrading. The activation energy for diffusion of hydrogen in columbium was found to be about 9000 cal./mol. Below a temperature of 600°C, the sorption process evidently undergoes a change from a diffusion controlled reaction to a surface controlled reaction. Bulk or volume diffusion appears to mask diffusion along short circuiting paths such as grain boundaries, as the sorption behavior was insensitive to grain size at all temperatures studied.

3) Hydrogen has little or no effect on the strength of columbium. In addition, no increase in work hardening is associated with the presence of hydrogen.

4) Hydrogen will embrittle columbium; the embrittlement is a function of hydrogen concentration, temperature, and microstructure. At 300°K an abrupt loss in ductility is observed at a hydrogen concentration of about 160 ppm. whereas, at 77°K the ductility of columbium is reduced more gradually with increasing hydrogen concentration. This results in a ductile-brittle-ductile transistion as the temperature is lowered from 300°K to 77°K. Maximum embrittlement is observed at a temperature near 191°K.

5) Coarse grained columbium is more sensitive to the presence of hydrogen than either wrought or fine grained material. This increased sensitivity is believed to be related to the lower initial ductility of the coarse grained structure.

6) The addition of hydrogen results in the development of porosity in fractured tensile samples of fine grain recrystallized material and wrought material. At 300°K voids are evident in the recrystallized columbium at hydrogen concentrations above 160 ppm., but is virtually eliminated at 114 ppm. The wrought material shows no porosity at 300°K, but rather, blunted surface cracks. At 191°K, a small amount of pitting was found near the fracture surface of the wrought material. At 77°K both the fine grained recrystallized and wrought structures exhibited porosity. In both cases, pit size increased gradually with increasing hydrogen concentration. The pits appear to form preferentially at grain boundaries. Factors favoring crack propagation appear to preclude pit formation in the coarse grained material at all test temperatures.

7) The formation of microcracks in hydrogenated columbium appears to be associated with the precipitation of a brittle hydride in

regions of high hydrogen concentration. The lowering of crack surface energy, due to adsorbed hydrogen, or the lowering of columbium atom bond strength due to diffusion of hydrogen to crack tips is presumed to be responsible for crack propagation.

8) At 300°K crack propagation is evidently controlled by the ability of columbium to flow plastically at crack tips, whereas at 77°K, the rate of diffusion of hydrogen to microcracks appears to be the controlling factor.

9) No slow strain rate embrittlement is observed in columbium at 300°K. An increase in strain rate results in an increased yield strength and, at the 300°K hydrogen tolerance limit, a loss in ductility compared to lower strain rates. This ductility loss appears to be due to the observed increase in yield strength. Prestraining at 300°K has little overall effect on the ductility of hydrogenated columbium at 77°K.

LIST OF REFERENCES

1. Hahn G. T., Gilbert A., and Jaffee R. I., Refractory Metals and Alloys II, Semchyshen M. and Perlmutter I., ed., Interscience Publishers, New York, 1963, p. 23.

2. Seigle L. L. and Dickinson C. D., Refractory Metals and Alloys II, Semchyshen M. and Perlmutter I., ed., Interscience Publishers, New York, 1963, p. 65.

3. Hultgren R., Orr R. L., Anderson P. P., and Kelly K. K., Selected Values of Thermodynamic Properties of Metals and Alloys, Wiley and Sons, New York, 1963, p. 188.

4. McKinley T. D., Paper presented before Regional AIME meeting, Cleveland, 1957.

5. Elliott R. P. and Komjathy S., Armour Research Foundation Report No. ARF 2120-8, May, 1960.

6. Albrecht W. M., Mallett M. W., and Goode W. D., Jour. Electrochem. Soc., 105, 1958, p. 219.

7. Albrecht W. M., Mallett M. W., and Goode W. D., Jour. Electrochem. Soc., 106, 1959, p. 981.

8. Gulbransen E. A. and Andrew K. F., Jour. Met. Trans. AIME, 188, 1950, p. 586.

9. Paxton H. W. and Sheehan J. M., Atomic Energy Commission Report No. NYO-8040, September 1957.

10. Sieverts A. and Moritz H., Z. anorg. u. allgem. Chem., 247, 1941, p. 124.

11. Imgram A. G., Bartlett E. S., and Ogden H. R., Trans. Met. Soc. AIME, 227, 1963, p. 131.

12. Eustice A. L. and Carlson O. N., Trans. ASM, 53, 1961, p. 501.

13. Wilcox B. A., Brisbane A. W., and Klinger R. F., Trans. ASM, 55, 1962, p. 179.

14. Wood T. W. and Daniels R. D., Trans. Met. Soc. AIME, 223, 1965, p. 898.

15. Fast J. D., Phillips Tech. Rev., 6, 1941, p. 365.

16. Fast J. D., Interaction of Gases and Metals I, Academic Press, New York, 1965.

17. Cotterill P., Progress in Materials Science, 9, Chalmers B., ed., Pergamon Press, London, 1961, p. 201.

18. Walter R. J. and Chandler W. T., Trans. Met. Soc. AIME, 223, 1965, p. 762.

19. Smithells C. J., Metals Reference Book II, Butterworths, London, 1962, p. 569.

20. Webb R. W., North American Aviation Report No. NAA-SR-10462, July, 1965.

21. Livanov V. A., Bukhanova A. A., Kolachev B. A., Hydrogen in Titanium, Daniel Davy & Co., New York, 1965, p. 92.

22. Cottrell A. H., Trans. Met. Soc. AIME, 212, 1958, p. 192.

23. Petch N. J., Progress in Metal Physics, 5, Chalmers B. and King R., ed., Pergamon Press, London, 1954, p. 1.

24. Griffith A. A., Phil. Trans. Roy. Soc., A221, 1920, p. 470.

25. Stroh A. N., Adv. in Phys., 6, 1957, p. 418.

26. Tetelman A. S., Fracture of Solids, Drucker D. C. and Gilman J. J., ed., Interscience Publishers, New York, 1963, p. 671.

27. Hobson J. D. and Sykes C., Journ. Iron and Steel Inst., 169, 1951, p. 209.

28. Hill M. L. and Johnson E. W., Trans. Met. Soc. AIME, 215, 1959, p. 717.

29. Siede A. and Rostoker W., Trans. Met. Soc. AIME, 212, 1958, p. 852.

30. Tetelman A. S. and Robertson W. D., Trans. Met. Soc. AIME, 224, 1962, p. 775.

31. Maringer R. E., Swetnam E. B., Marsh L. L., and Manning G. K., National Advisory Committee for Aeronautics Technical Note TN 4328, Sept., 1958.

32. Brown J. T. and Baldwin W. M., Trans. AIME, 6, 1954, p. 298.

33. Zapffe C. A. and Sims C. E., Trans. AIME, 145, 1941, p. 225.

34. Petch N. J., Phil. Mag., Series 8, 1, 1956, p. 331.

35. de Kazinczy F., Journ. Iron and Steel Inst., 189, 1958, p. 37

36. Bastien P. G., Physical Metallurgy of Stress Corrosion Fracture, Rhodin T. N., ed., Interscience Publishers, New York, 1959, p. 311.

37. Garofalo F., Chou Y. T., and Ambegaokar V., Acta. Met., 8, 1960, p. 504.

38. Morlet J. G., Johnson H. H., and Troiano A. R., Jour. Iron and Steel Inst., 189, 1958, p. 37.

39. Troiano A. R., Trans. ASM, 52, 1960, p. 52.

40. Roberts B. W. and Rogers H. C., Trans. AIME, 8, 1956, p. 1213.

41. Eustice A. L. and Carlson O. N., Trans. Met. Soc. AIME, 221, 1961, p. 238.

42. Van Fossen R. H., M. S. Thesis, Iowa State University, Feb., 1965.

43. Hunes J., Anctil A. A., and Kula E. B., U. S. Army Materials Research Agency Report No. AMRA TR 64-22, August, 1964.

44. Weissmann J., Lement B. S., Dickinson C. D., Refractory Metals and Alloys II, Semchyshen M. and Perlmutter I., ed., Interscience Publishers, New York, 1963, p. 117.

45. Smallman R. E., Modern Physical Metallurgy, Butterworths, London, 1962, p. 246.

46. Wilcox B. A. and Huggins R. A., Jour. Less. Com. Met., 2, 1960, p. 292.

47. Adams M. A., Roberts A. C., and Smallman R. E., Acta Met., 8, 1960, p. 328.

48. Johnson A. A., Acta Met., 8, 1960, p. 737.

49. Tankins E. S. and Maddin R., Columbium Metallurgy, Douglass D. L. and Kunz F. W., ed., Interscience Publishers, New York, 1960, p. 343.

50. Conrad H., Phil. Mag., 5, 1960, p. 745.

51. Conrad H. and Hayes W., Trans. ASM, 56, 1963, p. 125.

52. Conrad H. and Hayes W., Trans. ASM, 56, 1963, p. 249.

53. Wessel E. T., France L. L., and Begley R. T., Columbium Metallurgy, Douglass D. L. and Kunz F. W., ed., Interscience Publishers, New York, 1960, p. 459.

54. Keh A. S. and Weissmann S., Electron Microscopy and the Strength of Crystals, Thomas G. and Washburn J., ed., Interscience Publishers, New York, 1963, p. 881.

55. Van Torne L. I. and Thomas G., Acta Met., 11, 1963, p. 881.

56. Longson B., United Kingdom Atomic Energy Authority TRG Report No. 1035(C), 1966.

57. Wood T. W., Ph.D. Thesis, University of Oklahoma, August, 1962.

58. Wilson A. H., Phil. Mag., Ser. 7, 39, 1948, p. 48.

59. Crank J., Mathematics of Diffusion, Clarendon Press, Oxford, 1956.

60. Gelezunas V. L., Conn P. K., and Price R. H., Jour. Electrochem. Soc., 110, 1963, p. 797.

61. Mc Hargue C. J. and Mc Coy H. E., Trans. Met. Soc. AIME, 227, 1963, p. 1170.

APPENDIX I

CALIBRATION OF HYDROGENATION SYSTEM

A description of the construction and operation of a hydrogenation system of the type employed here has been given by Wood (57). A brief review of the use of the system employed in this investigation will be given here.

Considering hydrogen to be an ideal gas, it has been shown that (57)

$$\bar{r} = \frac{2\ V_e\ m}{R\ M}\ \frac{P_b V_b}{V_e T_{si}} - \frac{P_f}{T_{sf}} \qquad (1)$$

where $\bar{r}$ is the H/Nb atomic ratio desired, m is the atomic weight of columbium, M is the mass of the columbium specimen(s), R is the ideal gas constant in appropriate units, P_f is the final equilibrium pressure of hydrogen for any desired $\bar{r}$ at a given temperature, P_b is the starting pressure in the calibrated reservoir, V_b is the volume of the reservoir, T_{si} and T_{sf} are the initial and final ambient temperatures, and V_e is the "effective" or "hot" volume of the system.

All of the terms above are self explanatory with the exception of V_e which requires some clarification. As was discussed in Chapter II, an initial quantity of hydrogen is pumped into the calibrated reservoir, while the reaction tube remains under vacuum. This quantity is proportional to the product $P_b V_b$. When the gas is expanded into the reaction

tube, a new PV product, just prior to sorption, is obtained. This second PV product depends not only on the physical volume of the entire system, but also on the furnace temperature, since the pressure over the specimen will increase as the temperature increases. To account for this, a pseudo or "effective" volume of the system must be determined at several furnace temperatures.

This calibration was accomplished by first determining the volume of the reservoir by filling it with water. Hydrogen gas at a given pressure, P_b, in the reservoir, was allowed to expand into the reaction chamber with no specimen present. Thus:

$$P_b V_b = P_e V_e \qquad (2)$$

where P_e is the actual pressure measured at any furnace temperature. V_e was computed and graphed as a function of furnace temperature. These results for the system used here are plotted in Figure 44. V_e alone should be independent of P_b. This was verified by determining V_e at several values of P_b for each furnace temperature. The amount of hydrogen absorbed by a columbium specimen will be a function of the difference between $P_e V_e$ and $P_f V_e$.

It has been shown from elementary considerations that the parts by weight of hydrogen per million parts of Cb-H solution is given by (57):

$$\text{ppm} = \frac{10^6 \, \bar{r}}{92.91 + \bar{r}} \qquad (3)$$

where 92.91 is the atomic weight of columbium. Thus, for any desired ppm., a value of $\bar{r}$ may be calculated. The corresponding value of P_f may be determined from appropriate solubility data at a given temperature.

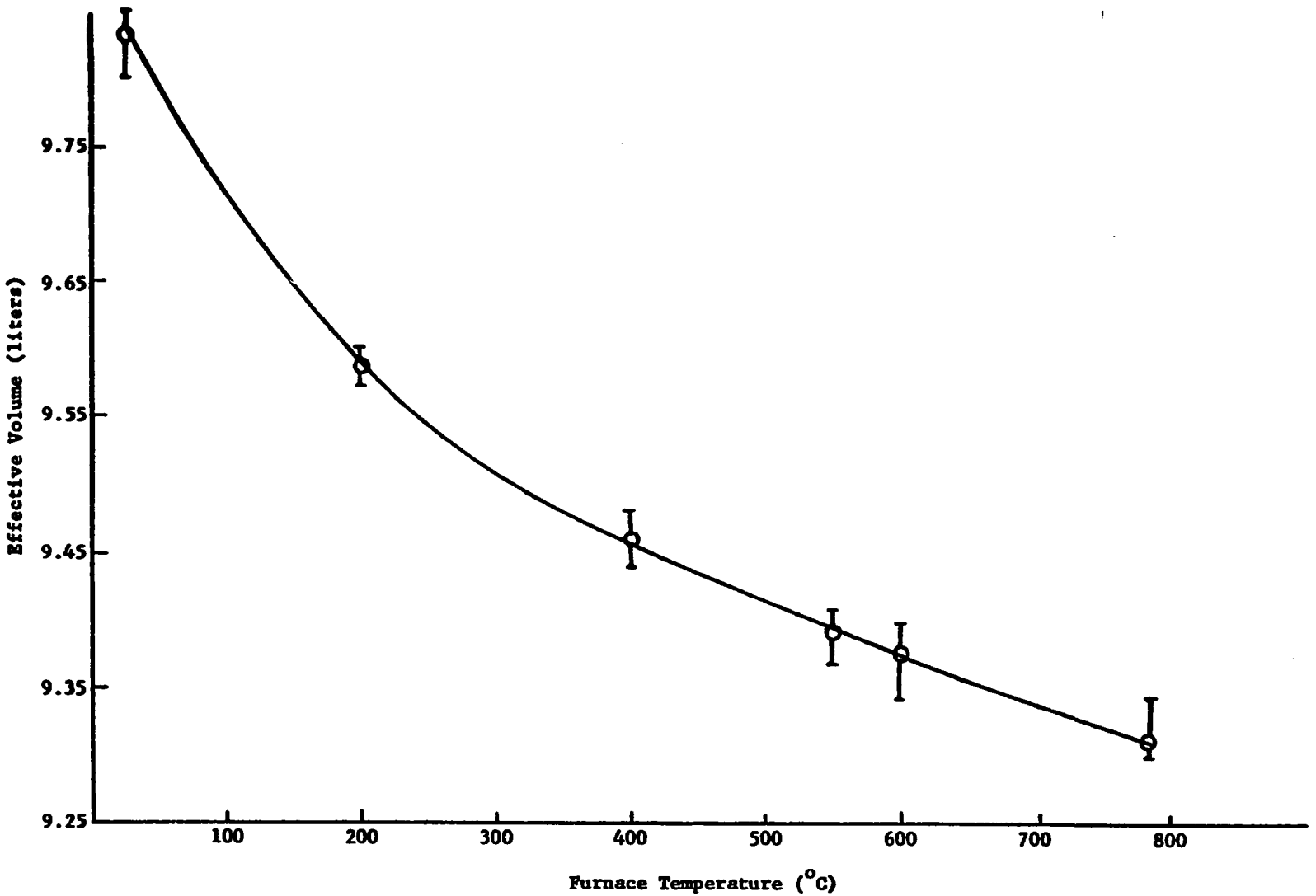

Figure 44. Effective volume of hydrogenation system as a function of furnace temperature.

Knowing $\overline{r}$ and P_f, Equation (1) will give the necessary value of P_b to obtain a desired hydrogen concentration. The solubility data used in this investigation was that of Elliott and Komjathy (5) shown in Figure 45.

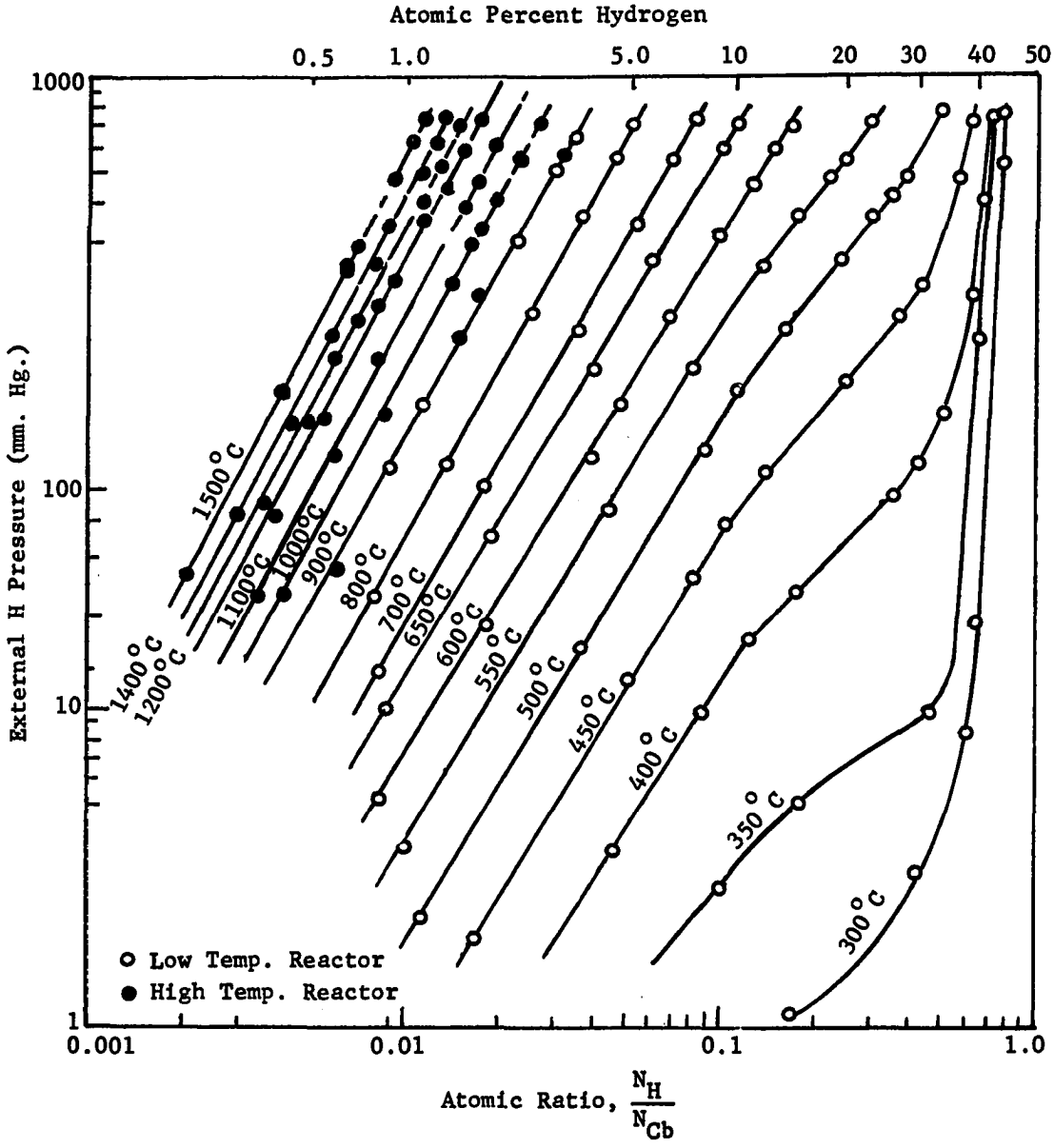

Figure 45. Equilibrium isotherms in the columbium-hydrogen system after Elliott and Komjathy (5).

APPENDIX II

SOLUTION OF DIFFUSION EQUATION WHERE AMOUNT OF DIFFUSING SUBSTANCE IS FINITE

The derivation to be presented here is taken directly from the work of Wilson (see Ref. 58). A discussion of this particular solution to the diffusion equation may also be found in Crank's monologue (see Ref. 59).

We use cylindrical polar coordinates, and consider a cylinder to be immersed in a bath of finite volume with initial concentration C_0 per unit volume. The cylinder occupies space $r \leq a$, and the cross section of the bath is $\underline{A}$, excluding the space occupied by the cylinder. We assume unit length of both the cylinder and the bath so that only the radial coordinate of diffusion appears explicitly.

For radial diffusion in a solid right circular cylinder, Fick's second law may be written as:

$$\frac{\partial C}{\partial t} = D \frac{1}{r} \frac{\partial}{\partial r} \left(r \frac{\partial C}{\partial r} \right) \tag{1}$$

where C is the concentration of diffusing substance, r is the radius, t is the time, and D is the diffusivity. Let $y(r,t)$ equal the amount of solute contained inside the cylinder at radius r and time t. Therefore

$$y(r,t) = 2\pi \int_0^r r'C(r',t)dr' \tag{2}$$

Now:

$$\frac{\partial(y)}{\partial t} = 2\pi \int_0^r r' \frac{\partial}{\partial t} C(r',t)dr' \tag{3}$$

or:

$$\frac{\partial(y)}{\partial t} = 2\pi D \int_0^r \frac{\partial}{\partial r'} \left(r' \frac{\partial C}{\partial r'}\right) dr' \tag{4}$$

$$= 2\pi D\, r \frac{\partial C}{\partial r} \tag{5}$$

since by symmetry, $\partial C/\partial r = 0$ at $r = 0$

Now:

$$\frac{\partial(y)}{\partial r} = 2\pi rC \tag{6}$$

$$\frac{\partial^2(y)}{\partial r^2} = 2\pi\left[C + r \frac{\partial C}{\partial r}\right] \tag{7}$$

$$= 2\pi\left[\frac{1}{2\pi r} \frac{\partial(y)}{\partial r} + r \frac{\partial C}{\partial r}\right] \tag{8}$$

Combining (8) with (5):

$$\frac{\partial(y)}{\partial t} = D\, r \frac{\partial}{\partial r} \left(\frac{1}{r} \frac{\partial(y)}{\partial r}\right) \tag{9}$$

which is the differential equation to be solved.

The boundary condition must now be specified. From (6), the concentration at the surface of the cylinder is given by:

$$C(a,t) = \frac{1}{2\pi a} \frac{\partial(y)}{\partial r}_{r=a} \tag{10}$$

Also the total concentration of solute in the bath and in the cylinder

must be a constant at any time t, and, since there must be a homogeneous distribution of solute, the concentration at the surface of the cylinder must equal that in the bath. Therefore:

$$AC(a,t) + y(a,t) = AC_0 \quad (r=a) \tag{11}$$

or:

$$\frac{A}{2\pi a} \left.\frac{\partial(y)}{\partial r}\right|_{r=a} + y(a,t) = AC_0 \quad (r=a) \tag{12}$$

We also have the initial condition that $y = 0$ for $0 \leq r \leq a$ at $t = 0$.

It is convenient to change to a new independent variable $f(r,t)$ defined by:

$$y(r,t) = \frac{AC_0\, r^2}{a^2 + A/\pi} + f(r,t) \tag{13}$$

The new variable now satisfies the differential equation:

$$\frac{\partial r}{\partial t} = D\, r \frac{\partial}{\partial r} \left(\frac{1}{r} \frac{\partial f}{\partial r}\right) \tag{14}$$

the boundary condition:

$$\frac{A}{2\pi a} \left.\frac{\partial f}{\partial r}\right|_{r=a} + f(a,t) = 0 \quad (r=a) \tag{15}$$

and the initial condition:

$$\frac{AC_0}{a^2 + A/\pi} + f(r,0) = 0 \quad (0 \leq r \leq a,\ t = 0) \tag{16}$$

The elementary solutions of (14) are:

$$f_n(r,t) = e^{-P_n t}\, f_n(r) \tag{17}$$

where $f_n(r)$ are solutions of:

$$\frac{d^2 f_n}{dr^2} - \frac{1}{r}\frac{df_n}{dr} + \frac{1}{D} P_n f_n = 0 \tag{18}$$

The solution of (18) which is regular at r = 0 is $rJ_1(q_n r/a)$ where J_1 is the Bessel function of order 1 and $q_n^2/a^2 = p_n/D$, q_n being taken strictly positive.

Now define two parameters:

$$\alpha = A/\pi a^2, \; \beta = D/a^2 \tag{19}$$

The general solution of (14) is:

$$f = \sum_n B_n e^{-P_n t} \, rJ_1(q_n r/a) \tag{20}$$

The boundary condition (15) gives:

$$\frac{A}{2\pi a}\frac{d}{dr}\{rJ_1(q_n r/a)\}_{r=a} + aJ_1(q_n) = 0 \tag{21}$$

which by the use of the relation:

$$\frac{d}{dZ}\{ZJ_1(Z)\} = ZJ_0(Z) \tag{22}$$

along with (19) becomes:

$$\alpha \, q_n J_0(q_n) + 2J_1(q_n) = 0 \tag{23}$$

To determine the constants B_n, the relation

$$\int_0^a \frac{1}{r} f_m(r)dr = \int_0^a rJ_1(q_m r/a)J_1(q_n r/a)dr = 0 \quad (m \neq n) \tag{24}$$

is employed. The initial condition gives:

$$\frac{AC_0 \, r^2}{a^2 + A/\pi} + \sum_n B_n rJ_1(q_n r/a) = 0 \quad (0 \leq r \leq a, \; t = 0) \tag{25}$$

Multiplying by $J_1(q_m r/a)$, integrating, and using (24), we obtain:

$$B_m \int_0^a r\{J_1(q_m r/a)\}^2 dr + \frac{AC_0}{a^2 + A/\pi} \int_0^a r^2 J_1 \frac{q_m r}{a} \, dr = 0 \tag{26}$$

This can be simplified by using the relations:

$$\int_0^X Z^2 J_1(Z) dZ = X^2 J_2(X) \tag{27}$$

$$2 \int_0^X Z\{J_1(Z)\}^2 dZ = X^2\{J_1(X)\}^2 - 2XJ_1(X)J_0(X) + X^2\{J_0(X)\}^2 \tag{28}$$

$$XJ_2(X) = 2J_1(X) - XJ_0(X) \tag{29}$$

After substituting for $J_1(q_n)$ from (23),

$$B_n = \frac{8a\ AC_0}{a^2 + A/\pi} \frac{1 + \alpha}{q_n(4 + 4\alpha + \alpha^2 q_n^2)} \frac{1}{J_0(q_n)} \tag{30}$$

The total amount of solute in the cylinder at time t is $M_t = y(a,t)$ and the equilibrium amount at $t = \infty$ is:

$$M_\infty = \frac{a^2\ AC_0}{a^2 + A/\pi} = \frac{AC_0}{1 + \alpha} \tag{31}$$

Thus:

$$M_t = M_\infty + \sum_n B_n a J_1(q_n) e^{-P_n t}$$

which, using (23) and (30) becomes:

$$\frac{M_t}{M_\infty} = 1 - \frac{4\alpha(1 + \alpha)}{4 + 4\alpha + \alpha^2 q_n^2} e^{-\beta q_n^2 t}$$

where the q_n's are positive non-zero roots of (23).

Crank has graphed Equation (32) for various percentages of the

total amount of solute taken up from the bath by the cylinder in the form M_t/M_∞ vs. $(Dt/a^2)^{1/2}$. Note that the parameter α and the percentage of uptake are related by:

$$\% \text{ uptake} = 1/(1 + \alpha) \tag{33}$$

Thus, for a given percentage of uptake, an α can be obtained and a theoretical curve plotted. Such curves are approximately linear in the initial portion (see Figure 4) and the slope increases as the percentage of uptake increases. As was mentioned in Chapter III, experimental data in the form M_t/M_∞ (or C/C_0) vs. $t^{1/2}$ may be fitted to a theoretical curve, determined by the percentage of uptake used experimentally, through a proper choice of D.

A difficulty arises in the application of Equation (31) in that the series converges very slowly for the small values of Dt/a^2 used in this investigation. Thus computing a theoretical curve for each percentage of uptake becomes quite tedious and inconvenient. However, from the theoretical curves of Crank, it can be seen that, for small percentages of uptake, the effect of percentage of uptake on the slope of the theoretical curve is small. Since, in this work, the percentage of uptake rarely exceeded 10 per cent, all of the experimental curves were fitted to the 0 per cent uptake curve as determined by Crank with presumably minimal error.

A second difficulty which arises is that Equation (32) neglects diffusion along the axis of the cylinder, i.e., it considers radial diffusion only. To circumvent this problem, the D values obtained were calculated only from a fit of the linear portions of the experimental C/C_0 curves to the linear portion of the theoretical curve. Thus the D values were obtained at short diffusion times were logitudinal diffusion along the axis of the cylinder can be reasonably neglected.

APPENDIX III

TENSILE PROPERTIES OF HYDROGENATED COLUMBIUM

TABLE 8

MECHANICAL PROPERTIES OF PURE COLUMBIUM

Spec. No.	Structure	Test Temp. °K	Strain Rate ipm/0.750	Prop. Limit Load/A_0	0.2% Offset Yield Strength Load/A_0	Ultimate Tensile Strength Load/A_0	Estimated Fracture Strength Load/A_f	% Elong.	% RA
2A-5	As swaged	300	0.02	50,400	55,300	58,300	247,400	21.5	94.0
2A-1	As swaged	191	0.02	61,100	66,000	70,800	217,500	28.4	89.2
2A-2	As swaged	77	0.02	125,100	129,400	129,400	255,700	20.1	77.5
2A-20	Stress Rel. 750°C	300	0.02	38,500	41,800	50,800	277,500	25.7	95.7
2A-19	Stress Rel. 750°C	191	0.02	48,100	51,100	62,500	244,300	35.7	92.6
2A-21	Stress Rel. 750°C	77	0.02	123,000	128,700	128,700	251,100	17.3	77.8
2A-21a	Stress Rel. 750°C	300	2.00	41,100	45,200	53,500	356,000	27.6	95.5
2A-36	Recrys. 1200°C	300	0.02	18,200	21,700	33,200	178,100	41.1	97.5
2A-37	Recrys. 1200°C	191	0.02	29,500	35,000	45,400	228,800	37.7	96.5
2A-38	Recrys. 1200°C	77	0.02	90,300	97,700	103,400	232,700	23.2	83.4
2A-98	Recrys. 1850°C	300	0.02	17,000	19,400	24,000	1 1,400	27.0	60.3
2A-99	Recrys. 1850°C	191	0.02	28,300	32,200	37,900	900	39.5	68.8
2A-100	Recrys. 1850°C	77	0.02	88,800	98,800	100,500	108,800	15.8	49.5

TABLE 9

MECHANICAL PROPERTIES OF STRESS RELIEVED (WROUGHT) HYDROGENATED COLUMBIUM

Spec. No.	ppm. Hydrogen	Test Temp. ^{o}K	Strain Rate ipm/0.750	Prop. Limit Load/A_0	0.2% Offset Yield Load/A_0	Ultimate Tensile Strength Load/A_0	Estimated Fracture Strength Load/A_f	% Elong.	% RA
2A-24	29.6	300	0.02	37,600	42,700	58,800	201,200	32.9	92.6
2A-27	29.6	191	0.02	45,800	50,700	57,200	60,000	5.2	15.7
2A-25	29.6	77	0.02	129,300	136,500	136,500	235,600	20.7	63.1
2A-7	47.1	300	0.02	34,300	39,400	51,500	187,300	29.9	89.6
2A-8	47.1	191	0.02	46,700	50,600	57,400	61,800	6.4	7.1
2A-9	47.1	77	0.02	128,000	132,700	132,700	216,700	26.2	57.0
2A-15	47.8	300	0.20	37,500	42,600	55,100	199,000	31.7	89.2
2A-16	47.8	300	2.00	40,000	45,700	56,000	244,000	31.8	90.7
2A-74	114.8	300	0.02	37,000	41,100	53,800	162,000	35.0	90.4
2A-73	114.8	191	0.02	41,300	48,300	57,200	61,300	5.5	6.7
2A-75	114.8	77	0.02	117,700	127,700	132,000	186,300	18.5	42.1
2A-77	114.8	300	2.00	34,800	40,900	55,200	187,900	31.0	85.6
2A-78	114.8	300	2.00	40,900	46,500	57,700	233,000	29.1	89.0
2A-61	166.0	300	0.02	34,500	40,100	52,600	75,000	24.5	32.0
2A-63	166.0	191	0.02	42,500	49,300	51,200	63,400	5.0	9.8
2A-62	166.0	77	0.02	118,000	127,300	134,600	167,100	15.8	32.6
2A-65	166.0	300	0.20	37,200	42,200	54,200	62,500	9.6	13.3
2A-66	166.0	300	2.00	42,900	45,100	54,100	65,300	7.4	17.0
2A-67	207.0	300	0.02	36,200	40,300	53,700	74,500	20.9	29.4
2A-69	207.0	191	0.02	41,200	48,200	57,400	64,400	5.5	10.9
2A-68	207.0	77	0.02	120,400	127,700	131,200	174,200	15.5	35.9
2A-72	207.0	300	2.00	39,600	44,800	54,100	65,700	8.1	17.8

TABLE 10

MECHANICAL PROPERTIES OF STRESS RELIEVED (WROUGHT) HYDROGENATED COLUMBIUM

Spec. No.	ppm. Hydrogen	Test Temp. °K	Strain Rate ipm/0.750	Prop. Limit Load/A_0	0.2% Offset Yield Load/A_0	Ultimate Tensile Strength Load/A_0	Estimated Fracture Strength Load/A_f	% Elong.	% RA
2A-33	23.8	300	0.02	16,500	19,600	35,100	152,300	47.6	94.0
2A-34	23.8	191	0.02	28,600	33,200	39,200	42,400	5.8	7.5
2A-35	23.8	77	0.02	107,100	112,600	114,600	203,900	31.9	62.9
2A-31	23.8	300	0.20	19,100	22,600	38,100	190,200	44.6	94.0
2A-32	23.8	300	2.00	24,600	26,400	39,600	236,000	42.1	95.0
2A-39	50.7	300	0.02	17,200	21,300	36,800	155,000	43.6	93.0
2A-40	50.7	191	0.02	27,500	33,000	42,100	48,000	6.7	12.3
2A-41	50.7	77	0.02	99,400	106,500	113,600	182,500	21.2	53.2
2A-42	117.0	300	0.02	19,700	23,000	37,600	145,700	45.1	90.2
2A-43	117.0	191	0.02	29,300	34,500	41,700	45,300	5.7	7.9
2A-44	117.0	77	0.02	98,000	108,000	115,300	160,600	24.9	38.0
2A-55	163.0	300	0.02	14,600	18,000	37,400	55,800	33.7	33.4
2A-58	163.0	191	0.02	27,300	33,000	43,100	46,700	7.10	7.67
2A-57	163.0	77	0.02	101,500	109,600	116,200	136,100	20.8	29.3
2A-60	163.0	300	0.20	18,100	21,000	39,700	52,200	21.8	24.0
2A-56	163.0	300	2.00	26,700	29,000	41,800	49,000	22.3	14.4
2A-49	205.0	300	0.02	14,700	18,100	37,300	47,800	23.8	22.0
2A-50	205.0	300	0.02	14,700	17,500	37,300	50,000	27.5	25.4
2A-52	205.0	191	0.02	29,000	34,800	43,900	46,800	6.6	6.1
2A-51	205.0	77	0.02	99,400	107,900	117,100	143,100	21.0	28.5
2A-46	216.0	300	0.02	17,400	21,700	38,700	50,000	26.8	22.6
2A-47	216.0	300	0.02	17,600	21,700	38,900	55,400	32.1	29.9
2A-48	216.0	77	0.02	98,500	108,700	117,000	148,300	17.0	29.6

TABLE 11

MECHANICAL PROPERTIES OF RECRYSTALLIZED (1850°C) HYDROGENATED COLUMBIUM

Spec. No.	ppm. Hydrogen	Test Temp. °K	Strain Rate ipm/0.750	Prop. Limit Load/A_0	0.2% Offset Yield Load/A_0	Ultimate Tensile Strength Load/A_0	Estimated Fracture Strength Load/A_f	% Elong.	% RA
2A-79	47.8	300	0.02	18,200	21,000	28,900	15,300	30.20	59.80
2A-80	47.8	191	0.02	30,400	33,200	36,200	40,100	4.80	9.70
2A-81	47.8	77	0.02	103,900	110,700	112,600	124,200	13.50	10.70
2A-84	47.8	77	2.00	109,200	112,000	114,500	122,000	7.55	9.36
2A-85	115.1	300	0.02	17,000	20,200	29,700	37,400	15.60	20.50
2A-86	115.1	191	0.02	30,500	33,300	36,400	38,600	5.70	5.80
2A-87	115.1	77	0.02	-	-	-	85,200	0	0
2A-91	115.1	77	2.00	-	-	-	95,200	0	0
2A-92	165.0	300	0.02	16,700	20,000	29,400	38,100	17.70	22.90
2A-95	165.0	191	0.02	28,400	33,000	37,500	39,700	5.02	5.60
2A-93	165.0	77	0.02	-	-	-	97,200	0	0
2A-96	165.0	77	2.00	-	-	-	83,500	0	0

TABLE 12

PRESTRAIN TESTS ON STRESS RELIEVED (WROUGHT) HYDROGENATED COLUMBIUM

Spec. No.	ppm. Hydrogen	Amount of Prestrain (% Elong.)	Prestrain Temp. ^{o}K	Tensile Test Temp. ^{o}K	Prop. Limit Load/A_0	0.2% Offset Yield Load/A_0	Ultimate Tensile Strength Load/A_0	Estimated Fracture Strength Load/A_f	% RA
2A-108	0	4.65	300	77	105,000	116,200	119,100	254,000	78.80
2A-23	29.6	4.50	300	77	121,000	127,800	127,900	207,400	52.50
2A-26	29.6	4.70	300	77	121,000	127,900	127,900	212,500	54.80
2A-10	47.8	5.80	300	77	118,500	125,000	126,000	195,000	49.10
2A-76	114.8	4.86	300	77	108,000	119,400	127,900	178,200	42.58
2A-64	166.0	4.75	300	77	92,000	116,400	131,300	160,400	28.28
2A-70	207.0	4.70	300	77	93,600	114,900	130,900	172,800	33.68

TABLE 13

PRESTRAIN TESTS ON RECRYSTALLIZED (1200°C) HYDROGENATED COLUMBIUM

Spec. No.	ppm. Hydrogen	Amount of Prestrain (% Elong.)	Prestrain Temp. °K	Tensile Test Temp. °K	Prop. Limit Load/A_0	0.2% Offset Yield Load/A_0	Ultimate Tensile Strength Load/A_0	Estimated Fracture Strength Load/A_f	% RA
2A-107	0	5.25	300	77	76,100	88,800	101,200	222,000	83.20
2A-30	23.8	5.40	300	77	105,000	110,780	113,450	201,390	59.20
2A-45	117.0	4.85	300	77	95,000	104,520	115,820	155,800	36.70
2A-59	163.0	4.96	300	77	82,400	98,000	114,700	152,700	36.80
2A-53	205.0	5.02	300	77	80,500	96,200	113,100	122,300	7.52
2A-54	205.0	4.77	300	77	86,800	98,300	113,600	124,400	10.51

TABLE 14

PRESTRAIN TESTS ON RECRYSTALLIZED (1850°C) HYDROGENATED COLUMBIUM

Spec. No.	ppm. Hydrogen	Amount of Prestrain (% Elong.)	Prestrain Temp. °K	Tensile Test Temp. °K	Prop. Limit Load/A_0	0.2% Offset Yield Load/A_0	Ultimate Tensile Strength Load/A_0	Estimated Fracture Strength Load/A_f	% RA
2A-101	0	4.79	300	77	71,000	95,000	94,100	86,700	57.5
2A-82	47.8	4.55	300	77	-	-	-	98,400	0
2A-83	47.8	4.59	300	77	-	-	-	49,400	0
2A-88	115.1	4.70	300	77	-	-	-	49,400	0
2A-89	115.1	4.65	300	77	-	-	-	49,900	0
2A-94	165.0	4.83	300	77	-	-	-	46,900	0